

# TOYOTA Technical Review

---



Continued: Toyota's Full Lineup Strategy  
for Carbon Neutrality

2023/12 **Vol.69 No.1**

## Preface

The special feature of this issue of the *Toyota Technical Review* (volume 69-1) continues the theme of the previous issue (volume 68): Toyota's Full Lineup Strategy for Carbon Neutrality.

The situation and environment surrounding the question of energy differs on the country and region. With the aim of achieving carbon neutrality everywhere around the world, Toyota is preparing a wide range of options to help reduce CO<sub>2</sub> emissions. This will enable customers to choose the most suitable vehicles for them from a full lineup of models. To achieve carbon neutrality, it is also important to consider the best ways to reduce CO<sub>2</sub> emissions at each stage of energy production, transportation, and use.

Volume 68 primarily focused on battery electric vehicles (BEVs) and fuel cell electric vehicles (FCEVs). In addition to BEVs and FCEVs, volume 69-1 also focuses on options such as hybrid electric vehicles (HEVs) and plug-in hybrid electric vehicles (PHEVs), as well as on the production of fuel. Specifically, the articles in this issue place the spotlight on (1) the fifth generation of the Prius HEV and PHEV, which first appeared on the market in 1997 as the world's first mass-production HEV and has maintained its status as a car cherished by customers to this day, (2) the O-Uchi Kyuden System, Toyota's first home battery, which incorporates the sophisticated battery technologies, parts, and units nurtured through the company's long history of electrified vehicle development, (3) technological developments, government policy trends, and Toyota's initiatives related to carbon-neutral fuels, and (4) the enhancement of mixture formation in hydrogen direct-injection (DI) engines using model-based development (MBD) of jet flows.

As vehicles become increasingly electrified, intelligent, and diversified, stronger links will develop between vehicles and society. Under the slogan "Let's Change the Future of Cars," Toyota intends to continue moving toward the mobility society of the future by mass producing happiness together with all its partners, while spreading the value of vehicles to the whole of society.

Starting from this issue, the *Toyota Technical Review* will be available to read on our homepage. As ever, we are striving to enrich the contents of the magazine to widen its appeal and usefulness to as many people as possible. We would like to thank our loyal readers and look forward to your continued feedback in the future.

Head of Planning, *Toyota Technical Review*

## Contents

---

### ▷Special Feature: Continued: Toyota's Full Lineup Strategy for Carbon Neutrality

- **The Toyota Prius**

Lead authors: Satoki Oya, Yuji Fujiwara, Sho Kawanabe,  
Katsuyuki Owa, Hironori Fujita, Takaji Kikuchi      ······3

- **Development of the O-Uchi Kyuden System Home Battery**

Natsuki Tanaka, Kazuki Kubo, Toshio Uchiyama, Kazuo Ebata      ······24

- **Carbon-Neutral Fuels**

Oji Kuno, Takeshi Nobukawa, Hiroyuki Fukui, Nozomi Yokoo, Koichi Nakata      ······29

- **Improvement of Mixture Formation in Hydrogen DI Engine Using Fuel Jet MBD**

Jun Miyagawa, Yoshinori Miyamoto, Shiro Tanno, Yoshihisa Tsukamoto,  
Tetsuo Omura, Daishi Takahashi, Koichi Nakata      ······38

---

### ▷Technical Papers/Technical Articles

- **The WAVEBASE Cloud-Based Material Data Analysis Service**

Masao Yano, Takeo Yamaguchi, Ryo Aoki, Kazuto Ide, Hanae Ikeda,  
Yasuhiro Toyama, Yusuke Murai, Kanta Ono, Tetsuya Shoji      ······47

---

### ▷Technical Award News

- **Development of Remote Control Autonomous Driving System**

Takuro Sawano, Takeshi Kanou, Shogo Yasuyama, Kento Iwahori, Keigo Ikeda      ······61

- **Initiatives to Reduce Power Demand through Peak Shifting and Demand-Response**

Yoshitaka Ohtake, Iwao Akaida, Nobutake Suzuki      ······64

---

### ▷List of Externally Published Papers of FY2022

·····69

# The Toyota Prius

Lead authors:

Satoki Oya\*<sup>1</sup>

Yuji Fujiwara\*<sup>2</sup>

Sho Kawanabe\*<sup>3</sup>

Katsuyuki Owa\*<sup>4</sup>

Hironori Fujita\*<sup>5</sup>

Takaji Kikuchi\*<sup>6</sup>

## Abstract

Toyota is pursuing a wide range of options following multiple pathways in accordance with the future energy situation and the conditions existing in each country and region. Since its launch, the Prius has led the mass popularization of dedicated hybrid electric vehicles (HEVs). For the fifth generation, Toyota focused on developing hybrid and plug-in hybrid electric models that would have an immediate effect on reducing CO<sub>2</sub> emissions under a concept called “Hybrid Reborn.” This article outlines the objectives of the fifth-generation Prius and the technologies to realize these objectives.

**Keywords:** *Prius, HEV, PHEV, TNGA, Hybrid Reborn, car cherished by customers, design that inspires love at first sight, captivating driving performance, Prius*

## 1. Introduction

Since its launch as the world’s first mass-production hybrid electric vehicle (HEV), the Prius has pioneered the popularization of dedicated HEVs. For the fifth generation, Toyota focused on developing hybrid and plug-in hybrid electric models that would have an immediate effect on reducing CO<sub>2</sub> emissions under a concept called “Hybrid Reborn.”

This article outlines the objectives of the fifth-generation Prius and the technologies developed to realize its main selling points of a design that inspires love at first sight and captivating driving performance.

## 2. Development Aims

### 2.1 The history of the Prius

Toyota inaugurated the Global 21st Century (G21) project with the objective of building the car of the 21st century. This project aimed to develop a vehicle that delivered overwhelmingly impressive fuel economy as part of measures to address the resource-related and environmental issues affecting the vehicle-based society of the day. After overcoming a wide range of development challenges, the first-generation Prius was

launched in 1997 as the world’s first mass-produced HEV under the tagline, “Just in time for the 21st century.” Given a Latin name that means “to go before,” the Prius was a true pioneer for a new age of mobility.

With the aim of realizing the mass-popularization of HEVs, the second-generation Prius was launched in 2003 with an updated version of the Toyota Hybrid System (the THS II) that emphasized both environmental and driving performance and a radically different silhouette.

Launched in 2009, the engine displacement of the third generation Prius was increased from 1.5 to 1.8 liters, helping to boost both fuel economy and dynamic performance. To appeal to more customers and popularize HEVs even further, this generation became the first model to be sold across all of Toyota’s sales channels.

Finally, in 2015, the fourth generation Prius was launched as the first model developed under the Toyota New Global Architecture (TNGA) design philosophy and realized improvements in both fuel economy and driving feel.

### 2.2 Hybrid Reborn

With the Prius as the pioneer, followed by the Aqua and many other HEVs, Toyota’s total global HEV sales have reached 20 million units. By itself, the Prius has sold 5 million units. The popularity of HEVs around the world has reduced global CO<sub>2</sub> emissions by up to 160 million tons.

As an icon of electrified vehicles, the Prius has successfully accomplished its role of popularizing HEVs (**Fig. 1**).

\*1 TCZ, Toyota Compact Car Company

\*2 Techno Art Research Co., Ltd.

\*3 TC Body Design Div., Toyota Compact Car Company

\*4 TC Vehicle Evaluation & Engineering Div., Toyota Compact Car Company

\*5 Chassis Development Div. No. 1, Vehicle Development Center

\*6 Powertrain Product Planning Div., Vehicle Development Center

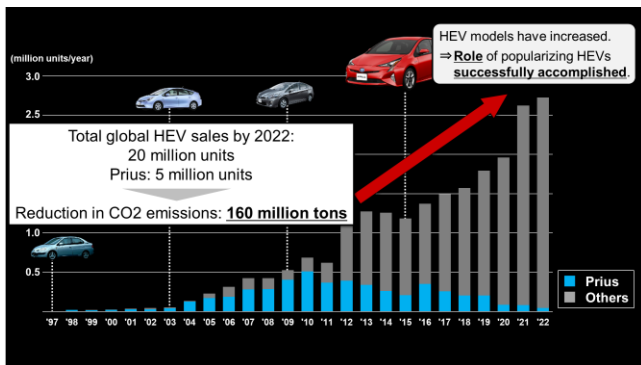


**Fig. 1 Global Sales of Toyota's Electrified Vehicles**

With this background, planning for the redesigned Prius began under the Hybrid Reborn concept with the aim of developing a model that would live up to its name and lead the way for the next generation of HEVs.

### 2.3 Commodity or car cherished by customers?

At the beginning of the planning phase before the team head settled on a direction, the president of Toyota suggested that the fifth-generation Prius might be developed as a dedicated taxi. The true intention behind this suggestion was the idea of contributing to the environment by turning the Prius into a commodity and increasing sales by emphasizing its longevity and durability.

This suggestion questioned the core role of the Prius, and the development team were unable to come up with a convincing response. In this difficult situation, the team asked the designers to come up with a sketch of a cool looking car. **Fig. 2** shows the design sketch that was submitted.



**Fig. 2 Design Sketch**

This single design sketch motivated the team to set aside the president's suggestion of developing a commodity like a taxi and decide to create a car that would be truly cherished and attract as many customers as possible.

### 2.4 Selling points

To create a car that would be truly cherished by customers, the development team aimed to create an

uncompromising model that would combine the environmental performance for which the Prius is traditionally renowned with a thorough dedication to both emotionally inspiring styling and driving performance. Reflecting this attitude, the selling points of the redesigned Prius were defined as (1) a design that inspires love at first sight and (2) captivating driving performance.

## 3. Design that Inspires Love at First Sight

To embody the idea of Hybrid Reborn in the styling of the fifth-generation Prius, the inspiration of love at first sight was set as the design concept. The objective was to create a design that appeals to people's emotions through a language that cannot be expressed through numbers or logic alone.

### 3.1 Exterior

#### 3.1.1 Exterior design

Design aims:

The following three key phrases were adopted to help express a styling design that appeals to the emotions.

(1) Sporty body silhouette (realizing a unique sporty silhouette for the Prius)

Inheriting the signature monoform silhouette that started with the second-generation Prius, the new generation realizes a sleek and sportier silhouette through the adoption of a lower center of gravity and large tires (**Fig. 3**).

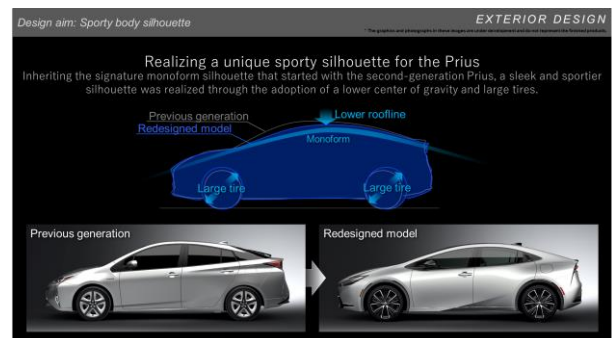


**Fig. 3 Body Silhouette**

(2) Emotional body shape (a body shape that appeals to the emotions)

Resembling natural flows of air, a dynamically accented body shape was created that reflects the emotions of the natural world through regularity amidst disorder (**Fig. 4**).

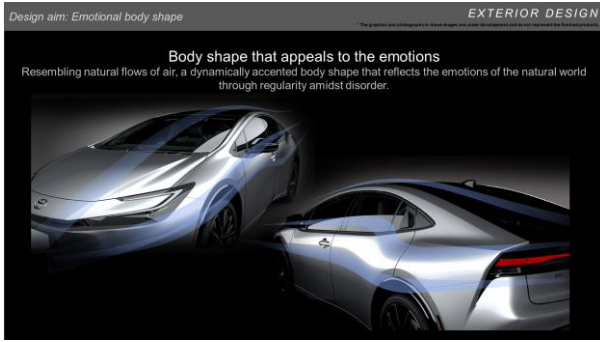


**Fig. 4 Body Shape**

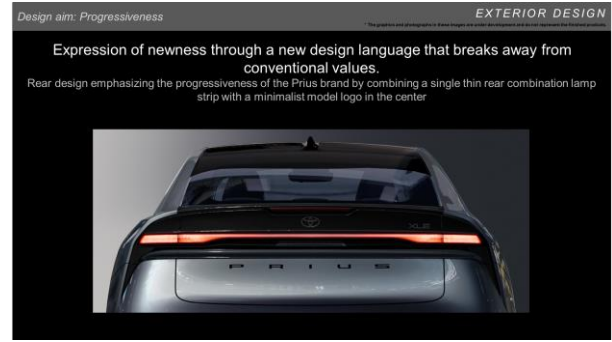


**Fig. 7 Rear Design**

- (3) Progressiveness (an expression of newness through a new design language)  
 The redesigned Prius has a design expression that is simple yet robust, clean yet impressive, and worth looking at (Fig. 5).

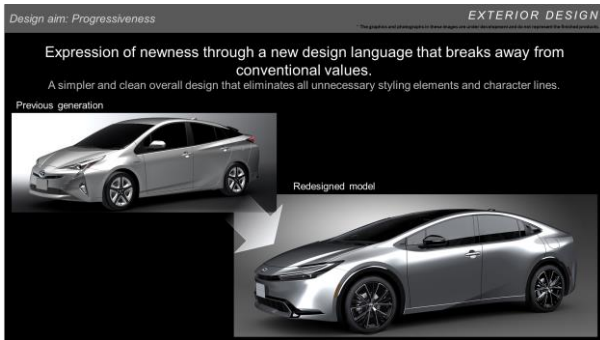


**Fig. 5 Expression of Progressiveness**

A simple and iconic front design was created that integrates functions and graphics based on the hammerhead design theme (Fig. 6).

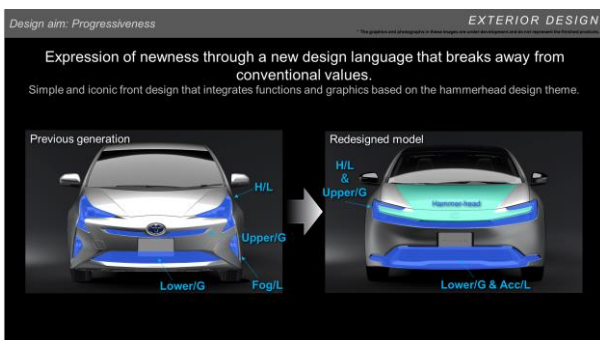


**Fig. 6 Front Design**

The rear design emphasizes the progressiveness of the Prius brand by combining a single thin combination lamp strip with a minimalist model logo in the center (Fig. 7).

**3.1.2 Achieving the exterior design**

(1) Packaging

The roofline was lowered to create a vehicle package that realizes the monoform silhouette and a lower center of gravity. The height of the vehicle was lowered by 40 mm compared to the previous generation, and the peak position of the roof was shifted to the rear (Fig. 8).

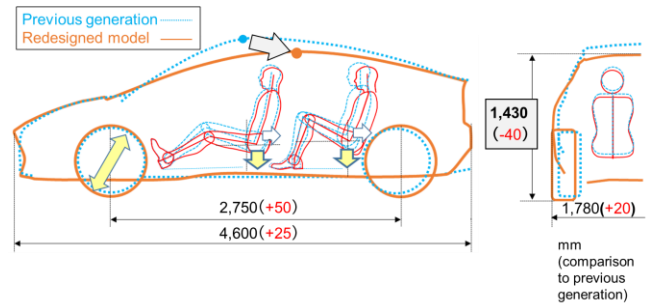


**Fig. 8 Packaging**

(2) A pillars

With the lower roof, the angle of the A pillars increases. Although this makes it more difficult to provide a good field of view around the pillars, the visible range through the fixed glass was maximized by pushing the outer mirrors rearward within the permitted range of the mirror reflection angle (Fig. 9).



**Fig. 9 Rearward Mirror Layout**

## (3) Rear door handles

The rear door handles were positioned above the belt line to help realize dynamic outer panels (**Fig. 10**). The trade-off impacts on the diagonally rear field of view and the handle operation space were both addressed by reducing the size of the interior mechanism.

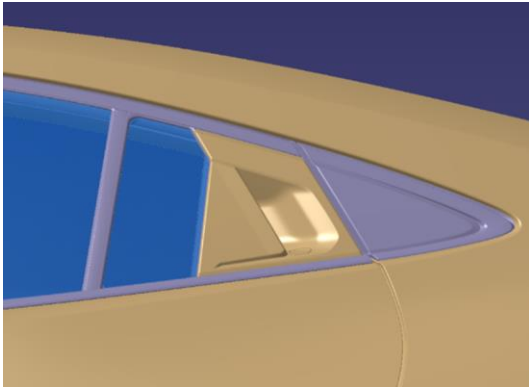


**Fig. 10 Rear Door Handle**

## (4) Hammerhead design theme

Issues for realizing the hammerhead design theme in the redesigned Prius included rigidity, pedestrian protection performance, and compliance with North American regulations (for mild collisions) of the parts at the front of the vehicle that extend from the headlights. These issues were addressed by examining structures with downward folding deformation modes (**Fig. 11**). The desired styling was realized by achieving the target deformation (**Fig. 12**).

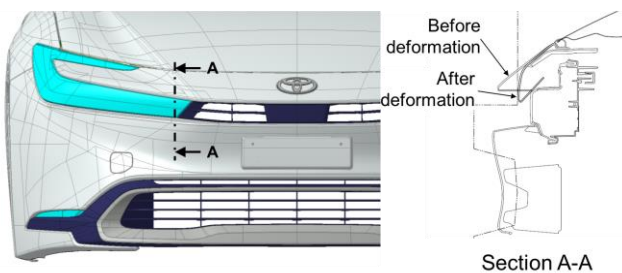


**Fig. 11 Target Deformation Mode**



**Fig. 12 Actual Vehicle Test**

## (5) Dedication to manufacturing that closely realizes the design aims

To maximize its emotional expression and achieve a design that inspires love at first sight, the shapes envisioned by the designers needed to be formed out of single sheets of steel. One of the main issues in expressing this styling was forming a steel sheet to create a wraparound effect at the rear lamp area (**Fig. 13**). At the sharply formed corners of the outer panel, the steel sheets must be formed without overlapping, since this might lead to wrinkling. **Fig. 14** shows a simple illustration of the issue. The desired shape was formed in the stamping process by adopting the following three steps: (1) drawing to form the basic product shape, (2) trimming to cut off excess material, and (3) bending of the outer parts of the sheet to form the flanges that connect with other parts (**Fig. 15**). In this case, the issue was the wrinkling that occurred in step (3). To address this issue, forming simulations were carried out that modified the shape of the sheet in 1-mm and 1-degree intervals to verify manufacturing methods for multiple patterns of pre-forming shapes, flange forming angles, and so on. This allowed the optimum manufacturing method that realizes the target shape to be proposed.

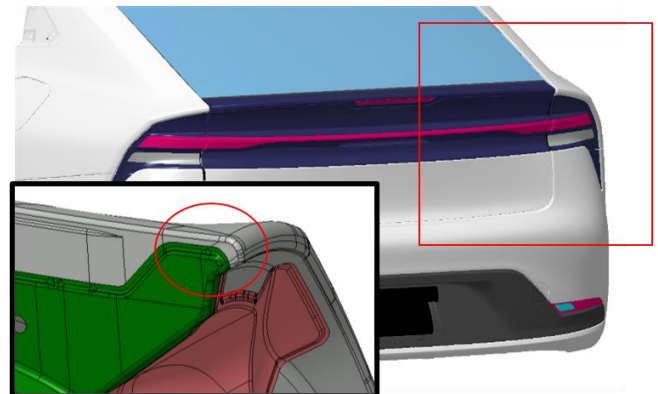


**Fig. 13 Difficult-to-Form Area**

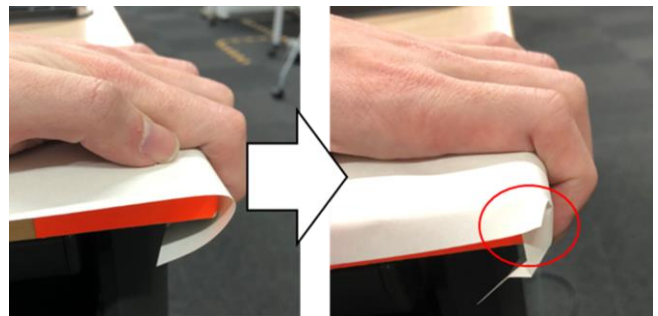


**Fig. 14 Illustration of Forming Issue**

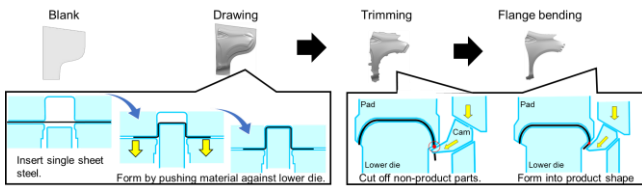


**Fig. 15 Stamping Process**

## 3.2 Interior

### 3.2.1 Interior design

Design aims:

The following three key phrases were adopted to help realize a high-quality cockpit that also enables an exciting driving experience.

(1) The “island architecture” concept

A low-stress, spacious cockpit that makes it easy to concentrate on driving was realized through the design of three areas called the “surrounding tub,” “driving module,” and “floating instrument panel” (Fig. 16).

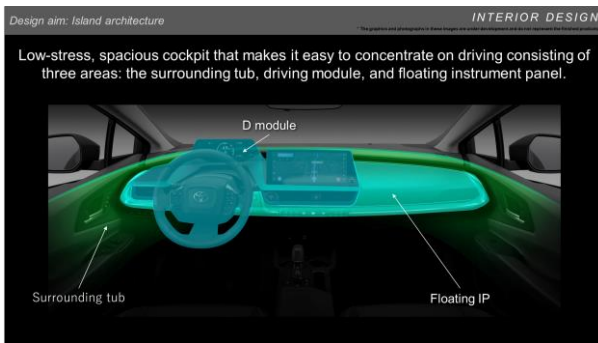


**Fig. 16 Island Architecture**

The driving module is centered on a meter cluster located in a position that sets the driver’s viewpoint further away than in a conventional vehicle. This encourages a more intuitive driving focus and helps to create an exciting driving experience (Fig. 17).



**Fig. 17 Driving Module**

(2) Sporty and high quality

A sporty and high-quality space was realized by synchronizing the instrument panel and seat decoration with a black-toned interior (Fig. 18).

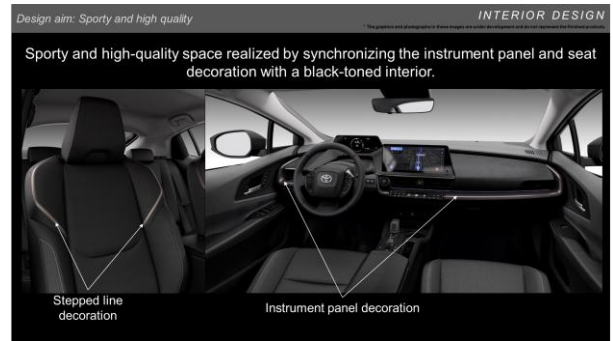


**Fig. 18 Interior Space**

(3) Progressiveness (creation of new value)

The interior includes illumination that expresses new value synchronized with the TSS functions (Fig. 19).

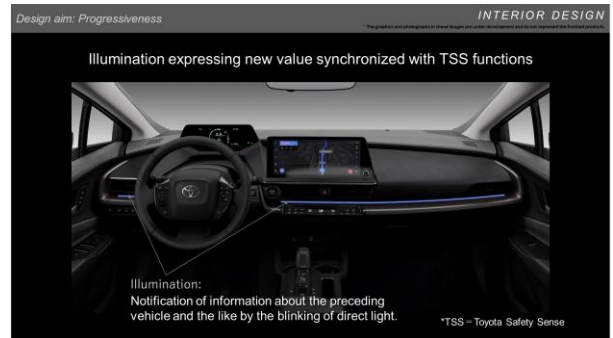


**Fig. 19 Illumination**

New sensations are expressed by coordination between the color of the illumination and the decoration (Fig. 20).

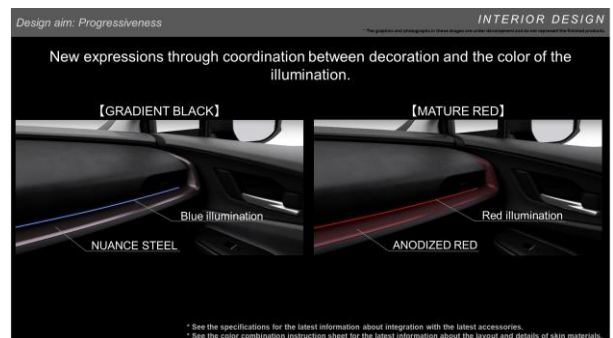


**Fig. 20 Expression of New Sensations**

### 3.2.2 Reproduction of interior design mockups by mass-production parts

To replicate the design aims in the real world as closely as possible, the interior design development focused on the following key points.

#### (1) Island architecture

- Reduction of cockpit stress

Detailed sectional studies were carried out from the initial phase of development to reduce any potential stress generated by the perception of being cramped by the low-roofed sporty package. The height of the top edge of the top mounted meter cluster was minimized by splitting up parts and designing innovative structures. The center display was designed not to project above the instrument panel with the driver seated (Fig. 21). In addition, a two-tone illumination color was adopted to reduce stress created by the perception of being cramped by the A pillar garnish and to reduce reflection onto the windshield.

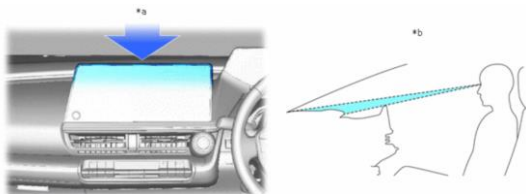


Fig. 21 Lowered Center Display Layout

- Optimum layout around cockpit including the center console

To facilitate intuitive operation of the switches around the driver's seat by the vehicle occupants, the layout prioritized switch visibility by grouping the switches into those used while driving, those indicated on the display, and those that are only used when the vehicle is stopped.

The console layout was designed in consideration of the frequency of use of the shift lever, cup holders, and smart phone storage spaces (the slit tray and wireless charger). The first horizontal cup holder layout on the GA-C platform was adopted to prevent interference with heater control panel and shifting operations, helping to enhance accessibility to the drinks by the occupant of each seat. The smart phone storage spaces were determined after studying fields of vision and wrist discomfort. Items that need to be used and touched naturally and without stress were positioned close to the driver.

#### (2) New value creation in sporty and high-quality design

- Fusion of ambient illumination and film decoration

The ambient illumination colors were set to match the interior color. Direct illumination was deliberately adopted instead of indirect illumination to create an expression as part of the interior decoration. A uniform light distribution

was achieved by eliminating inconsistencies in this distribution caused by the adoption of direct illumination through countless iterations of optical analysis, prototyping, and subjective evaluation. Alerts synchronized with the advanced driver assistance system (ADAS) functions were also designed to be more easily discernible by the vehicle occupants.

Seamless and long film decoration panels, which would be difficult to accomplish using conventional forming technologies, were developed through joint studies between suppliers and the style designers and engineers by a process involving the analysis of film forms (Fig. 22), trials using prototype film forming molds, and the development of films with large forming tolerances.

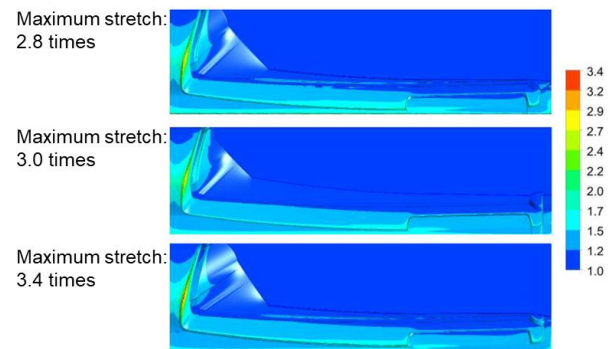


Fig. 22 Film Forming Analysis

### 3.2.3 Meter cluster

The meter cluster is positioned above the steering wheel, which moves the viewpoint of the driver further away and realizes a low depression angle. This layout also reduces the necessary movement of the driver's focus point, facilitates instant understanding of displayed information, and aids intuitive operations. The aim of this design was to create a futuristic-looking cockpit that makes it easy to concentrate on driving. In addition, measures to make the meter cluster casing appear thinner and achieve narrower bezel edges help to create an uncluttered and stylish impression (Fig. 23).

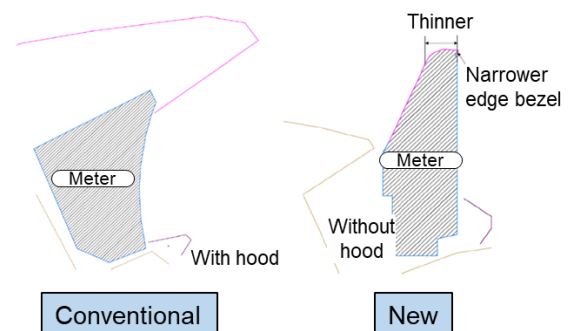


Fig. 23 Meter Geometry

Since eliminating the hood of the meter cluster exposes the meter to direct sunlight, anti-reflection and anti-glare measures were applied to the meter display area, ensuring visibility and suppressing reflection. At the same time, measures were also incorporated into the design to suppress reflection of meter cluster lights on the surrounding glass at night. The challenge of this meter cluster layout and the adoption of a thinner casing was the concentration of the fixing points on one side since the conventional approach to meter cluster attachment could not be copied. To ensure the necessary vibration resistance for this fixing structure, an innovative internal structure was selected, and a bracket layout and angle settings less susceptible to the effects of center of gravity acceleration were adopted. In addition, the overall stiffness of the meter cluster was increased by selecting the appropriate materials for the component parts of the meter cluster and adopting innovative shapes.

The meter cluster was designed under the concept of providing the necessary information at the necessary time and in the optimum form. The display layout only includes the absolute minimum content required while driving. At the same time, an even simpler layout was realized by allowing the HEV system indicator to be hidden if the driver wants to reduce the volume of items on display. With this layout, the driver can be notified of the necessary information by pop-up displays at the appropriate timing if an emergency or similar situation occurs. For drivers who require more information, a display layout with a larger amount of content can be selected by a single press of a steering wheel switch. In this way, the meter cluster display can be customized in accordance with the driver's needs (Fig. 24).

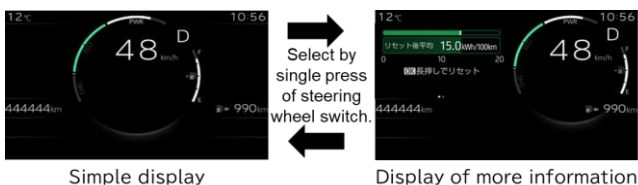


Fig. 24 Graphic Layout

### 3.3 Color design

Design aims:

The following three key phrases were adopted to help realize a concept called “sophisticated specialty,” which refers to the combination of a hidden sensation of exhilaration and anticipation that presages the coming age with a sense of playfulness.

- (1) Modern: the pursuit of new value
- (2) Sporty: agile sportiness
- (3) Intriguing: interest and passion

Color lineup:

- (1) Exterior colors (newly developed colors): The aim of the exterior colors is to express solidity at first glance and create a sparkling effect when the light hits the particles in the paint.

- 1M2/ASH: A color that draws the eye without garishness and expresses hidden sophistication (Fig. 25).



Fig. 25 1M2/ASH

- 5C5/MUSTARD: A vivid color that also expresses a mature, glossy, and sporty appearance (Fig. 26).



Fig. 26 5C5/MUSTARD

- (2) Interior colors: A sporty and high-quality space was realized by synchronizing the instrument panel decoration with the stepped line seat decoration (Fig. 27).

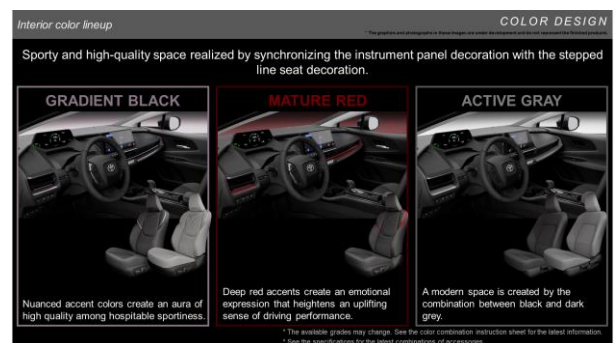


Fig. 27 Interior Colors

## 4. Captivating Driving Performance

### 4.1 Aims of the redesigned Prius

Following the key concept of “Hybrid Reborn,” it was important to completely rejuvenate the driving performance of the redesigned Prius in line with its inspiring design to make it an appealing option for customers of HEVs and PHEVs.

The slogan “captivating driving performance” was chosen for this reason. After considering the character of the Prius as a model, it was decided to appeal to the majority of customers who would drive the Prius in everyday scenarios rather than aim to realize aggressive driving performance suitable for a racetrack. Consequently, performance that enables the driver to drive as intended and makes the driver feel more skillful was defined as one development aim. Then, to express the Hybrid Reborn concept in a more tangible form, it was decided to utilize the excellent acceleration feel that provides an important part of the appeal of an HEV or PHEV. As a result, an exhilarating acceleration feeling and driving performance that follows the intention of the driver were defined as the two aims of the development.

To realize these two aims, desktop studies and test track trials were combined with driving tests in actual real-world scenarios. This was regarded as particularly important for the redesigned Prius as a way of breaking down target performance from the perspectives of where and how customers would like to drive the vehicle. As a result, the following three scenario and performance combinations were emphasized.

- (1) City streets: the capability to adjust speed easily
- (2) Mountainous roads: the capability to follow the intended driving line
- (3) Expressways: the capability to realize powerful and enjoyable acceleration

The following sections describe the evolution of the TNGA, which is the foundation of the required performance in these scenarios, and the basic technologies that were adopted to support each of the target scenarios.

### 4.2 Evolution of the TNGA

As the first model to use the TNGA, the previous generation of the Prius adopted the fourth-generation HEV/PHEV system and the GA-C platform. The redesigned model features further advanced versions of TNGA components and the vehicle platform.

#### 4.2.1 Fifth-generation HEV/PHEV system

New fifth-generation 1.8/2.0-liter HEV systems and a new 2.0-liter PHEV system were developed for the redesigned Prius. The HEV systems feature transaxle motors and power control units (PCUs) that realize higher power with lower loss, as well as a compact high-power lithium-ion battery. As a result, the 2.0-liter HEV system achieves 1.6 times higher power than the previous generation with the equivalent or better fuel economy. In addition to even greater acceleration performance and lower noise than the HEV, the EV driving range of the redesigned PHEV system was improved by at least approximately 50% compared to the previous generation. This range is long enough to cover most of the daily driving needs of the user (Table 1).

**Table 1 Comparison of Previous and Redesigned System Specifications**

|                       |   | Hybrid (HEV)                            |  |  | Plug-in hybrid (PHEV)                     |  |            |
|-----------------------|---|---|--|--|---|--|------------|
|                       |   | Redesigned model                        | Previous generation                    | Redesigned model   | Previous generation                       |  |            |
| Engine                | Type/displacement                       | M20A-FXS<br>Inline 4-cylinder, 1,986 cc | 2ZR-FXE<br>Inline 4-cylinder, 1,797 cc | 2ZR-FXE<br>Inline 4-cylinder, 1,797 cc                       | M20A-FXS<br>Inline 4-cylinder, 1,986 cc   | 2ZR-FXE<br>Inline 4-cylinder, 1,797 cc   |            |
|                       | Maximum power<br>(kW [PS]/rpm)          | 112 [52]/6,000                          | 72 [98]/5,200                          | 72 [98]/5,200  | 111 [51]/6,000                            | 72 [98]/5,200                            |            |
|                       | Maximum torque<br>(N·m [kgf·m]/rpm)     | 188 [19.2]/4,400 to 5,200               | 142 [14.5]/3,600                       | 142 [14.5]/3,600   | 188 [19.2]/4,400 to 5,200                 | 142 [14.5]/3,600                         |            |
| Motor                 | Front                                   | Maximum power<br>(kW [PS])              | 83 [113]                               | 70 [95]  | 53 [72]                                   | 120 [163]                                | 53 [72]    |
|                       |   | Maximum torque<br>(N·m [kgf·m])         | 206 [21.0]                             | 185 [18.9]   | 163 [16.6]                                | 208 [21.2]                               | 163 [16.6] |
|                       | Rear<br>(E-Four grades only)            | Maximum power<br>(kW [PS])              | 30 [41]                                | Same as left   | 5.3 [7.2]                                 | —  | —          |
|                       |   | Maximum torque<br>(N·m [kgf·m])         | 84 [8.6]                               | Same as left   | 55 [5.6]                                  | —  | —          |
| Main traction battery | Capacity<br>(Ah)                        | 4.08 (lithium-ion)                      |  | FWD: 3.6 (lithium-ion)<br>E-Four: 6.5 (nickel-metal hydride) | 51 (lithium-ion)                          | 25 (lithium-ion)                         |            |
| Maximum system power  | kW [PS]<br>* Value calculated by Toyota | FWD: 144 [196]<br>E-Four: 146 [199]     | 103 [140]                              | 90 [122]   | 164 [223]                                 | 90 [122]                                 |            |
| EV driving range      | km                                      | —                                       |  |  | 87 (19-inch tires)<br>205 (17-inch tires) | 60 (15-inch tires)<br>50 (17-inch tires) |            |

### 4.2.1.1 Technologies incorporated into HEV systems

- (1) Transaxle motor  
 In addition to achieving lower electrical losses by reducing the size of the coil ends and changing the magnet layout, mechanical losses were reduced by adopting a new lubrication structure and new low-viscosity oil. As a result, the redesigned Prius realizes lower loss and higher power than the previous generation.
- (2) PCU  
 The PCU features newly developed reverse conducting insulated gate bipolar transistors (RC-IGBTs). The inductance of internal conduction parts was also reduced, thereby increasing the switching speed and resulting in lower loss. These measures improved electrical loss by 13% compared to the previous generation (Figs. 28 and 29).

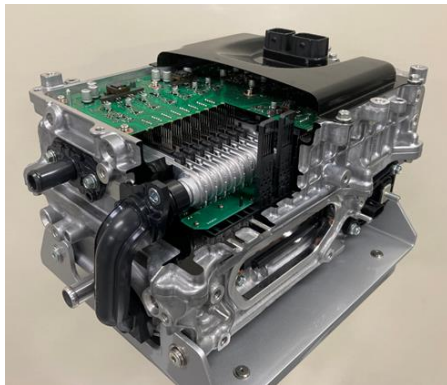


Fig. 28 External Appearance of PCU

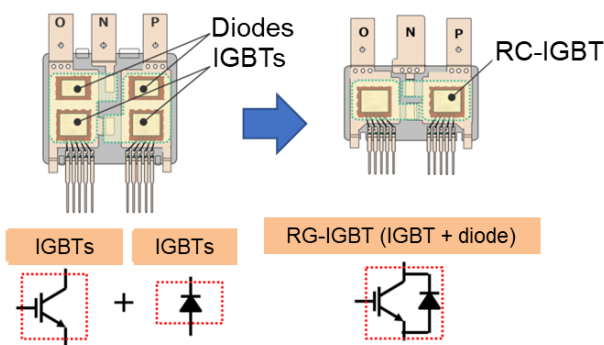


Fig. 29 Outline of RC-IGBT

- (3) HEV battery  
 The power density of the HEV battery was increased 16% by adopting newly developed lithium-ion cells. The battery cell stack and battery pack casing functions were integrated using an aluminum diecast case. Flexible printed circuits (FPCs) were adopted for the voltage detection circuits, reducing the space required for

the wiring (Fig. 30). These measures helped to reduce the size of the 2.0-liter HEV battery by 25% without increasing the weight.

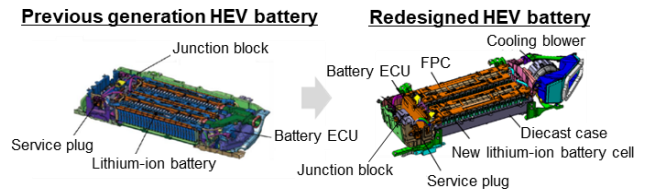


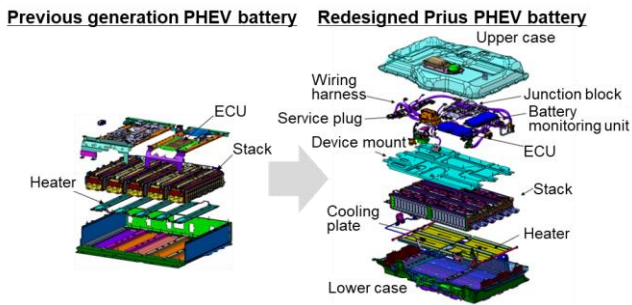
Fig. 30 Comparison of Previous and Redesigned HEV Battery Pack Structures

### 4.2.1.2 Technologies incorporated into PHEV system

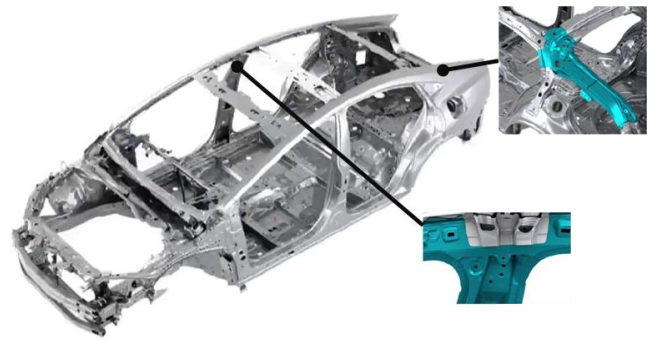
- (1) Transaxle motor  
 The motor magnet layout was changed from the layout in the HEV system motors and a new lubrication structure was adopted. These measures resulted in increased power and better cooling performance in EV mode.
- (2) PCU  
 A double boost system with two HEV boost converters arranged in parallel was adopted, enabling high-power motor drive without increasing the size of the PCU compared to the HEV system.
- (3) PHEV battery  
 The battery cells from the RAV4 were adopted. This battery is the same size as the battery in the previous generation Prius PHEV, but has 1.5 times the capacity. In addition, higher power was realized by modifying the cooling structure to use air conditioning coolant (Table 2). Furthermore, a double layer structure was adopted for the stack and auxiliary devices inside the battery pack, helping to save space and enabling the battery to fit below the rear seats (Fig. 31).

Table 2 Comparison of Previous and Redesigned PHEV Batteries

|                 | Previous generation | Redesigned model |
|-----------------|---------------------|------------------|
| Number of cells | 95 cells            | 72 cells         |
| Capacity        | 8.8 kWh             | 13.6 kWh         |
| Weight          | 129 kg              | 129 kg           |
| Cell capacity   | 25 Ah               | 51 Ah            |
| Cell voltage    | 3.7 V               | 3.7 V            |



**Fig. 31 Comparison of Previous and Redesigned PHEV Battery Pack Structures**



**Fig. 32 Body Structure**

#### 4.2.2 Second-generation TNGA platform

Captivating driving performance cannot be realized through powertrain advances alone. Since the vehicle body plays an important role in transmitting the driving force from the powertrain and operational inputs from the driver, body innovations were also necessary to realize vehicle behavior that follows the driver's intentions. The second-generation TNGA platform was developed for the redesigned Prius as an enhanced version of the previous GA-C platform. This platform advances the foundations underpinning the driving performance of the vehicle through enhancements to both the powertrain and body.

##### 4.2.2.1 Technologies incorporated into the body

Based on the previous generation GA-C platform, a lighter and more rigid body was adopted to enhance vehicle response to driver inputs. Noise and vibration (NV) performance was enhanced at the same time to enable an even more sophisticated driving experience. The rigidity of the suspension attachments (i.e., the front lower control arms and front suspension struts) was increased by optimizing the geometry of the front sub-frame and front side members, and by refining the structure of the cowl end portion and joining method. These measures also enhanced the transmission characteristics of vibration input sources. In addition, while helping to realize the intended design that inspires love at first sight, annular structures were incorporated in various locations around the body and torsional rigidity equal to or higher than the previous generation was achieved (Fig. 32). These measures were complemented by the adoption of enhanced front bumper reinforcements and an enhanced structure around the radiator supports to increase the lateral bending rigidity of the front body (Section 4.3.2 (2)), which plays an essential role in realizing the targeted captivating driving performance. At the same time, the layout of the damping materials on the dash and floor panels was revised to improve the NV performance (Fig. 33, Section 4.3.3 (2)).

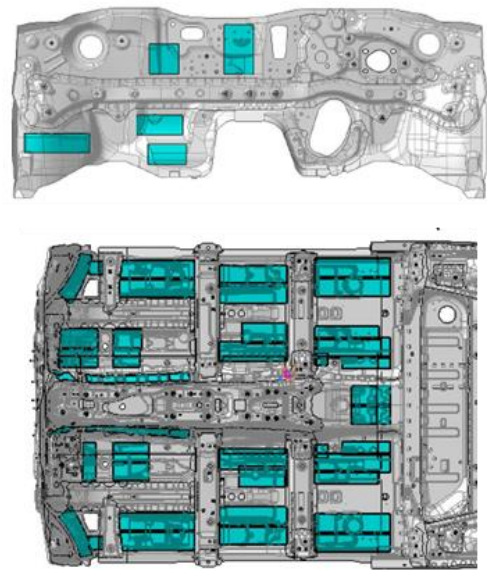


**Fig. 33 Coating Type Damping Materials**

##### 4.2.2.2 Technologies incorporated into the suspension

To realize further improvements in vehicle stability and response, the suspension geometry and characteristics of each component part were optimized based on the previous generation GA-C platform (Fig. 34).



**Fig. 34 Overall View of Suspension**

Modifications were made to components such as the suspension arms, knuckles, and carriers, expanding the tread dimension of the tire contact points outward by 30 mm. This helps to realize greater stability both when driving straight on and around corners. The characteristics of joint parts such as the suspension bushings and ball joints were optimized to enhance vehicle response to small steering inputs (Section 4.3.2 (3)). These measures were combined with enhancements to the body suspension supports, suppressing excess vibration and helping to realize more refined driving performance.

### 4.3 Basic technologies for each driving scenario

Section 4.1 outlined the particularly important driving scenarios for the redesigned Prius. This section describes the technologies developed to support the necessary performance in these scenarios.

#### 4.3.1 City streets

Driving on city streets involves repeated cycles of acceleration and deceleration at low speeds. Being able to adjust speed and stop smoothly and as intended is an effective way of making the driver feel more skillful. To accomplish this objective, the development incorporated the two following approaches.

- Enhance accelerator response at low speed to ensure that the vehicle accelerates in accordance with the intention of the driver.
- Lower the aftershock when the vehicle stops to eliminate harsh vehicle movements.

##### (1) Enhanced accelerator response at low speed

The development team of the redesigned Prius aimed to enhance vehicle response to accelerator inputs. This was achieved by heightening the time-based acceleration response (acceleration jerk) (Figs. 35 and 36). Since the normal speed of accelerator operation in day-to-day driving scenarios is 40% per second or less, the enhancements in response were mainly implemented in this range (Fig. 37).

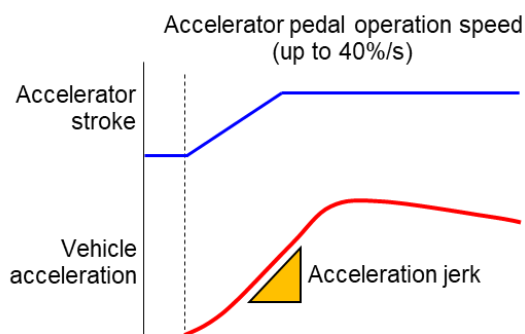


Fig. 35 Acceleration Response to Accelerator Inputs

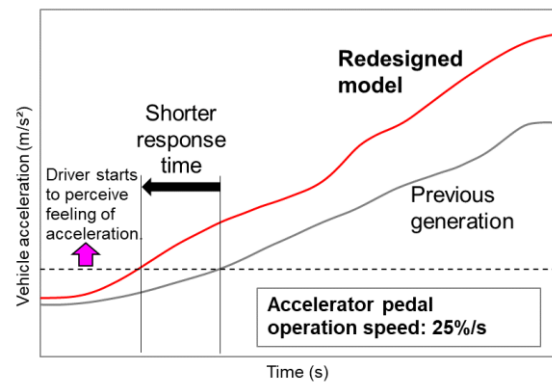


Fig. 36 Vehicle Acceleration (Response)

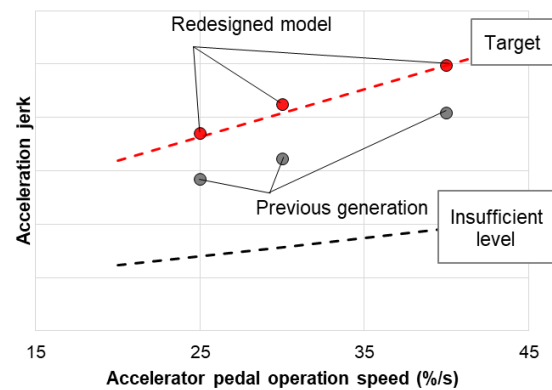


Fig. 37 Acceleration Jerk

##### (2) Lower aftershock when vehicle stops

The redesigned model features a new electronically controlled braking system. The previous high hydraulic pressure accumulation system was replaced with a system that generates pressure on demand. This approach allows more precise control of the brake fluid pressure (Fig. 38). This system enables the brake fluid pressure to follow small pedal inputs, such as when the driver releases the brake pedal gradually before the vehicle comes to a stop. As a result, the driver can stop the vehicle smoothly and without generating any aftershock (Fig. 39).

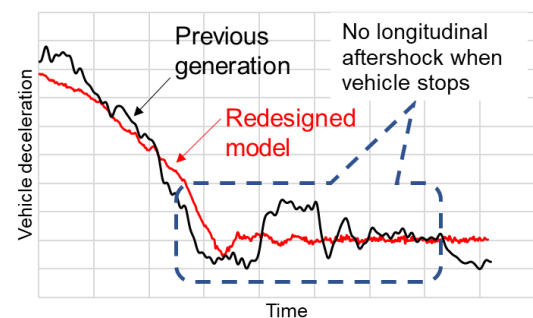
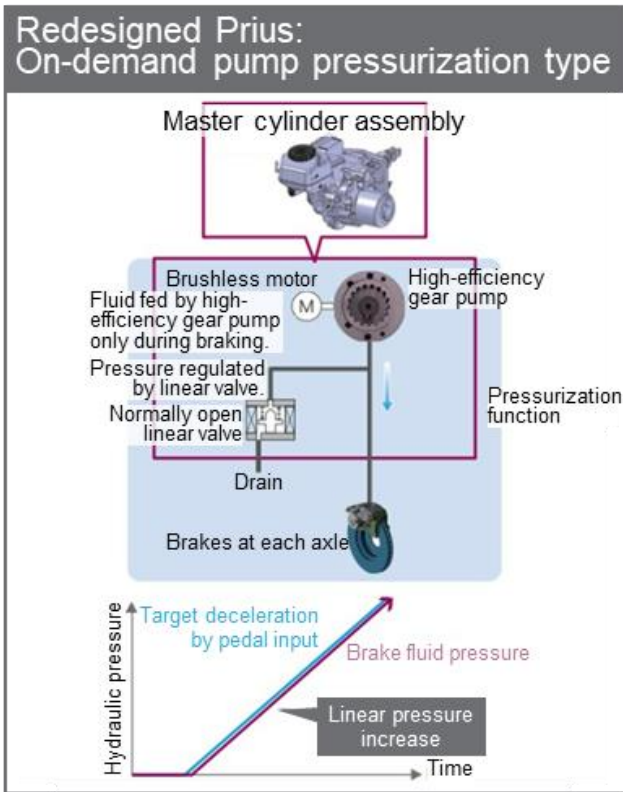


Fig. 38 Aftershock



**Fig. 39 On-Demand System**

**4.3.2 Mountainous roads**

Captivating driving performance can be realized on mountainous and other types of winding roads by enhancing the capability of the vehicle to follow the driving line intended by the driver. The following three measures were implemented.

- Enhance the effect of motor regenerative braking to enable the driver to control the speed of the vehicle without delay and at the intended timing immediately before entering a curve.
- Adopt a highly rigid body to ensure that it follows steering wheel inputs without delay when entering the curve.
- Optimize the suspension settings to ensure that the vehicle stably follows the target driving line when driving through the curve.

The following basic technologies were developed to realize these measures and achieve captivating driving performance on winding roads.

(1) Enhanced motor regenerative braking effect

The new HEV system (2.0-liter) is capable of stronger deceleration due to motor regeneration in the D range. This gives the driver a greater capability to control the vehicle speed using the accelerator. Sport Mode features even stronger deceleration to match the aggressive acceleration feeling generated in this driving mode.

The redesigned PHEV system features three selectable levels of motor regenerative braking in the B range (low, medium, and high (Fig. 40)) and is

designed to ensure the driver or other vehicle occupants are not discomfited during deceleration. More specifically, the deceleration jerk caused by motor regeneration was designed to closely replicate the deceleration jerk generated from the start of foot brake operation (time-based changes in deceleration) (Figs. 41 and 42).

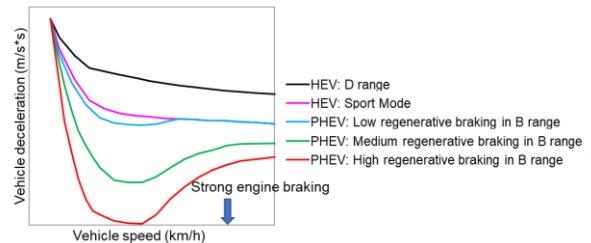


**Fig. 40 Deceleration of Redesigned Prius by Motor Regeneration**

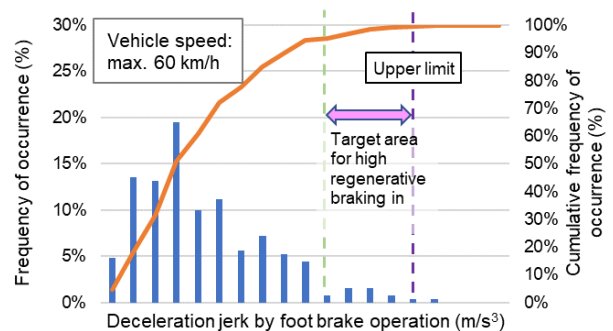


**Fig. 41 Deceleration Jerk due to Braking (Time-Based Changes in Deceleration)**

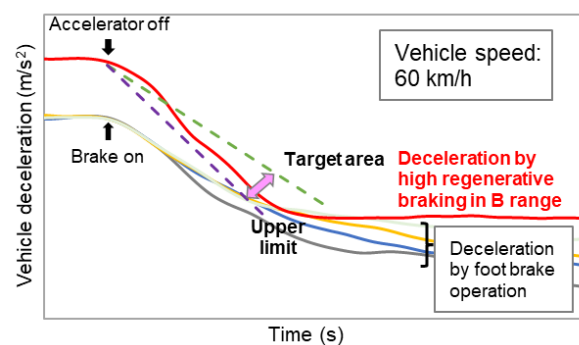


**Fig. 42 Comparison of Deceleration in B Range (High Regenerative Braking) and Deceleration by Foot Brake Operation**

(2) Highly rigid body

As the vehicle enters a curve, the driver fixes on the target driving line and then turns the steering wheel. At this point, lateral bending deformation occurs at the front of the vehicle, in which the front part of the body bends and deforms either to the left or right

(Fig. 43). Therefore, the bending rigidity of the front body was increased to enable the vehicle to respond to these initial steering wheel inputs without delay. The development identified that increasing the rigidity of the reinforcement that connects the radiator supports and apron upper member, and increasing the rigidity of joining with the surrounding parts would be an effective way of accomplishing this aim. Rigidity was increased by designing this reinforcement with a ridge line structure without major bending points, reducing steps between the surrounding parts, and creating joining structures with a minimum number of intermediate parts (Fig. 44). These measures increased the front lateral bending rigidity by a maximum of 15% compared to the previous generation.

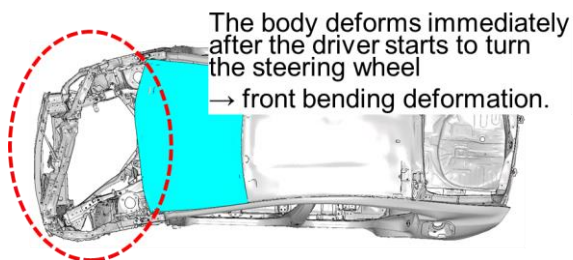


**Fig. 43 Front Lateral Bending Deformation**

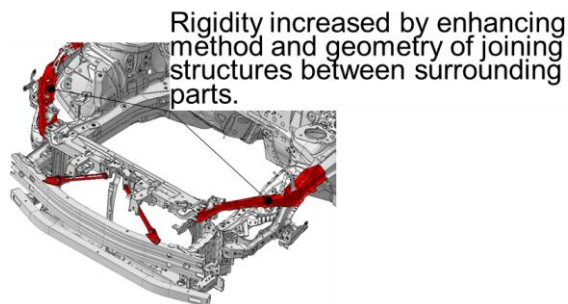


**Fig. 44 Structure for Enhancing Front Body Rigidity**

### (3) Suspension settings

To enable the driver to follow the target driving line more stably, linear vehicle behavior without delay is necessary in response to driver inputs. However, this is not enough by itself. The driver must also be able to feel how the vehicle is behaving and drive with full awareness that the vehicle is responding as intended (Fig. 45).



**Fig. 45 Information Transmission between Vehicle and Driver**

For this purpose, the following targets were established for the suspension: realize linear response characteristics without delay to steering wheel inputs, and generate the appropriate steering reaction forces that can be perceived by the driver. The characteristics of the component parts were optimized to achieve these targets. More specifically, linear rigidity characteristics were realized for joint parts such as the suspension bushings and ball joints to lower the suspension hysteresis that is a contributing factor to response lag (Fig. 46). In addition, enhancements were made to the linear suspension response characteristics (Fig. 47) and steering torque in response to small steering inputs (Fig. 48).

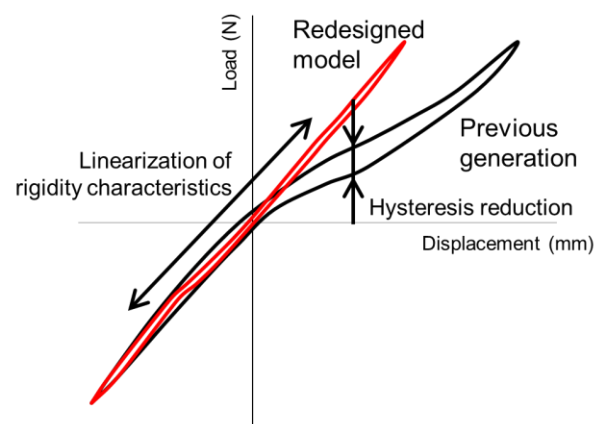


**Fig. 46 Rigidity Characteristics of Suspension Component Parts**

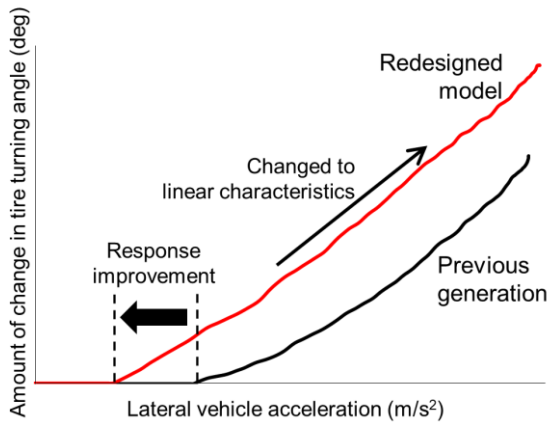


Fig. 47 Suspension Response Characteristics

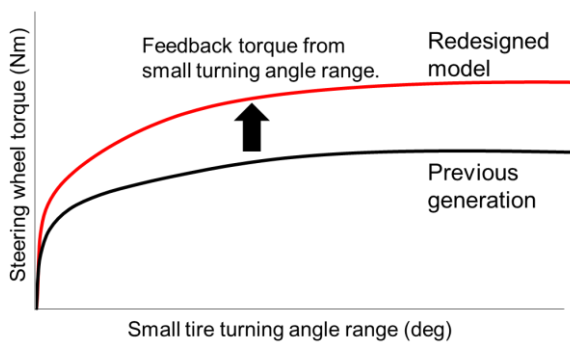


Fig. 48 Steering Wheel Torque in Response to Small Steering Inputs

Furthermore, roll stability was enhanced by expanding the tread outward by 30 mm in the redesigned Prius compared to the previous generation. The amount that the eye line of vehicle occupants changes in response to lateral G while cornering was reduced (Fig. 49), helping to realize driving performance that generates a greater sense of stability in the driver and passengers.

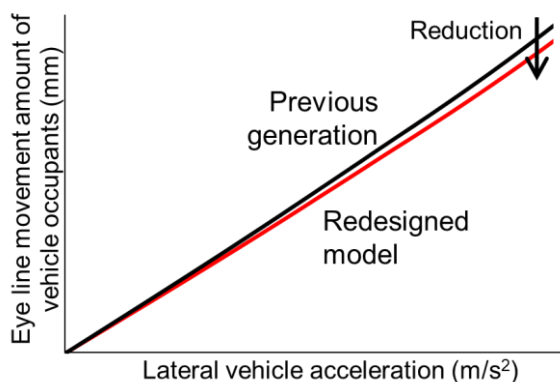


Fig. 49 Eye Line Movement Amount of Vehicle Occupants

### 4.3.3 Expressways

In scenarios requiring forceful use of the accelerator, such as on an expressway or access ramp, the capability to realize powerful and fun-to-drive acceleration is the moment when the driver will experience the Hybrid Reborn concept most strongly. The following two measures were applied to achieve this kind of performance.

- Deliver a feeling of power that creates a tangible sense of thrilling acceleration.
  - Create an engine sound that creates a tangible sense of pure fun-to-drive acceleration.
- (1) Feeling of power during acceleration

Based on the results of surveys into the accelerator pedal stroke and acceleration when entering an expressway, the vehicle was designed to deliver a tangible sense of power immediately after launch. The sense of power realized at the same accelerator stroke is clearly different to the previous generation (Fig. 50).

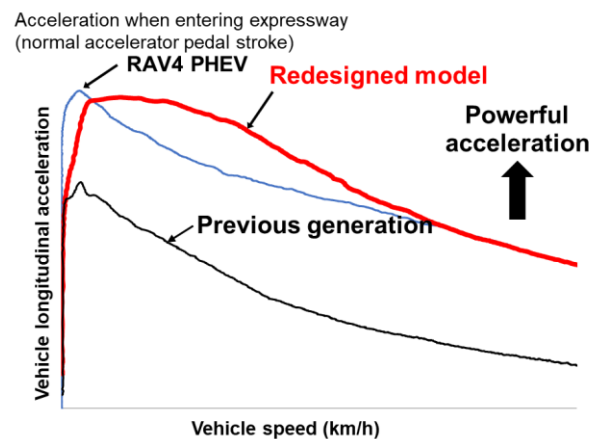


Fig. 50 Acceleration of Redesigned Prius

- (2) Engine sound during acceleration

An interior noise environment that matches the sense of power delivered during acceleration was defined as follows. The engine sound and road noise generated from the tires should not be noticeable under low acceleration. In contrast, the engine sound should be clearly audible under strong acceleration to express a sense of pure power, while simultaneously suppressing the road noise. Road noise was reduced by the measures to increase the rigidity of the platform and upper body and the enhanced damping materials as described in Section 4.2.2.1, as well as refinements to the suspension bushings. The engine sound under low acceleration was translated into lower interior noise by the greater dynamic performance of the fifth-generation HEV and PHEV systems, as well as enhanced engine mounts. In contrast, the engine sound under strong acceleration was realized by adopting newly

designed damping materials in the dash panel. These materials help to lower high-frequency sound pressure level (SPL) components and raise the low-frequency SPL in relative terms, resulting in a powerful and pure engine sound (Fig. 51). Additionally, the PHEV is equipped with an engine balance shaft that quietens the engine sound in the low frequency range and further reduces interior noise compared to the HEV.

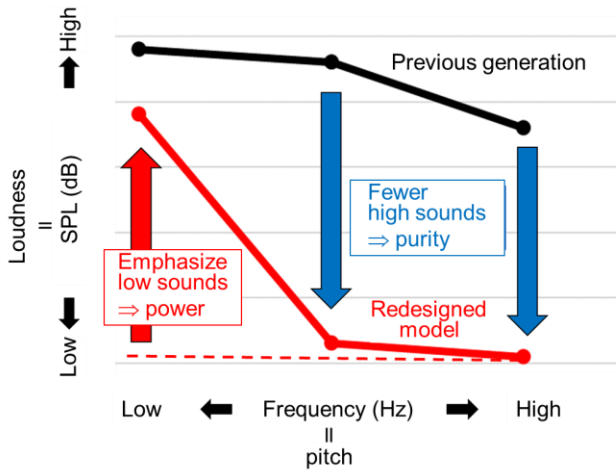


Fig. 51 Frequency Balance of Engine Sound

#### 4.4 The “One Team” approach to dynamic performance development

The previous sections described the incorporation of individual elements into the redesigned Prius. However, individual elements alone were not enough to realize the targeted driving performance. For example, Fig. 52 shows a scenario of a vehicle entering and driving through a curve. Even in this scenario, driver operations and vehicle behavior are not independent but occur continuously while overlapping each other. Therefore, so that the driver perceives these elements as naturally as possible, the development team needed to tune the vehicle while factoring in the phenomena (operations) immediately before and immediately after the current point in time. Therefore, the conventional approach of tuning each function individually was changed to an integrated team-based approach in which the engineers in charge of tuning each separate phenomenon worked together to develop the dynamic performance as a series of interconnected actions (Fig. 53).

Toyota’s guiding policy for dynamic performance can be summarized by the slogan “confident and natural.” In more specific terms this refers to stable and confident vehicle response to outside disturbances and inputs, and natural vehicle response to driver inputs that follows the driver’s intention. These words do not refer to concrete objects or specific values, but represent perceived performance. This requires a people-centric approach to vehicle development.

Confident and natural performance cannot be realized simply by individual members of the development team defining certain items or specifications. This type of performance can only be accomplished by constantly considering how these items or specifications would be perceived by the driver. In this development project, to facilitate proper understanding of this concept and ensure that individual team members did not become confined within defined areas of responsibility, progress was made toward the ideal approach by carrying out team-based development (referred to in Toyota as the “One Team” approach).

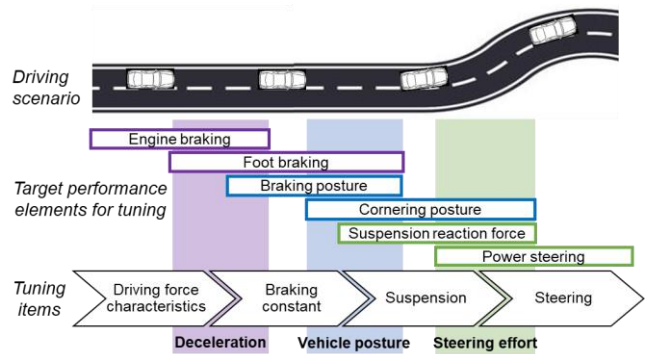


Fig. 52 Illustration of Approach to Tuning Driving Performance

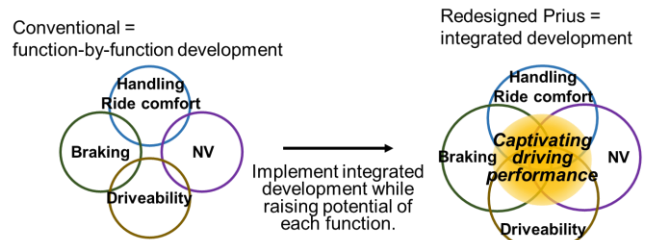


Fig. 53 Integrated Development of Redesigned Prius

## 5. Realizing a Car Cherished by Customers

### 5.1 Advanced safety

One objective of the redesigned Prius was to build a cherished car that customers would want to keep and use for a long period of time. This section describes the functions that were adopted for the first time within the Toyota brand with the aim of helping to provide even greater safety and confidence.

### 5.1.1 Proactive Driving Assist Steering Assist (PDA SA): function that provides constant support to the driver to keep the vehicle in its lane

To help build a car that would be cherished by as many customers as possible, the PDA SA system was developed as support technology to reduce driver stress due to a lack of driving experience or excessive driving burden during hands-on driving. Factors contributing to driver stress or an excessive driving burden include corrective driving operations made in response to unstable vehicle behavior caused by unnecessary or delayed operations that run counter to the intention of the driver. Therefore, enabling appropriate changes in steering effort in accordance with the driving scenario was suggested as an important way of reducing unnecessary operations while the driver holds the steering wheel in a turned position or minimizing delayed operations when entering a curve (Fig. 54). For example, when the vehicle lane is straight, the system raises the steering effort in both the left and right directions to make it easier for the driver to continue driving in a straight line. In contrast, at the entrance to a curve, the system lowers the steering effort in the direction of the inside of the curve to help minimize steering delays. As a result, this system facilitates confident driving through smooth vehicle behavior.

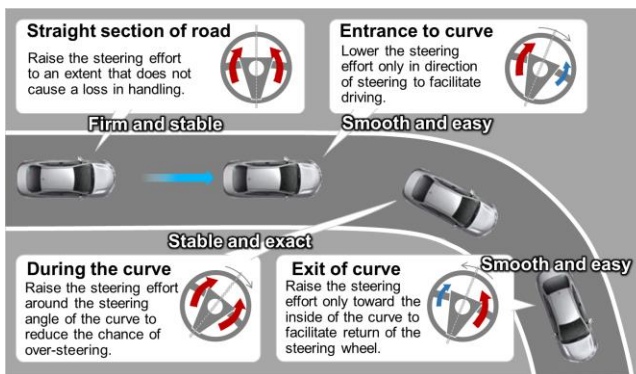


Fig. 54 Illustration of Changes in Steering Effort by PDA SA

Changing the steering effort in accordance with the scenario as shown in Fig. 54 requires lane detection using a monocular camera or the like, steering angle calculations that anticipate driver operations, and electric power steering (EPS) output control based on these inputs. To apply this system in a wide range of driving environments (including ordinary roads), it must enable easy-to-handle characteristics that minimize any sense of discomfort generated by system intervention. PDA SA achieves this by only changing the steering effort without any autonomous steering controls. As a result, it can be activated in many different situations without inconveniencing the driver. System activation can also be switched on or off and its effects (i.e., the strength of

system intervention) made more or less prominent in accordance with driver preferences and driving scenarios. There are three selectable levels of system intervention that make the extent of support more obvious in sequence.

The steering feel of the redesigned Prius was very carefully designed. For this reason, the development team was concerned that the vehicle might become harder to drive as the support characteristics were tuned. Therefore, repeated vehicle assessments were carried out with the members of the dynamic performance evaluation team, resulting in a tuning that realizes natural support characteristics.

### 5.1.2 Rear Vehicle Approaching Indication

A function was developed that notifies the driver via the instrument cluster if the rear millimeter wave radar detects a vehicle approaching from the rear. This function encourages the driver to look at the rear view mirror and determine whether evasive action is required (Fig. 55). When driving on expressways or other unfamiliar roads, drivers that lack confidence or are tired may not have the presence of mind to check to the rear of the vehicle. If the driver suddenly notices an approaching vehicle, the driver may hastily and dangerously change lanes without checking around the vehicle first. Alternatively, if the driver does not notice the vehicle at all, this may lead to an incident of road rage. Notifying the driver before this occurs enables the driver to change lanes safely, reduces the driving burden, and helps to proactively prevent road rage incidents.

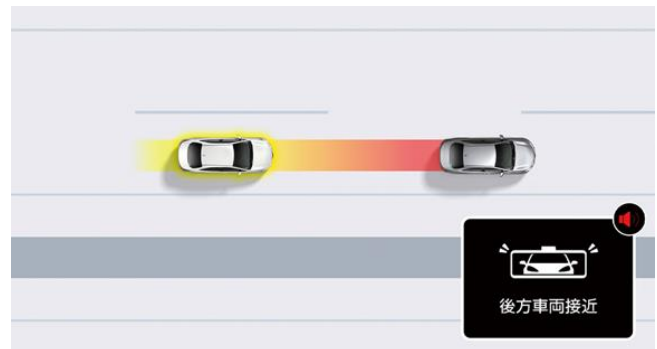


Fig. 55 Rear Vehicle Approaching Indication

### 5.1.3 Approaching Vehicle Support (Recording Function, Report Notification Function)

Road rage has become a social issue of concern in recent years. To help mitigate the damage caused by road rage incidents, technology was developed that automatically detects potential road rage and proposes recommended measures for drivers facing this situation (Fig. 56). If the driver's vehicle is approached extremely closely from behind (more closely than the situation described in Section 5.1.2), the developed system uses

audio and instrument cluster messages to propose calling the police. The system makes the call automatically if the driver decides that the police should be called and approves the proposal. As a result, the driver can speak to the police while the road rage incident is occurring and can receive help from the police remotely. In addition, if the vehicle is equipped with drive recorders (front and rear), an event will be registered to supplement the constant recording function. The incident will be automatically recorded and saved to a dedicated part of the memory so that it is not recorded over.



**Fig. 56 Approaching Vehicle Support (Recording Function, Report Notification Function)**

#### 5.1.4 Secondary Collision Brake (Rear Impacts while Stopped)

The following system was developed. If the rear millimeter-wave radar detects a vehicle approaching from the rear and the system determines a high possibility of a rear-end collision while the driver's vehicle is stopped, the system will activate the brakes. Subsequently, if a rear-end collision has occurred, the developed system will slow the driver's vehicle to help prevent or mitigate damage caused by a secondary collision as a knock-on effect from the first collision (Fig. 57). Compared to the conventional Secondary Collision Brake system that activates the brakes only after a frontal or side impact collision occurs while driving, this system uses the rear millimeter-wave radar to also respond to potential rear-end collisions and can slow the vehicle down more quickly by activating the brakes before the collision occurs.



**Fig. 57 Secondary Collision Brake (Rear Impacts while Stopped)**

## 5.2 Solar panel

As part of global efforts to realize a sustainable society and Toyota's objective of achieving carbon neutrality by 2050, the company is aiming to reduce the CO<sub>2</sub> emissions of its new models by 50% in 2035.<sup>(1)</sup> To help achieve this target, the redesigned Prius PHEV sold in Japan, Europe, and North America is equipped with a solar charging system. This solar charging system supplies energy to the vehicle, enabling zero-emission, zero-running cost, and location-free charging. In addition to daily use, this system also helps to secure a supply of power in an emergency. This section describes the solar roof of the redesigned Prius PHEV (Fig. 58).



**Fig. 58 Solar Roof of Redesigned Prius PHEV<sup>(2)</sup>**

In addition to the adoption of heterojunction back-contact type solar cells, the structure of the system and material colors were unified to hide the wiring from sight, making the solar roof system look like a more integral part of the vehicle than the previous generation. Since the adoption of uniform coloring for the component materials makes even slight differences in color stand out more clearly, the supplier and relevant internal departments worked closely together to define quality criteria for the exterior appearance. The resulting solar roof contributes to a design that inspires love at first sight.

Shingling connections were adopted for the solar cells to realize an efficient cell layout within a limited area. As a result, although the roof area is 10% smaller than the previous generation PHEV, power per unit area was increased by 15%, maintaining a power generation capacity that is the same or higher than the previous generation. When calculated using the average annual solar irradiation data for Nagoya, the system is capable of generating approximately 166 kWh, which is equivalent to an annual driving distance of roughly 1,200 km. This power is used to charge the drive battery or supplied to the auxiliary battery to help reduce tailpipe CO<sub>2</sub> emissions.

### 5.3 Reservation design

The U grade of the redesigned Prius is a special grade for Toyota's KINTO vehicle subscription service. This grade includes functions and equipment that can only be selected when a new vehicle contract is concluded. The design enables these functions and equipment to be added whenever the customer desires, even after vehicle delivery. Conventional hardware retrofitting is a very time-consuming operation that involves working with wiring harnesses and is difficult to realize. Therefore, assuming future hardware upgrades, the vehicle has been designed in advance to allow the retrofitting of hardware even after delivery. The time required to add equipment and make changes to wiring connections has been greatly reduced by adopting a structure that factors in serviceability and allows these changes to be made more easily.

## 6. Conclusion

Hybrid Reborn is the key concept of the fifth-generation Prius. Under this concept, a united One-Team approach was adopted with the aims of realizing a design that inspires love at first sight and captivating driving performance. The authors would like to take this opportunity to express their sincere gratitude for the invaluable contribution of the suppliers, sales staff, and everyone who participated in this development.

The development team intends to continue its efforts to help achieve carbon neutrality by nurturing the development of the Prius to increase its appeal to as many people as possible and make it a car that is truly cherished by customers.

## References

- (1) *New Management Policy & Direction Announcement*. Toyota Global Newsroom. <https://global.toyota/en/newsroom/corporate/39013233.html>
- (2) *Toyota Launches All-New Prius PHEV in Japan*. Toyota Global Newsroom. <https://global.toyota/en/newsroom/toyota/38869594.html>

## Authors

Section 1. Introduction  
Section 2. Development Aims  
Section 6. Conclusion



S. Oya

M. Nitano

TCZ, Toyota Compact Car Company

Section 3. Design that Inspires Love at First Sight



Y. Fujiwara

Techno Art Research Co., Ltd.



M. Hirokawa

Design Div., Toyota Compact Car Company



T. Oba

Vision Design Div., Vehicle Development Center



K. Taniguchi

Color & Sensory Design Dept., Vehicle Development Center



K. Matsumura

Productization Manufacturing Engineering Div., Vehicle Development Center



S. Kawanabe

TC Body Design Div., Toyota Compact Car Company



T. Yamamoto

MS Vehicle Design Div., Mid-Size Vehicle Company



M. Matsui

Lexus Body Engineering Div., Lexus International Co.

Section 4. Captivating Driving Performance



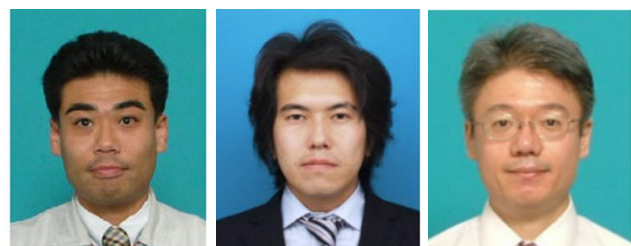
K. Owa



T. Takayama



S. Nakahara



M. Amano

M. Azuma

M. Ito

TC Body Design Div., Toyota Compact Car Company



H. Masaki

TC Vehicle Evaluation & Engineering Div., Toyota Compact Car Company

Section 5. Realizing a Car Cherished by Customers



T. Itsuji  
TC Chassis Engineering Div., Toyota Compact Car Company



S. Sugamoto  
Automated Driving Technology Development Div., Vehicle Development Center



H. Fujita  
Chassis Development Div. No. 1, Vehicle Development Center



T. Nakado  
E/E Architecture Development Div., Vehicle Development Center



S. Ito  
Chassis Development Div. No. 2, Vehicle Development Center



K. Nii  
MS Vehicle Design Div., Mid-Size Vehicle Company



T. Kikuchi      T. Abe      K. Hashimoto  
Powertrain Product Planning Div., Vehicle Development Center



T. Kohara  
Advanced Safety Technology Development Div., Vehicle Development Center



T. Hamaguchi  
Automated Driving Technology Development Div.,  
Vehicle Development Center

# Development of the O-Uchi Kyuden System Home Battery

Natsuki Tanaka\*<sup>1</sup>

Kazuki Kubo\*<sup>1</sup>

Toshio Uchiyama\*<sup>1</sup>

Kazuo Ebata\*<sup>1</sup>

## Abstract

Toyota is promoting the introduction of a wide range of practical products and services using the battery technologies, parts, and units nurtured over its long history of electrified vehicle development. As part of this initiative, Toyota has been focusing on the massive and lengthy power outages caused by the growing number of natural disasters in recent years, as well as the energy crisis spurred by global instability. Consequently, Toyota has developed the O-Uchi Kyuden System home battery with the objective of enabling carbon neutral lifestyles with ever-greater peace of mind and safety. This article describes the development history and characteristics of the O-Uchi Kyuden System.

**Keywords:** *home battery, utilization of electrified vehicle technologies, carbon neutrality, resilience*

## 1. Introduction

Toyota is working to achieve its mission to mass-produce happiness by delivering innovative, safe, and high-quality manufactured goods and services that bring peace of mind to its customers.

As part of this mission, Toyota has developed its first home battery, called the O-Uchi Kyuden System, using battery technologies, parts, and units nurtured through the company's long history of electrified vehicle development. With this system, Toyota is aiming to promote a smarter lifestyle that brings greater peace of mind by encouraging the use of renewable energy generated from solar power in normal times and supplying power to whole households in the event of a power outage after a natural disaster. This article describes the performance and characteristics of the O-Uchi Kyuden System.

## 2. Motivation behind the Development

In September 2019, typhoon number 15 of the 2019 Pacific typhoon season (Typhoon Faxai) brought fierce winds and heavy rains to the Izu Islands and southern Kanto region around Tokyo, knocking out power to up to 930,000 homes in Chiba Prefecture. It took 280 hours, or 12 days, to fully restore power. The series of natural disasters that struck Japan that year prompted the company to ask a number of questions, such as: What can Toyota do in an emergency? What is demanded of vehicles as a part of social infrastructure? How can Toyota contribute to the community through its vehicle manufacturing know-how? With this motivation, Toyota started to examine how it could deliver greater peace of

mind to people's lifestyles in today's society.

At the same time, the ten-year contracts organized under Japan's Feed-in Tariff Scheme for Renewable Energy (FIT) system, which began in 2009, were starting to expire. Under this system, power companies agreed to pay a fixed price for power generated by renewable energy. However, with the ending of these contracts, the purchase price of this electricity would drop, resulting in lower income for the contract holders.

Under this background, Toyota began developing a home battery under the policy of utilizing the company's safe and reliable battery technologies to contribute to society at large (**Fig. 1**).



**Fig. 1 The O-Uchi Kyuden System after Installation**

\*<sup>1</sup> Carbon Neutral Development Div., Carbon Neutral Advanced Engineering Development Center

### 3. Development Concept

For this home battery development project, two objectives were defined for the adoption of a storage battery at people's homes: the realization of economic and carbon-neutral lifestyles, and the provision of a safety net in the event of a power outage caused by a natural disaster. To realize these objectives, the following three concepts were proposed and used to define the specific items that would be needed. The team then began development.

- (1) Maximize the effectiveness of having a home storage battery by combining solar power generation with nighttime electricity supply. → Two charge/discharge cycles per day (Section 6.1)
- (2) Secure electricity supply in the event of an extended power outage. → Electricity supply from electrified vehicles (Section 6.2)
- (3) Toughness to withstand a natural disaster → Waterproofing (Section 6.3) and robustness (Section 6.4)

To turn these concepts into reality, it was decided to make widespread use of the technologies that Toyota has nurtured through its long history of electrified vehicle development.

### 4. Utilization of Vehicle Parts

The storage battery of the O-Uchi Kyuden System uses the highly reliable and large-capacity lithium-ion battery installed in the RAV4 and Prius PHEVs (Fig. 2).



**Fig. 2 Concept of Lithium-Ion Battery Utilization**

To bring peace of mind to users of the system, half of the component parts were repurposed from automotive applications. This includes the battery, which was originally developed to deliver safety, a long lifespan, high quality at a reasonable price (*ryohin-renka*), and high performance, as well as key parts such as the electronic control unit (ECU) and relays that control the power supply. The controls of these parts were then optimized for use in the O-Uchi Kyuden System (Fig. 3).

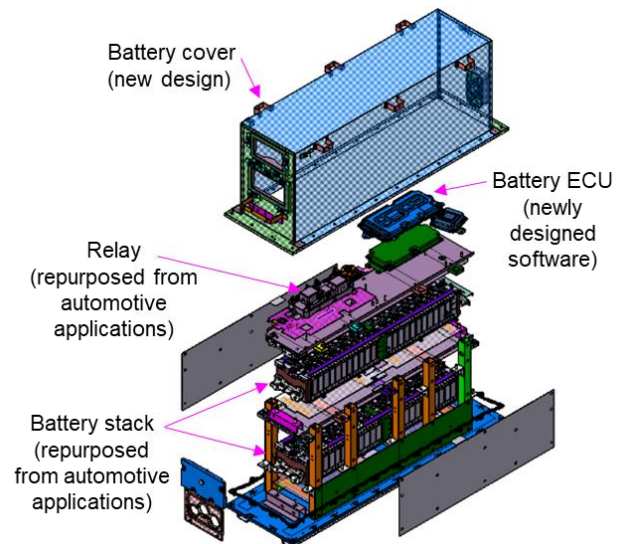


**Fig. 3 Examples of Vehicle Parts Used in the O-Uchi Kyuden System**

### 5. System Outline

#### 5.1 System configuration

After considering the weight of the system during transportation and installation flexibility, the O-Uchi Kyuden System was divided into the following four separate units (Fig. 4).

- (1) A battery unit for storing electricity
- (2) A DC-DC converter that converts voltage using voltage direct current (DC)
- (3) A hybrid power conditioner that inputs power from the storage battery and solar panels as DC and converts it to alternating current (AC) for use in the home.
- (4) A vehicle power supply adapter and vehicle connection cable that enables an electrified vehicle (hybrid (HEV), plug-in hybrid (PHEV), battery (BEV), or fuel cell electric vehicle (FCEV)) to supply electricity to the home in an emergency.

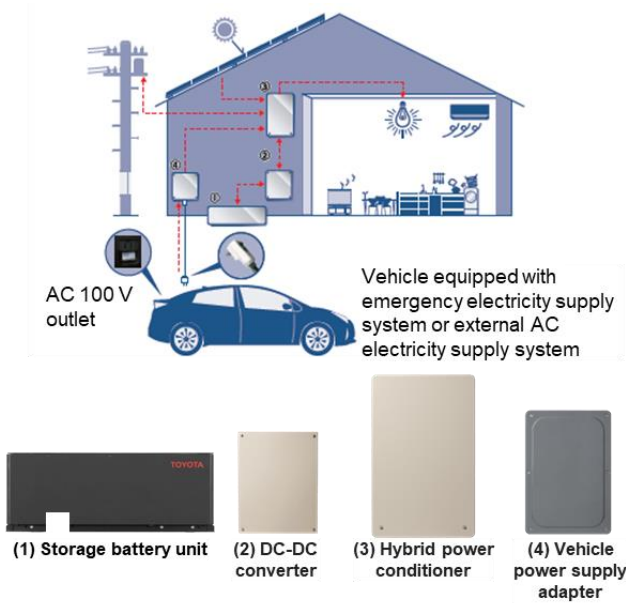


**Fig. 4 Configuration and Outline of the O-Uchi Kyuden System**

**5.2 System specifications**

The maximum power of the system was set to 5.5 kW, which is sufficient for normal daily applications since the contracted current of ordinary homes is 50 A (i.e., a power of 5 kW), 90% of this value (Table 1).

The system is also capable of acting as a whole-home backup by supplying all the necessary electricity for a home via the storage battery in the event of a power outage. The system was designed with sufficient storage battery capacity to run the minimum necessary household appliances, such as a refrigerator and lights, during a power outage for at least one day.

**Table 1 Specifications of the O-Uchi Kyuden System**

| General specifications          |   |
|---------------------------------|---|
| Rated capacity                  | 8.7 kWh   |
| Maximum power                   | 5.5 kW  |
| Operating temperature           | -20 to +45° C<br>* Autonomous operation and vehicle power supply adapter: -20 to +40° C |
| Electricity supply from vehicle | 1.1 kW  |
| Solar power input               | 5.5 kW  |
| Storage battery weight          | 142 kg  |
| Whole-home backup               |   |

**6. System Characteristics**

**6.1 Two charge/discharge cycles per day**

Many ordinary storage batteries are designed to carry out only a single charge/discharge cycle per day. The O-Uchi Kyuden System takes advantage of the

reliability of automotive batteries and Toyota’s control technologies to achieve two cycles per day. As a result, the battery can be charged using the lower cost of electricity supplied at night as well as using solar power, and can be discharged to cover the periods of low power generation early in the morning and during the night. This helps the user save money on electricity bills (when smart mode is selected (Fig. 5)).

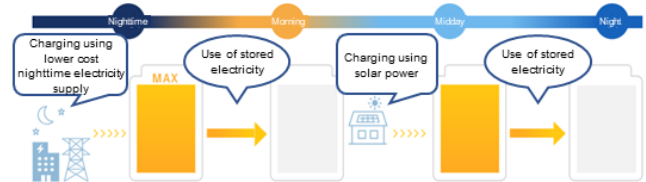


**Fig. 5 Illustration of Two Charge/Discharge Cycles per Day Operation**

**6.2 Electricity supply from electrified vehicles**

Although the storage battery is designed to operate when a power outage occurs, it is possible that the battery charge may not be sufficient to supply power throughout a lengthy outage caused by a large-scale natural disaster or the like.

Therefore, to provide greater peace of mind, the O-Uchi Kyuden System comes with a vehicle power supply adapter as standard equipment. Maximum power of 1.1 kW can be supplied to the whole household by plugging the vehicle connection cable into the 100 V outlet installed on Toyota’s electrified vehicles (HEVs, PHEVs, BEVs, and FCEVs, Fig. 6).

For example, the Prius HEV can supply five days of electricity to the storage battery using its engine and battery, helping to create further peace of mind and safety in an emergency.

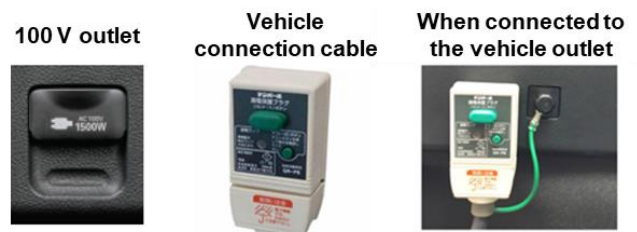


**Fig. 6 Overview of Vehicle Connections of the O-Uchi Kyuden System**

**6.3 Waterproofing**

As this storage battery is meant to be relied upon in a natural disaster, it was designed to be extremely waterproof to protect it from damage or malfunctions

caused by the disaster.

The same sealing rubber structure as used by a vehicle battery pack was adopted to create a fully closed storage battery with a waterproof rating equivalent to IP67.

#### 6.4 Robustness

In the same way as the approach toward waterproofing, the structure was designed to withstand the external forces of a natural disaster.

New in-house standards for home batteries were established assuming impacts from flying debris in typhoons, earthquake vibrations, crushing caused by collapsing structures in an earthquake, snowfalls, and the like. For example, steel plates were added to the sides and front to protect the battery against flying debris in a typhoon (Fig. 7).

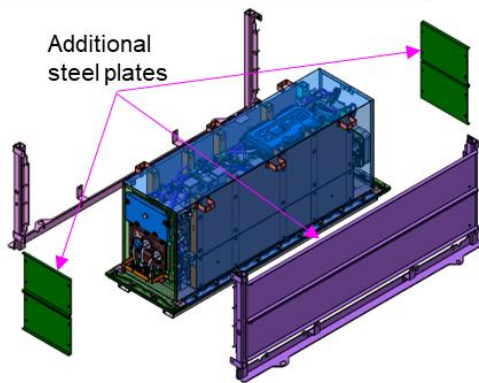


**Fig. 7 Additional Steel Plates to Protect against Flying Typhoon Debris**

#### 6.5 Safety

A home battery has various safety requirements in addition to the requirements applicable to automotive parts. For example, the O-Uchi Kyuden System complies with the following two Japanese Industrial Standards (JIS).

JIS C 4412: Safety requirements for electric energy storage equipment

JIS C 8715: Secondary lithium cells and batteries for use in industrial applications

As a result, the O-Uchi Kyuden System has been certified by the third-party Japan Electrical Safety & Environment Technology Laboratories (JET), which demonstrates to customers that the system can be used safely and with peace of mind.

The development realized various other safety features. For example, the structure is shielded and insulated against heat so that external parts are not affected if parts in the battery pack overheat. This approach also makes use of battery technologies and parts developed for electrified vehicles.

#### 6.6 Smart phone synchronization

In an age where many household appliances can be operated by smart phone, a dedicated app was also developed for the O-Uchi Kyuden System. The system communicates with the power conditioner through the wireless LAN router of the house, allowing the user to confirm the electricity flows and history of power consumption. The app can also be used to select from various operation modes and set a range of parameters (Fig. 8).

One of the development team's key focus points was the app interface design. The team paid particular attention to details, following user feedback and thoroughly benchmarking other companies' products to ensure the interface is easy to understand and intuitive to use.



| Setting            | Characteristics   | Recommended users   |
|--------------------|---|---|
| Normal mode        | Lower consumption of solar power generated by the house<br>Higher amounts of electricity available for sale | Users with FIT contract<br>Use of cheaper electricity at nighttime            |
| Energy-saving mode | Higher consumption of solar power generated by the house<br>Less electricity purchased                      | Users whose FIT contract has ended<br>Metered electricity payment plan        |
| Smart mode         | Charging using nighttime electricity and solar power  | Users whose FIT contract has ended<br>Use of cheaper electricity at nighttime |
| Power storage mode | Keeps battery constantly fully charged<br>Electricity supply in a power outage                              | Users with high electricity demand in a power outage                          |

**Fig. 8 Image of Dedicated App Interface and Operation Modes**

## 7. Conclusion

Toyota developed its first home battery, the O-Uchi Kyuden System using technologies repurposed from automotive applications to help realize a carbon-neutral society and to ensure greater peace of mind and safety in a natural disaster. To repurpose vehicle technologies for use in a home battery, the development focused on the differences between vehicle and home battery development.

Toyota plans to develop the next model with feedback from the market and intends to continue contributing to the achievement of an ever-safer and more secure carbon-neutral society.

## Reference

- (1) K. Sato. "Spotlighting Toyota's New Home Battery Business." *Toyota Times*.  
[https://toyotatimes.jp/en/toyota\\_news/1005.html](https://toyotatimes.jp/en/toyota_news/1005.html)  
(2022).

## Authors



N. Tanaka



K. Kubo



T. Uchiyama



K. Ebata

# Carbon-Neutral Fuels

Oji Kuno\*<sup>1</sup>Takeshi Nobukawa\*<sup>2</sup>Hiroyuki Fukui\*<sup>3</sup>Nozomi Yokoo\*<sup>1</sup>Koichi Nakata\*<sup>1</sup>

## Abstract

To achieve carbon neutrality, it will be essential to pursue a wide range of options following multiple pathways. In addition to promoting hybrid (HEVs), plug-in hybrid (PHEVs), battery (BEVs), and fuel cell electric vehicles (FCEVs), as well as hydrogen engines, Toyota is also working to popularize carbon-neutral fuels while partnering with the energy industry in research and development projects. This article describes Toyota's initiatives related to carbon-neutral fuels for the purpose of reducing the CO<sub>2</sub> emissions of vehicles that are already on the road. It also discusses the types of carbon-neutral fuels, as well as the relevant government policies and trends.

**Keywords:** *e-fuel, synthetic fuel, carbon intensity, biofuel, bioethanol, biodiesel*

## 1. Introduction

Terminology such as “carbon-neutral fuel,” “e-fuel,” and “biofuel” are appearing at an increasing frequency in newspapers, television news programs, and other media. In Japan, wider awareness of the concept of carbon-neutral fuels was probably triggered by a press conference held on April 22, 2021, by Akio Toyoda in his role as Chairman of the Japan Automobile Manufacturers Association, Inc. In this press conference, Chairman Toyoda laid down a policy for carbon neutrality and explained the importance of correctly understanding the essence of what carbon neutrality means. With this understanding, he stated that it should be possible to see a whole new world with significantly lower CO<sub>2</sub> emissions by combining Japan's strengths in high-efficiency engines and electric motor technologies with carbon-neutral fuels.<sup>(1)</sup>

First, it is important to define what is meant by a carbon-neutral (or CO<sub>2</sub>-neutral) fuel. The following definition is taken from a draft document published by the European Commission (EC) at the time that this article was written.

“CO<sub>2</sub>-neutral fuels are defined as fuels, including biofuel, biogas, biomass fuel, renewable liquid and gaseous transport fuel of non-biological origin (RFNBO) or a recycled carbon fuel (RCF), that emit only biogenic CO<sub>2</sub> or recycled CO<sub>2</sub> when burned, resulting in circular CO<sub>2</sub> emissions and a net-zero impact on the climate. This definition is already in line with the REDII, indicating

that all fuels listed in the directive should be considered as CO<sub>2</sub>-neutral fuels.”<sup>(2)</sup>

In summary, a carbon-neutral fuel is a type of synthetic fuel or biofuel called an e-fuel that, when burned, only emits CO<sub>2</sub> derived from biogenic sources or recovered CO<sub>2</sub>, resulting in a net-zero impact on the climate.

This article describes topics related to carbon-neutral fuels, such as government policies, national and regional trends, and impacts on vehicles.

## 2. Types and Effects of Carbon-Neutral Fuels

### 2.1 Synthetic fuel

The definition of synthetic fuel includes hydrogen produced from renewable energy and fuels converted into hydrocarbons through reactions with captured CO<sub>2</sub>. A general term used to describe these fuels is “e-fuel.” Some typical processes are as follows. (1) The production of hydrogen by applying electrolysis to water using electricity generated by renewable energy sources such as solar or wind power generation. (2) The use of CO<sub>2</sub> generated by the combustion or fermentation of biomass, CO<sub>2</sub> directly recycled from the air (a process known as direct air capture (DAC)), or CO<sub>2</sub> derived from industrial activities (such as chemical processes, cement, steelmaking, and so on) to reduce life cycle greenhouse gas (LC-GHG) emissions by 70% or more.<sup>(3)</sup> (3) The synthesis of hydrocarbons from captured CO<sub>2</sub> and hydrocarbons using Fischer-Tropsch (FT) reactions, and the fractional distillation of gasoline.

The main principle of e-fuel is that, even when it is burned in an engine, the only emissions are CO<sub>2</sub> that has been captured from the atmosphere, which means that overall CO<sub>2</sub> emissions do not increase. In addition, since the properties of e-fuel can be arranged in the same way as gasoline, e-fuel can be used in vehicles currently on

\*1 Carbon Neutral Development Div., Carbon Neutral Advanced Engineering Development Center

\*2 Electrification & Environment Material Engineering Div., Advanced R&D and Engineering Company

\*3 Environment Affairs and Engineering Management Div., Carbon Neutral Advanced Engineering Development Center

the road without modification. Consequently, existing refueling infrastructure such oil tanks, gas stations, and the like can also be used as-is. E-fuel represents a simple way to produce, store, and use energy while also suppressing CO<sub>2</sub> emissions (Fig. 1).

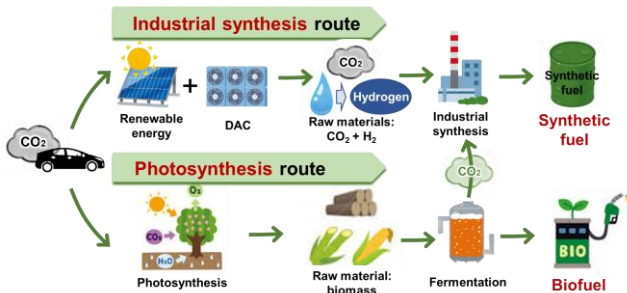


Fig. 1 Lifecycle of Carbon-Neutral Fuels

## 2.2 Biofuel

Biofuel includes ethanol produced from plants, and fuel components synthesized using vegetable or animal fats as a raw material. Biofuel can be produced by the following four main methods (Fig. 2).

- (1) Bioethanol: ethanol produced via fermentation or distillation using sugar cane or corn as the raw material. Many countries and regions blend approximately 10% of bioethanol into gasoline (a type of fuel known as E10). Bioethanol has the effect of increasing the octane number and lowering the particle number (PN) of exhaust gases.
- (2) Bio-derived gasoline: bioethanol is converted industrially to synthesize materials such as gasoline (known as ethanol to gasoline (EtG)), ethyl tertiary-butyl ether (ETBE), or the like.
- (3) Fatty acid methyl ester (FAME): fuel produced from vegetable oil derived from oil palms, rapeseed, or soybeans, or from animal fats. FAME is used by blending into diesel fuel. Diesel containing 30% FAME derived from palm oil is known as B30, and diesel containing 7% FAME derived from soybeans is known as B7.
- (4) Hydrotreated vegetable oil (HVO): fuel produced by the hydrogenation of fatty acid components in palm oil or the like or in waste oil, and used as an alternative to diesel. The use of waste oil as a raw material is attracting attention as a promising way of producing fuel with low CO<sub>2</sub> emissions. Since biofuels use renewable biological resources, these fuels are an effective way of reducing the CO<sub>2</sub> emissions of vehicles. However, these fuels have also been criticized as impacting food sources and resulting in the conversion of forest habitats into farmland. For this reason, measures must be taken to ensure the ongoing sustainability of supply.

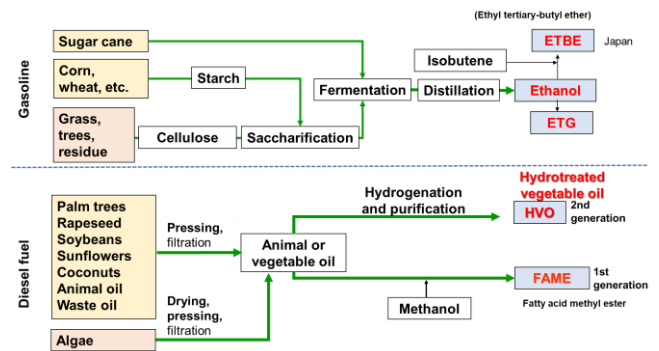


Fig. 2 Production Paths of Biofuels

## 2.3 Carbon intensity (CI)

CI is a value calculated by, for example, dividing the CO<sub>2</sub> emissions produced by the combustion of the fuel or the LC-GHG emissions generated in the production process by the heat released during combustion, using the amount of CO<sub>2</sub> generated per megajoule (g-CO<sub>2</sub>eq/MJ) as the unit. The amount of CO<sub>2</sub> generated by the combustion of biofuels is not counted since it derives from the CO<sub>2</sub> absorbed from the atmosphere by the plant. Therefore, the CI of biofuels is assessed using the CO<sub>2</sub> generated during production and transportation.

In the U.S., CI is defined by the Renewable Fuel Standard of the Federal Environmental Protection Agency (EPA) and the Low Carbon Fuel Standard (LCFS) of the California Air Resources Board (ARB). The LCFS includes official CI values for the products of each biofuel producer.<sup>(4)</sup>

In Japan, the Act on the Promotion of Use of Non-Fossil Energy Sources and Effective Use of Fossil Energy Materials by Energy Suppliers (Sophisticated Methods Act)<sup>(5)</sup> was revised in April 2023 to update the reasoning behind standard values for LC-GHG emissions. Compared to a CI of 88.74 g-CO<sub>2</sub>eq/MJ for volatile oils (gasoline), the GHG emissions of ethanol derived from corn produced in the U.S. is defined as having a CI of 36.86 (ratio to gasoline: -58%) and ethanol derived from sugar cane produced in Brazil as 28.59 (-68%). In this revision, both values decreased by 15%.

The GHG emissions of ethanol derived from corn produced in the U.S. was revised based on discussions with life cycle assessment (LCA) experts and the latest data from GREET 2022 (the Argonne National Laboratory in the U.S.). These revisions covered the emissions produced from fertilization and the use of mechanical energy during raw material cultivation, raw material transportation, energy consumption during ethanol production, ethanol transportation, and so on. Reductions in emissions due to electrification, fertilizer, and chemical substances, as well as improvements in fuel efficiency during international transportation helped lower CO<sub>2</sub> emissions.

## 2.4 Cross-industry projects involving bio and synthetic fuels

In July 2022, six companies (ENEOS Corporation, Suzuki Motor Corporation, Subaru Corporation, Daihatsu Motor Co. Ltd., Toyota Motor Corporation, and Toyota Tsusho Corporation) established the Research Association of Biomass Innovation for Next Generation Automobile Fuels (raBit) to study ways of optimizing the process of producing fuel. This association expanded to seven companies with the participation of Mazda Motor Corporation in March 2023.<sup>(6)(7)</sup>

The association was established to carry out research in the following four areas: (1) efficient ethanol production systems, (2) co-produced oxygen, CO<sub>2</sub> capture, and utilization, (3) efficient operation of overall systems, including fuel utilization, and (4) efficient raw material crop cultivation methods. Through research in these areas, the association is promoting technological research into the use of biomass, as well as the efficient production of bioethanol fuel for vehicles through the optimized circulation of hydrogen, oxygen, and CO<sub>2</sub> during production. Another aim of the association is to capture the CO<sub>2</sub> generated during ethanol fermentation for use as a source of green CO<sub>2</sub> in the production of synthetic fuels (**Fig. 3**).

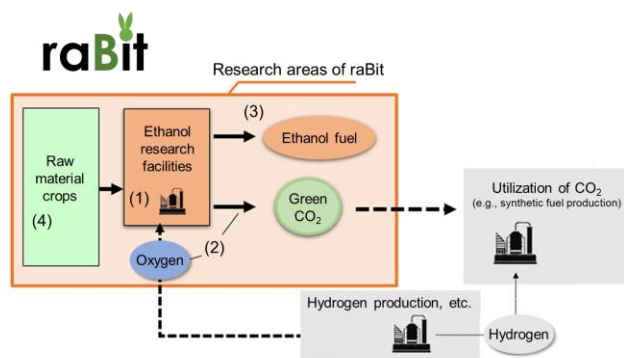


**Fig. 3 Research Areas of raBit**

In the cultivation of raw material crops, the association is focused on plants that will not create competition for foodstuffs. In 2022, various species of sorghum were grown in tests in Fukushima. **Fig. 4** shows a photograph taken on August 1, around three months after sowing on May 15. One species had grown to a height exceeding 4 meters. By October, it had exceeded 5 meters. The association plans to modify the crop species and cultivation methods to help realize more efficient ways of increasing biomass production.



**Fig. 4 Sorghum Cultivation in Fukushima**

## 3. Synthetic Fuels

### 3.1 Government policies

The communique issued by the G7 after the meeting held in Hiroshima in May 2023 included a commitment “to promote...sustainable carbon-neutral fuels including sustainable bio- and synthetic fuels” in addition to expanding the introduction of zero emission vehicles (ZEVs) as ways of achieving net-zero emissions in the road sector by 2050. This recognizes the potential role of synthetic fuels in the decarbonization of vehicles already on the road.

#### 3.1.1 Japan

In Japan, the Ministry of Economy, Trade and Industry (METI) hosted the Public-Private Council for Promoting the Introduction of Synthetic Fuels (e-Fuel) in May 2023. This council presented proposals for revising the existing e-fuel introduction roadmap. These proposals brought forward the target date for the commercialization of e-fuel from 2040 to the first half of the 2030s. To realize this objective, the proposals contained a timeline under which feasibility studies will be conducted using a bench-scale plant in 2025 and a pilot plant in 2028, with the aim of producing 10,000 barrels of fuel a day starting in 2035.

To encourage the practical adoption of e-fuel, ENEOS held a driving demonstration in May 2023. At the accompanying press conference, ENEOS declared the objective of starting the supply of low-carbon gasoline from around 2027, with the hope that this timeline might brought forward. As a result, there are promising signs for the introduction of e-fuel in Japan.<sup>(8)</sup>

#### 3.1.2 Europe

The European Union (EU) has stated a target of having advanced biofuels account for 5.5% of energy supplies in the transportation sector in 2030, of which at least 1% should be renewable fuels of non-biological origin (RFBNO). In addition to e-fuel, RFBNO also includes green hydrogen, ammonia, e-methane, and the like. Furthermore, due to German opposition, discussions about the limitation of new vehicle sales to ZEVs alone

from 2035 resulted in an exemption for internal combustion engine (ICE) vehicles that run on e-fuel alone. Remaining issues to be resolved include how to supply only e-fuel to specific vehicles and whether sufficient supplies of e-fuel can be secured.

### 3.1.3 U.S.

In the U.S. despite the lack of government policies covering the introduction of synthetic fuels, projects have been started to encourage wider use of hydrogen, which acts as a material for synthetic fuels.

In partnership with the major U.S. energy companies ExxonMobil and Chevron Corporation, Toyota has carried out driving demonstrations using low-carbon gasoline capable of reducing lifecycle CO<sub>2</sub> emissions by 75% and 40%, respectively (Fig. 5).<sup>(9)</sup> Through these demonstrations, the exhaust gases and driving performance of vehicles fueled by low-carbon gasoline supplied by these two companies were evaluated and confirmed to be the same as ordinary gasoline-fueled vehicles.



Fig. 5 Driving Demonstration Carried Out by Chevron and Toyota

## 3.2 Production methods

As described above, synthetic fuels are produced from hydrogen and CO<sub>2</sub> derived from renewable energy sources. Synthetic fuel production methods are compatible with existing processes developed to produce fuel from natural gas or coal. As a result, research, development, and demonstration tests using the FT process and the process for conversion into gasoline via methanol (methanol to gasoline (MTG)), which already have a proven record of commercial applications, are making progress. The FT process is capable of synthesizing hydrocarbon fuels with a wide range of molecular numbers. In addition to gasoline, it can be used to produce aviation, marine, and heavy-duty vehicle (diesel) fuels at the same time. In contrast, although the main product of MTG is gasoline, its intermediate product of methanol can be used as a raw material for chemicals.

### 3.2.1 FT synthesis

The FT process uses a synthesis gas (a blend of hydrogen and CO) as a raw material. It involves reactions capable of synthesizing a wide range of hydrocarbons from light olefins to heavy waxes. Hydrocarbons produced by this process have a carbon distribution known as the Schulz-Flory distribution, which changes in accordance with the chain growth probability. This synthesis gas can also be produced from coal, natural gas, and biomass. In particular, FT processes using coal and natural gas as raw materials have already been commercialized on a large scale.<sup>(10)</sup> In Japan, the Nippon GTL Technology Research Association carried out a project between 2006 and 2012 to develop GTL technology for the purpose of utilizing small-scale natural gas fields.

Since the main components in FT synthetic fuels are paraffin, olefins, and alcohol, hydrogenation and isomerization processes must be carried out to upgrade the fuel before use as gasoline or diesel. However, these processes can be carried out using existing petroleum refining facilities, and the resulting products are identical to gasoline or diesel derived from crude oil. It will be important to realize a number of technological breakthroughs to help popularize synthetic fuels, such as microreactors to ensure the more efficient use of renewable energy, co-electrolysis technologies capable of generating the synthesis gas directly from water and CO<sub>2</sub>, and the development of catalysts to enable direct FT synthesis from hydrogen and CO<sub>2</sub> without passing through the synthesis gas stage.

### 3.2.2 MTG

The MTG process involves the dehydration and concentration of methanol into dimethyl ester (DME) followed by reactions to generate aromatic hydrocarbons (aromatics) or paraffin via C<sub>2</sub> to C<sub>4</sub> olefins.<sup>(11)</sup> The main hydrocarbons generated by this process are gasoline products. In the same way as FT synthesis, MTG has already been commercialized as a process using coal or natural gas as raw materials. ExxonMobil carried out commercial production using the MTG process in New Zealand for ten years between 1985 and 1995. Currently, in China, the Jincheng Anthracite Mining Group (JAMG) is producing 15,000 barrels per day (BPD) of fuel via the MTG process.<sup>(12)</sup>

Gasoline obtained by the MTG process has a high aromatic and olefin content, and has the same octane number as modern regular-grade gasoline. Therefore, it can be used without carrying out any upgrades.

### 3.2.3 Cost

Since the production of synthetic fuels requires large amounts of green hydrogen, its price is strongly affected by the price of renewable energy. According to provisional calculations by METI, that price ranges

between 300 and 700 yen/liter, a value that is likely to be refined through future demonstration and study projects.<sup>(13)</sup>

### 3.2.4 Representative projects

The first project to demonstrate the potential of synthetic fuel was the “Audi e-gas” project. Audi carried out research to demonstrate the feasibility of e-fuel in the market, starting with compressed natural gas (CNG) produced using hydrogen synthesized using wind or solar power generation and CO<sub>2</sub> captured from biogas plants or agricultural residue in 2013, before moving onto diesel in 2017.<sup>(14)</sup> More recently, Porsche has started demonstration tests involving the synthesis of gasoline in Chile, a country with extensive renewable energy resources.

In Japan, a project by ENEOS to develop a production process for synthetic fuels using CO<sub>2</sub> was selected by the National Research and Development Agency New Energy and Industrial Technology Development Organization (NEDO) for the Green Innovation Fund.<sup>(15)</sup>

### 3.3 Vehicle and engine adaptation

As described above, FT and MTG technologies to produce synthetic fuels have already been commercialized, and gasoline and diesel derived from these processes are also already on the market. Since the properties and quality of these fuels comply with fuel standards across the world, no special adaptation process is required for vehicles or engines.

As an example, an evaluation was carried out using different engines and vehicles to examine the use of low-carbon gasoline produced from various renewable fuels. The results found that these fuels had no major impact on engine combustion or vehicle emissions, and confirmed the potential capability of these fuels to help reduce CO<sub>2</sub> emissions in the future, including emissions from vehicles already on the road.<sup>(16)</sup>

In the field of synthetic fuel research and development, studies have also been conducted into designing fuels with even lower emissions, such as the synthesis of fuels using fewer types of hydrocarbons than crude oil, and the use of fuels that contain no sulfur or similar components.<sup>(17)</sup>

## 4. Biofuels

### 4.1 Ethanol

#### 4.1.1 Vehicle and engine adaptation

Bioethanol is used as a blending agent at certain ratios with gasoline. Current gasoline standards in many countries limit this ratio to a maximum of 10%. However, measures to increase the concentration of ethanol are being increasingly adopted to lower dependence on fossil fuels. For this reason, technological advances are

required to improve raw material crop cultivation, increase the efficiency of ethanol production, and reduce the production costs of cellulosic ethanol.

There are three key points that must be considered when adapting vehicles and engines for use with ethanol blends: (1) material compatibility, (2) compliance with exhaust standards, and (3) factors affecting driveability such as noise and vibration (NV). For point (1), the compatibility of materials and surface treatments used for fuel system parts in direct contact with the fuel, such as delivery pipes, fuel hoses, injectors, and the like, must be verified. Fig. 6 shows the swelling properties of rubber materials. With ethanol blends of between 20 and 30%, rubber materials undergo drastic changes in volume, which makes it necessary to select the appropriate materials for the application. In addition, around an ethanol blend of 20% (E20), oxidation stability decreases and care must be taken about metallic part corrosion.

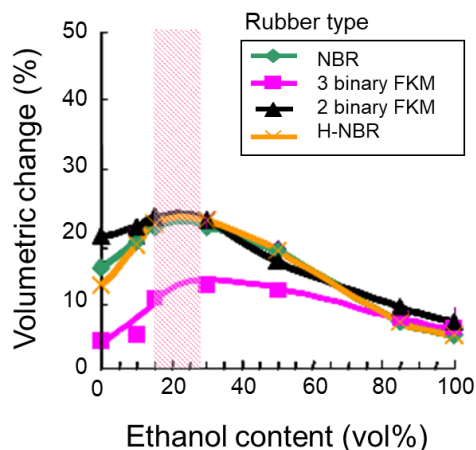
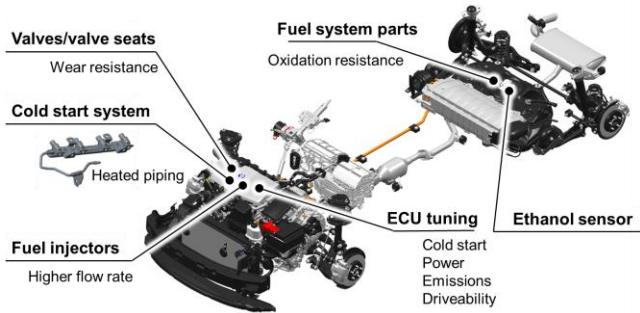


Fig. 6 Rubber Swelling Properties

Since ethanol has a high octane number, it helps to improve fuel economy by raising the octane number of gasoline. Consequently, ethanol can help to lower CO<sub>2</sub> emissions. At the same time, since ethanol is a compound that contains oxygen atoms, it also suppresses the PN of hydrocarbons and carbon monoxide.

In countries with a high degree of self-sufficiency in ethanol, domestically produced ethanol is used to reduce imports of crude oil and lower GHG emissions. In these countries, high ethanol blends such as E85 and E100 are sold alongside flexible fuel vehicles (FFVs) capable of using this type of fuel. Since FFVs run on ethanol, which is less volatile than normal gasoline, measures are taken such as installing a heater to vaporize the ethanol. Other measures include the adoption of surface treatments to reduce the corrosion of metallic parts (Fig. 7).



**Fig. 7 Main Changes in FFVs**

**4.1.2 U.S.**

Global ethanol production stands at approximately 100 million kL, around half of which (57 million kL) is produced in the U.S. Following the energy policies laid down in the 2005 Renewable Fuel Standard in Energy Policy Act, ethanol production rose from 14.2 million kL in 2004 to 51.4 million kL in 2010, a 300% increase in only five years. Since then, although production continued to increase gradually, it peaked at 62.4 million kL in 2018 before falling back to around 60 million kL.

E10 fuel has been sold in all 50 states since 2010 and, in reaction to recent high gasoline prices, the sale of E15 fuel in the summer months was approved to start in 2022. In the U.S., the number of registered E85 FFV models peaked at 90 in 2014, but declined to 40 models in 2019 and 17 models in 2022. Toyota introduced E85 FFV versions of the Tundra and Sequoia, but discontinued sales of FFVs in North America in 2019.

**4.1.3 Brazil**

In Brazil, the government has encouraged increases in ethanol production using sugar cane as a raw material. Brazil is the world’s second largest bioethanol producing and consuming nation after the U.S. In 2009, the Sugarcane Agroecological Zoning (SAZ) policy defined areas most suitable for sugar cane cultivation, while placing environmental protections on the Amazon area and the region near Paraguay. In addition, the RenovaBio policy plans to almost double ethanol production from 26.2 million kL in 2021 to 50 million kL in 2030. Using its abundant ethanol resources, Brazil encourages the sale of FFVs capable of running on both ethanol and gasoline. Currently, E100-compatible vehicles make up part of the standard lineup of all automakers in Brazil. Toyota has also looked to reduce well-to-wheel (WtW) CO<sub>2</sub> emissions using ethanol. The Corolla HEV-FFV that was launched in 2019 realizes approximately 80% lower CO<sub>2</sub> emissions than an E0 ICE gasoline vehicle (**Fig. 8**).

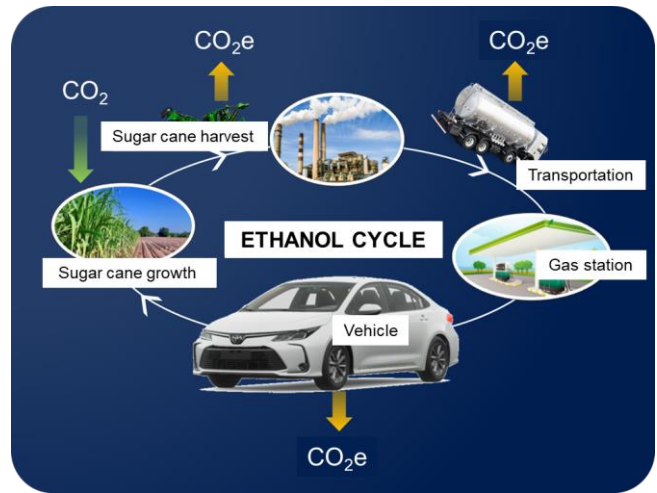


**Fig. 8 Initiative to Reduce WtW CO<sub>2</sub> Emissions**

**4.1.4 Europe**

Europe is the world’s fourth largest bioethanol producing and consuming region after the U.S., Brazil, and China. The Renewable Energy Directive (RED II), which was revised in 2020, mandates the use of renewable fuels and calls for renewable energy to make up 14% of fuel consumption by 2030. In the region as a whole, ethanol production is particularly strong in France. E85 fuel is sold at half the price of gasoline, which is driving demand for FFVs. The ePURE consortium accounts for approximately 85% of ethanol production in Europe. In terms of CI, a wide range of CO<sub>2</sub> reduction measures managed to achieve an average 78.4% decrease in GHG emissions compared with fossil fuels in 2022 (**Fig. 9**).<sup>(18)</sup>

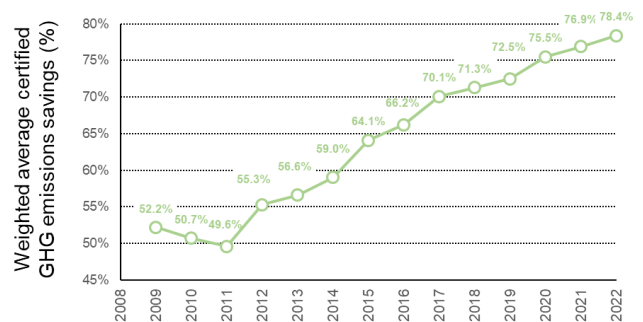


**Fig. 9 GHG Reduction Trend of Ethanol**

**4.1.5 Thailand**

Thailand is actively introducing ethanol and biodiesel fuels with the aim of halting a rise in crude oil imports. Virtually all biofuels produced locally from sugar cane, cassava, and palm oil are consumed domestically. An extremely high number of fuel types are on sale since the rates of biofuel blends change in accordance with the price of crude oil. Thailand was the first Asian country to introduce E85 FFVs, which became more popular under

a preferential tax scheme. However, as the price of bioethanol has increased and the burden of subsidies has broadened, the merits of E85 for users have started to evaporate. In response, the government has decided to scrap E85 and switch to E20 as the main type of fuel.

#### 4.1.6 India

In June 2021, Prime Minister Modi announced the Roadmap for Ethanol Blending in India 2020-25<sup>(19)</sup> to help ensure energy security while realizing a low-carbon society. India introduced E5 fuel to the market in 2003, and E5 to E10 blends have become widely available throughout the country, depending on the region. The average gasoline/ethanol blend concentration has increased from 1.53% in 2014 to 8.5% in 2021 (approximately 7 million kL). E20 was introduced in April 2023 with the aim of enabling the supply of E20 in all regions from 2025. This anticipates an approximate doubling of production from 2021 to 13.5 million kL. Although sugar cane and corn are expected to account for half of the necessary raw materials, twelve cellulosic ethanol plant projects are also under way with government support. These policies are expected to have the ancillary benefits of increasing new employment opportunities, raising the income of agricultural communities, expanding the utilization of unused biomass (thereby helping to prevent air pollution caused by the open burning of fields), and the like.

In response to the possibility of the introduction of higher ethanol blends and concerns about the effects on infrastructure, such as the tanks used at gas stations, the automotive industry is accelerating the development and introduction of FFVs compatible with blends from E20 to E100. As part of this trend, Toyota has launched the Flexi Fuel Strong Hybrid Electric Vehicles (FFV-SHEV) pilot project (Fig. 10).<sup>(20)</sup>



Fig. 10 FFV-SHEV Pilot Project in India

#### 4.1.7 Indonesia

Indonesia is the world's leading producer of palm oil, which it both exports and uses as domestic biodiesel. The government had aimed to introduce an E10 bioethanol

blend, but this policy was abandoned due to the price of ethanol and concerns about supply volumes. However, in response to the government's carbon-neutral strategy,<sup>(21)</sup> the Ministry of Energy and Mineral Resources announced the Strategic Roadmap for Accelerating Bioethanol Implementation in Indonesia in 2022. As part of this roadmap, demonstration tests of E5 fuel are scheduled to take place in some regions of the country.

#### 4.1.8 Japan

In Japan, bioethanol blends of up to 3% are permitted to be used as normal gasoline. Bioethanol was introduced into Japan on a trial basis in 2007. In 2020, approximately 500,000 kL (crude oil conversion) of bioethanol was imported for fuel. Of this, roughly 90% was converted into ETBE before use. Since ETBE is less susceptible to water absorption, it does not affect the quality of the gasoline. However, since it uses isobutene derived from fossil fuels in the production process, its CO<sub>2</sub> reduction effect is limited. Since direct blending up to E10 is permitted, it is likely that the use of bioethanol will expand in the future. In April 2023, the Sophisticated Methods Act entered its third public comment phase. This act maintains the annual 500,000 kL (crude oil conversion) target for bioethanol introduction over five years from 2023 while revising the criteria for GHG emissions, and lays down a policy about studying how to build an environment for expanding the use of bioethanol.

### 4.2 Biodiesel and renewable diesel

#### 4.2.1 Vehicle and engine adaptation

In general terms, when FAME is blended at defined ratios into biodiesel, the soot, hydrocarbons, and CO emitted from the engine tend to decrease compared with conventional diesel. However, the effects of the oxygen content in the fuel results in higher NO<sub>x</sub>, which requires tuning to comply with emissions standards or the addition of treatment devices. Currently, Indonesia permits the highest blend of biodiesel in the world (B35). HVO fuel that has undergone hydrogenation is also known as renewable diesel. The hydrogenation treatment removes the oxygen and results in clean combustion, which means that 100% blends can be used.

#### 4.2.2 FAME

FAME can be categorized into three types depending on the raw material: FAME derived from palm oil that is produced in large quantities in Indonesia and Malaysia, FAME derived from soybean oil that is produced in large quantities in Brazil and other South American countries, and FAME derived from rapeseed oil (oil compressed from seeds of the mustard family) that is produced in Europe. Foodstuffs account for at least 90% of the production of all of these materials. The area of cultivation used for fuels is only 8%. In addition, the World Wildlife Fund (WWF) is leading efforts to create

certification systems through the Roundtable on Sustainable Palm Oil (RSPO) and the like.

Since FAME contains components with carbon double bonds, FAME-blended diesel is generally susceptible to oxidation. It also contains heavy components that are less likely to vaporize, which makes the fuel more susceptible to solidification at low temperatures. In addition, oxidized fuel generates organic acids and sludge that affect fuel system part materials and induce clogging of fuel filters. For these reasons, the properties of blended biodiesels are controlled to comply with the standards for the fuel in question.

#### 4.2.3 Renewable diesel

Also known as HVO, renewable diesel is a type of hydrocarbon fuel produced by hydrogenating raw material oils such as palm oil, waste oil, and the like. Renewable diesel is attracting attention as a fuel with low GHG emissions (carbon intensity: 0.1 to 0.2), particularly when waste oil is used as the raw material. Similar to diesel derived from fossil fuels, renewable diesel consists of saturated hydrocarbons, and higher concentration blends can be used compared to FAME. However, due to issues such as poor fluidity at low temperatures and lower swelling of rubber parts, blended renewable diesels tend to be used at concentrations within a range that satisfies diesel standards. In Europe, a product called R33 Blue Diesel, which contains 26% HVO and 7% FAME blended into diesel, is on sale. This fuel can reduce CO<sub>2</sub> emissions by approximately 20% while being used in the same way as conventional diesel. In Japan, Itochu Enex Co., Ltd. has developed a biodiesel containing HVO as a renewable diesel, and is conducting demonstration tests around the country using existing vehicles.<sup>(22)</sup> Northern European countries have adopted 100% HVO with improved low-temperature fluidity. Toyota began offering models compatible with this fuel in 2023 (Fig. 11).<sup>(23)</sup>

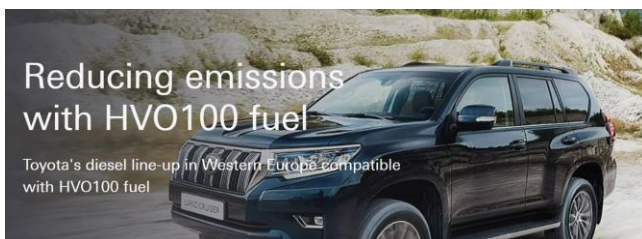


Fig. 11 HVO100-Compliant Model in Europe

## 5. Conclusion

To realize carbon-neutral mobility, it will not be enough to simply promote the adoption of BEVs or a hydrogen energy-based society. These efforts will require the participation of everyone who uses mobility, which means adopting measures for countries and

regions with insufficient supplies of renewable energy, as well as measures for vehicles currently on the road and older ICE vehicles. Carbon-neutral fuels are a valuable source of energy that can use existing infrastructure and social systems, and can be produced, transported, stored, and used easily while minimizing GHG emissions. The wider popularization of these fuels can play an important role in achieving carbon neutrality.

## References

- (1) Press Conference of the Japan Automobile Manufacturers Association.  
<https://www.jama.or.jp/english/news/press-conference/2021/195/>
- (2) European Committee on the Environment, Public Health and Food Safety.  
[https://www.europarl.europa.eu/doceo/document/ENVI-PR-746876\\_EN.pdf](https://www.europarl.europa.eu/doceo/document/ENVI-PR-746876_EN.pdf) (page 36).
- (3) *EUR-Lex - C(2023)1086 - EN - EUR-Lex*.  
Official Website of the European Union.
- (4) *LCFS Pathway Certified Carbon Intensities*.  
CARB.  
<https://ww2.arb.ca.gov/resources/documents/lcfs-pathway-certified-carbon-intensities>
- (5) Homepage of the Ministry of Economy, Trade and Industry (in Japanese).  
[https://www.meti.go.jp/shingikai/energy\\_environment/bio\\_nenryo/pdf/010\\_02\\_00.pdf](https://www.meti.go.jp/shingikai/energy_environment/bio_nenryo/pdf/010_02_00.pdf)
- (6) Toyota Global Newsroom.  
[https://global.toyota/en/newsroom/corporate/37543537.html?\\_ga=2.224282642.860679310.1694651693-1629418075.1694050070&\\_gl=1\\*r2o3hl\\*\\_ga\\*MTYyOTQxODA3NS4xNjk0MDUwMDcw\\*\\_ga\\_FW87SM9FNZ\\*MTY5NDY1MTY5Mi4yLjAuMTY5NDY1MTY5Mi42MC4wLjA](https://global.toyota/en/newsroom/corporate/37543537.html?_ga=2.224282642.860679310.1694651693-1629418075.1694050070&_gl=1*r2o3hl*_ga*MTYyOTQxODA3NS4xNjk0MDUwMDcw*_ga_FW87SM9FNZ*MTY5NDY1MTY5Mi4yLjAuMTY5NDY1MTY5Mi42MC4wLjA).
- (7) Toyota Global Newsroom.  
[https://global.toyota/en/newsroom/corporate/38999570.html?\\_gl=1\\*utwby0\\*\\_ga\\*MTYyOTQxODA3NS4xNjk0MDUwMDcw\\*\\_ga\\_FW87SM9FNZ\\*MTY5NDY1MTY5NDY3NzY4Ny4yLjAuMTY5NDY1MTY5NDY3NzY4Ny42MC4wLjA.&\\_ga=2.221847697.860679310.1694651693-1629418075.1694050070](https://global.toyota/en/newsroom/corporate/38999570.html?_gl=1*utwby0*_ga*MTYyOTQxODA3NS4xNjk0MDUwMDcw*_ga_FW87SM9FNZ*MTY5NDY1MTY5NDY3NzY4Ny4yLjAuMTY5NDY1MTY5NDY3NzY4Ny42MC4wLjA.&_ga=2.221847697.860679310.1694651693-1629418075.1694050070)
- (8) ENEOS Corporation News Release.  
[https://www.eneos.co.jp/english/newsrelease/2023/pdf/20230529\\_01.pdf](https://www.eneos.co.jp/english/newsrelease/2023/pdf/20230529_01.pdf)
- (9) Chevron Corporation Newsroom.  
<https://www.chevron.com/newsroom/2023/q2/renewable-gasoline-blend-hits-the-road>
- (10) Y. Onishi et al. "Transition and the Future of the GTL Technology Development." *Nippon Steel Engineering Co., Ltd. Technical Review* Vol. 1 (2010).

- (11) *Synthetic Fuels (Methanol to Gasoline)*. ExxonMobil.  
<https://www.exxonmobilchemical.com/en/catalysts-and-technology-licensing/synthetic-fuels> (accessed July 4, 2023).
- (12) A. Sanz-Martínez et al. “Methanol to Gasoline (MTG): Parametric Study and Validation of the Process in a Two-Zone Fluidized Bed Reactor (TZFBR).” *Journal of Industrial and Engineering Chemistry* Vol. 113 (2022) pp. 189-195.
- (13) Interim Summary of the Synthetic Fuel Research Council of the Ministry of Economy, Trade and Industry (in Japanese).  
[https://www.meti.go.jp/shingikai/energy\\_environment/gosei\\_nenryo/20210422\\_report.html](https://www.meti.go.jp/shingikai/energy_environment/gosei_nenryo/20210422_report.html) (accessed July 13, 2023).
- (14) *Audi e-gas*. Audi AG.  
[https://www.audi-technology-portal.de/en/mobility-for-the-future/audi-future-lab-mobility\\_en/audi-future-energies\\_en/audi-e-gas\\_en](https://www.audi-technology-portal.de/en/mobility-for-the-future/audi-future-lab-mobility_en/audi-future-energies_en/audi-e-gas_en) (accessed July 4, 2023).
- (15) ENEOS Corporation News Release.  
[https://www.eneos.co.jp/english/newsrelease/2022/pdf/20220419\\_01.pdf](https://www.eneos.co.jp/english/newsrelease/2022/pdf/20220419_01.pdf)
- (16) T. Yates, et al. “Evaluation of Fully Sustainable Low Carbon Gasoline Fuels Meeting Japanese E10 Regular and Premium Octane Specifications.” *JSAE/SAE Powertrains, Energy and Lubricants International Meeting* No. 20239175 (2023).
- (17) A.C. Kulzer, et al. “Sustainable Mobility Using Fuels with Pathways to Low Emissions.” *SAE Paper* No. 2020-01-0345 (2020).
- (18) ePURE asbl. Press Release.  
<https://www.epure.org/press-release/eu-renewable-ethanol-hits-new-record-level-for-greenhouse-gas-reduction-as-industry-drives-toward-carbon-neutrality/>
- (19) *Roadmap for Ethanol Blending in India 2020-25*. NITI Aayog, Ministry of Petroleum and Natural Gas (2021).
- (20) Toyota Kirloskar Motor Press Release.  
<https://www.toyotabharat.com/news/2022/launch-of-toyotas-first-of-its-kind-pilot-project-on-flexi-fuel-strong-hybrid-electric-vehicles-ffv-shev-in-india.html>
- (21) *Long-Term Strategy for Low Carbon and Climate Resilience 2050*. Government of Indonesia (2021).
- (22) Homepage of Itochu Enex Co., Ltd.  
<https://www.itcenex.com/en/index.html>
- (23) Toyota Europe Newsroom.  
<https://newsroom.toyota.eu/toyotas-diesel-line-up-in-western-europe-to-be-made-compatible-with-hvo100-diesel-fuel/>

## Authors



O. Kuno



T. Nobukawa



H. Fukui



N. Yokoo



K. Nakata

# Improvement of Mixture Formation in Hydrogen DI Engine Using Fuel Jet MBD

Jun Miyagawa\*<sup>1</sup>Yoshinori Miyamoto\*<sup>1</sup>Shiro Tanno\*<sup>1</sup>Yoshihisa Tsukamoto\*<sup>1</sup>Tetsuo Omura\*<sup>1</sup>Daishi Takahashi\*<sup>1</sup>Koichi Nakata\*<sup>1</sup>

## Abstract

This research compared fuel jet forms predicted by numerical calculation with Schlieren images, and verified that the jet angle and jet tip penetration of results obtained using computational fluid dynamics (CFD) matched values obtained by actual measurement. This jet prediction method was then used to investigate whether tumble or swirl is more suitable for a hydrogen direct injection (DI) engine. The results indicated that tumble is more effective than swirl in reducing the inhomogeneity of the mixture. This is because tumble flow, which is intensified by the hydrogen jet, decays during piston compression, creating turbulence that maximizes turbulent diffusion. Consequently, it was learned that tumble flow is suitable for application in a low-pressure DI (LPDI) hydrogen engine.

**Keywords:** carbon neutrality, hydrogen DI engine, mixture formation, gas jet, MBD, CFD, tumble, turbulent diffusion, NOx

## 1. Introduction

Vehicle powertrains are becoming more and more diverse as the concept of carbon neutrality drives increasing research into renewable energy. In addition to electrification and fuel cells, biofuels, synthetic fuels, and hydrogen are attracting attention as potential uses of mature internal combustion engine (ICE) technologies. As part of this background, extensive research is being conducted into hydrogen engines for heavy-duty commercial vehicles and agricultural machinery, particularly in Europe.<sup>(1)(2)(3)</sup>

Due to its fast laminar burning velocity and wide flammable range, hydrogen in an ICE has the potential to achieve both high efficiency due to lean combustion and low NOx. In contrast, it is known that high load operation is difficult to achieve in port fuel injection (PFI) hydrogen engines due to abnormal combustion phenomena such as backfire and pre-ignition. Although compression stroke injection by in-cylinder direct injection (DI) is an effective means of suppressing these phenomena,<sup>(4)(5)</sup> the short mixing time tends to result in inhomogeneous mixtures, making the reduction of NOx an issue. This research studied a model-based development (MBD) technique for simulating a fuel gas jet and examined guidelines for achieving homogeneous mixture formation.

## 2. Construction of Gas Jet MBD Model

Three-dimensional computational fluid dynamics (3D CFD) is widely used in gasoline DI engine development. Ordinarily, when calculating mixture formation, 3D CFD is used to verify the reproduction of the external shape of the spray in terms of parameters such as the spray penetration and spray angle in static fields. These results are then applied to engine calculations. Although the target of the analysis changed from a liquid-fuel spray to a gaseous-fuel jet, it was decided to adopt the same verification process. This section describes the tests carried out to visualize the external shape of the gas jet and how the accuracy of the gas jet MBD model was improved based on these visualization tests.

### 2.1 Gas jet visualization

Several methods are available for visualizing gas flow. The Schlieren method was adopted since it can clearly identify the boundaries of a jet and because it is capable of making high-speed continuous images. **Fig. 1** shows the testing equipment. Gas is injected in the area of a parallel light flux created by convex lenses. Changes in the refraction index caused by variations in density are converted into a light-to-dark ratio, and observed. By cutting the primary luminous flux with a knife edge, it is possible to identify minute density variations with a high sensitivity.

\*<sup>1</sup> Carbon Neutral Development Div., Carbon Neutral Advanced Engineering Development Center

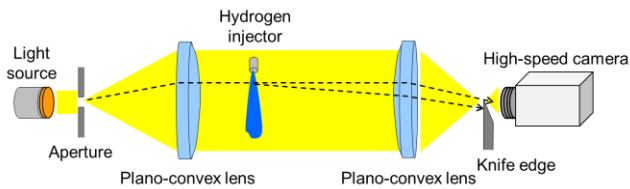


**Fig. 1 High-Speed Schlieren Jet Imaging Equipment**

**Table 1** lists the physical properties of hydrogen, helium, and nitrogen. When a compressible fluid is injected at high pressure, choked flow occurs that reaches the speed of sound at the injector throat. Since hydrogen and helium have a low molecular weight, the speed of sound of those gases is significantly higher than that of nitrogen. This may result in unique behavior. This research used helium instead of hydrogen as the combustible gas since helium is easier to handle and has similar physical properties.

**Table 1 Physical Properties of Gases**

| Gas   | Hydrogen (H <sub>2</sub> ) | Helium (He) | Nitrogen (N <sub>2</sub> ) |
|---|----------------------------|-------------|----------------------------|
| Molecular weight (g/mol)                          | 2.016                      | 4.003       | 28.01                      |
| Fuel density (0.1 MPa, 25°C) (kg/m <sup>3</sup> ) | 0.08994                    | 0.1785      | 1.251                      |
| Speed of sound (25°C, 12.5 MPa) (m/s)             | 1,426                      | 1,073       | 374                        |
| Viscosity (0.1 MPa, 20°C) (mPa-s)                 | 0.0088                     | 0.0196      | 0.0176                     |
| Specific heat ratio (0.1 MPa, 25°C) (-)           | 1.41                       | 1.66        | 1.4                        |

The measurement was carried out in a normal temperature atmospheric field. The injection pressure was between 11.5 and 13.5 MPa, the energizing time of the injector was 3 ms, and the frame rate of the camera was 39,000 frames per second. A straight single-holed nozzle injector was used.

**Fig. 2** shows three typical images taken from the start of injection at an injection pressure of 13.5 MPa. The angle of expansion of the helium gas jet in the vicinity of the nozzle hole was 21.6 degrees. The helium gas jet tip penetration calculated by processing the resulting visualization images is discussed in the next section.

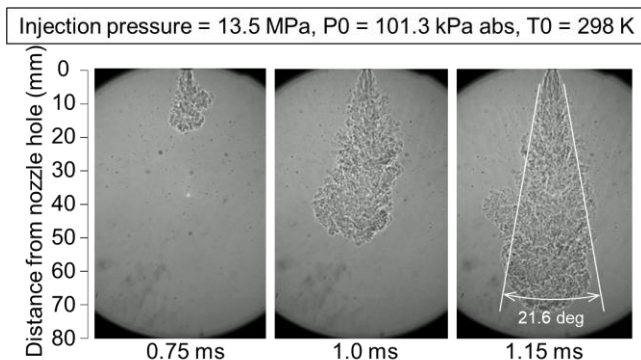


**Fig. 2 Schlieren Images of Helium Gas Jet**

## 2.2 Verification of gas jet MBD model

The CFD calculations used the CONVERGE software manufactured by Convergent Science (CSI). Turbulence was modeled using the RNG k- $\epsilon$  model in the Reynolds Averaged Numerical Simulations (RANS). The temperature, pressure, and gas composition of the atmosphere were set to the same conditions as the visualization test. As well as considering the nozzle hole shape, the measured injection rate was applied as a boundary condition.

**Fig. 3** compares the external shape of the jet. The expansion angle at the base of the jet was 20 degrees, which was closely consistent with the visualization results. **Fig. 4** compares the measured and calculated jet tip penetration. The gradients of the jet tip penetration in an injection pressure range between 11.5 and 13.5 MPa were almost identical at all injection pressures, and it was confirmed that the calculations were also consistent with these trends.

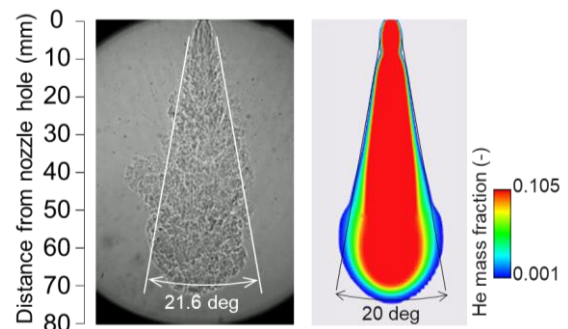


**Fig. 3 Comparison of Measured and Calculated (CFD) Jet Shapes**

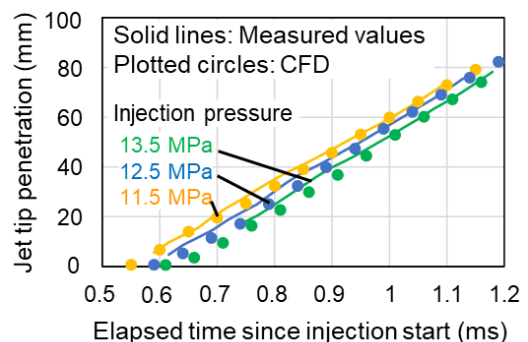


**Fig. 4 Jet Tip Penetration at Different Injection Pressures**

This method was then used to compare differences in behavior between a liquid spray and a gas jet. The liquid spray injection pressure was set to 30 MPa and the injection rate was aligned with that of the gas jet. The upper half of **Fig. 5** shows the oxygen concentration distribution. Higher oxygen concentrations are shown in blue and lower oxygen concentrations are shown in red. The gas jet has a larger internal red area (i.e., a larger

region with a low oxygen concentration) than the liquid spray, which is consistent with reports that gaseous fuels are more difficult to mix. However, this result is also inconsistent with research that reported a large quantity of entrained air in a gas jet.<sup>(6)</sup>

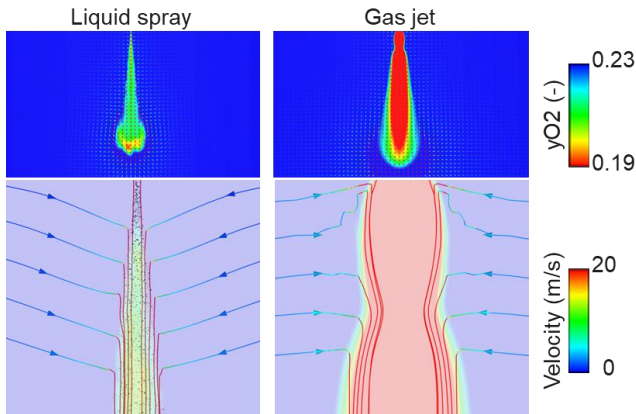


**Fig. 5 Air Entrainment Behavior of Liquid Spray and Gas Jet**

With a liquid spray, it has been reported that entrainment from the spray base is important for inducing air into the spray.<sup>(7)</sup> Therefore, the behavior of air at the base of the spray and the jet was analyzed. The lower half of **Fig. 5** shows the results. The entrainment of air from around the spray or jet is depicted as flow lines. The color of the flow lines indicates the speed. The gas jet has a faster air entrainment velocity and a higher amount of entrainment. However, the entrained air remains close to the surface of the jet and does not enter into the center. In contrast, although the liquid spray has a slower velocity of air entrainment, the air reaches the internal part of the spray. This is due to differences in the structures of the flows. Whereas a gas jet consists of a continuous flow without any gaps, a liquid spray consists of droplets existing discretely in the surrounding air. In other words, air is less likely to enter the center of a gas jet than a liquid spray. From the perspective of this fundamental issue, a gas jet MBD model can be regarded as extremely important.

### 2.3 Verification by engine calculations

The static field gas jet MBD model described in the previous section was applied to calculations inside an engine cylinder to confirm the behavior of the mixture. In this case, the chemical species of the injection gas and its injection rate was changed from helium to hydrogen. The test engine was based on a 2.0-liter inline 4-cylinder mass-production turbocharged gasoline engine. This engine was equipped with DI hydrogen gas injectors with straight single-hole nozzles below the intake ports. **Table 2** lists the engine specifications. Two hydrogen DI engine concepts have been put forward: the high-pressure DI (HPDI) concept that injects the hydrogen

close to top dead center (TDC), and the low-pressure DI (LPDI) concept that injects the hydrogen in the intake stroke or in the first half of the compression stroke when the in-cylinder pressure is low. This research focused on the LPDI concept. The engine speed was set to 2,800 rpm, the brake mean effective pressure (BMEP) to 0.95 MPa, and the start of injection (SOI) to 95 degrees before top dead center (BTDC). Tests and calculations were then carried out with the excess air ratio  $\lambda$  varied in a range between 1.0 and 2.2.

**Table 2 Engine Specifications**

| Engine                                | 2.0-liter inline 4-cylinder  |
|---------------------------------------|------------------------------|
| Bore (mm)                             | 86                           |
| Stroke (mm)                           | 86                           |
| Compression ratio (-)                 | 10                           |
| Injection system                      | Direct in-cylinder injection |
| Intake valve open timing (deg BTDC)   | 29                           |
| Intake valve close timing (deg ATDC)  | 35                           |
| Exhaust valve open timing (deg BBDC)  | 29                           |
| Exhaust valve close timing (deg ATDC) | 1                            |

**Fig. 6** shows the equivalence ratio ( $\Phi$ ) distribution at a cross section of the bore center at TDC with  $\lambda$  set to 1.2 and 2.0. A relative decrease in rich mixture occurs as  $\lambda$  becomes leaner.

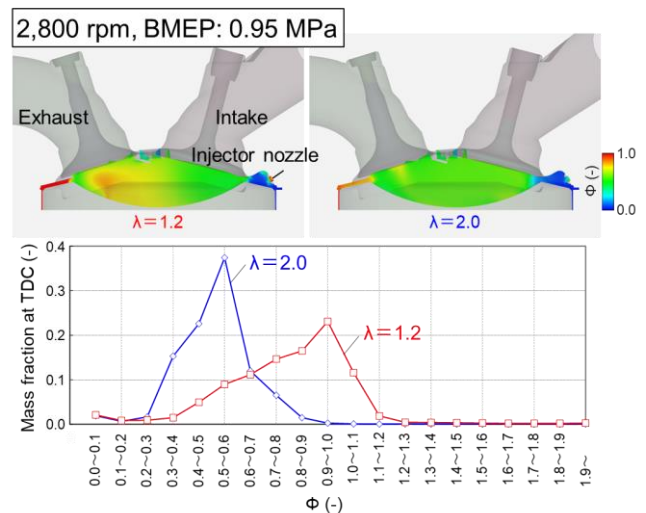


**Fig. 6 Equivalence Ratio Distribution at TDC**

Next, this research considered a method of quantitatively and simply indexing NO<sub>x</sub> emissions in an actual engine using the equivalence ratio distribution shown in **Fig. 6**. NO<sub>x</sub> generated within an engine cylinder depends closely on the local equivalence ratio. In the case of a hydrogen engine, NO<sub>x</sub> mostly consists of NO, which is also known as thermal NO<sub>x</sub>. The

relationship between the equivalence ratio and the NO generation amount was obtained using an elementary reaction calculation for a one-dimensional laminar premixed flame. CHEMKIN-PRO was used for the calculation software, and the initial conditions were as follows: 300 K, 0.1 MPa,  $\phi$ 0.3 to 1.6. GRI-Mech 3.0 was used for the reaction mechanism. Fig. 7 shows the relationship between the equivalence ratio and the amount of NO generation. The vertical axis shows normalized values divided by the equivalence ratio at the maximum NO generation amount.

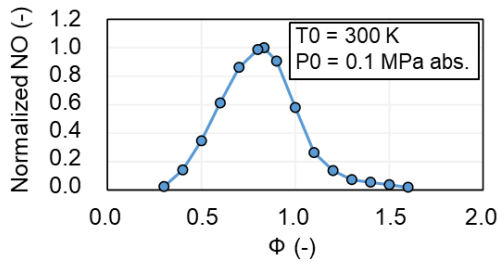


**Fig. 7 Relationship between Equivalence Ratio and NO Generation Amount**

The NO generation characteristics shown in Fig. 6 were multiplied by the mass fraction of each equivalence ratio of the mixture calculated by the gas jet MBD model at TDC. The resulting value was then defined as the NOx index in engine simulations. Fig. 8 shows the relationship between the NOx index on the horizontal axis and the measured NOx emissions on the vertical axis. The correlation forms a single curve over the whole range of in-cylinder conditions from  $\lambda = 1.0$  to 2.2, demonstrating that this index pertains quantitatively to actual NOx.

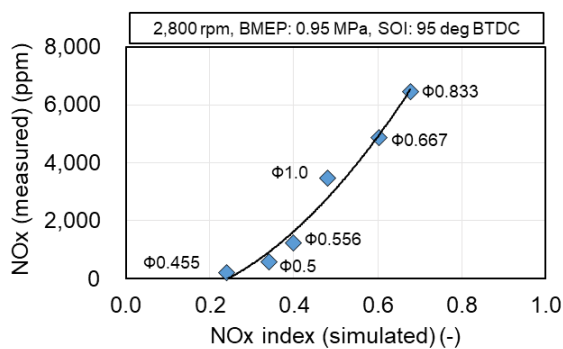


**Fig. 8 Correlation between NOx Emissions Index and Measured NOx**

### 3. Research into Mixture Formation Guidelines Using Gas Jet MBD Model

This section describes the research into creating guidelines for forming high efficiency and low-NOx mixtures in a hydrogen DI engine using the gas jet MBD model and mixture distribution NOx index detailed in the previous sections.

#### 3.1 Direction of improvements to realize both high efficiency and low NOx

As a first step, the direction of improvements to realize both high efficiency and low NOx in an actual engine were examined. Using the engine described in Table 2, tests were carried out at various SOI timings under the following conditions: engine speed = 2,800 rpm, BMEP = 0.95 MPa, excess air ratio  $\lambda = 2.0$ .

Fig. 9 shows the correlation of SOI with thermal efficiency and NOx. Thermal efficiency improves as the SOI timing becomes increasingly retarded. Fig. 10 is a pressure-volume (PV) diagram that shows curves for both a SOI of 95 degrees and a SOI of 180 degrees. As indicated by the hatched area in the diagram, the main reason for this improvement is the decrease in compression work with respect to the hydrogen injected into the cylinder as the SOI timing becomes increasingly retarded. This effect is equivalent to the recovery of work required to compress the hydrogen, and is called the pressure recovery effect below.<sup>(8)</sup> In a vehicle fueled by high-pressure hydrogen, this effect is directly connected to the driving range of the vehicle and must be maximized.

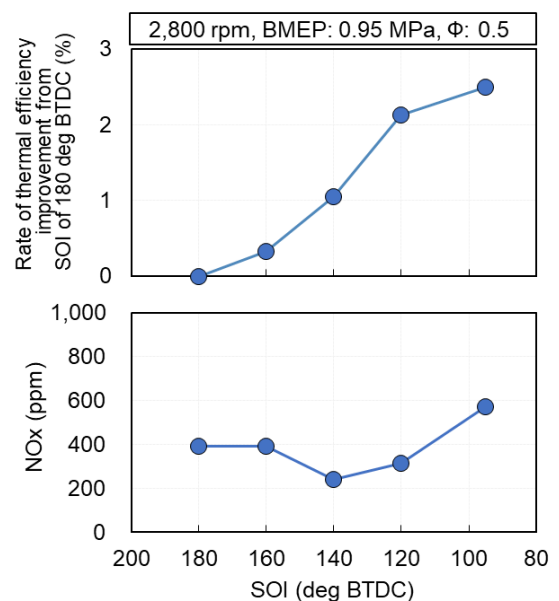


**Fig. 9 Correlation of SOI with Thermal Efficiency and NOx**

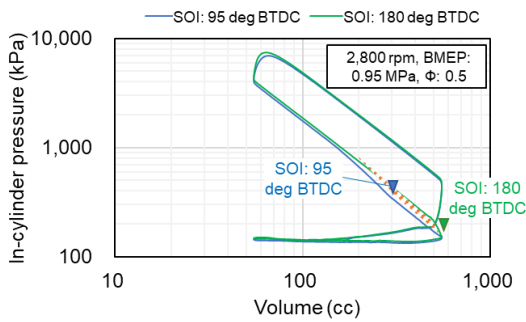


**Fig. 10 PV Diagram Showing Pressure Recovery Effect**

In contrast, NO<sub>x</sub> deteriorates when the SOI timing is retarded later than 140 deg BTDC. In general terms, it is known that NO<sub>x</sub> emissions increase when a locally rich mixture is present. Therefore, it is thought that retarding the SOI timing shortens the mixing duration, which results in a greater locally rich mixture.

Consequently, to realize both high efficiency and low NO<sub>x</sub>, the SOI timing needs to be retarded to maximize the pressure recovery effect. At the same time, the mixing process must be promoted within that limited time window to reduce the occurrence of a locally rich mixture.

**3.2 Quantification of molecular diffusion and turbulent diffusion of hydrogen**

Diffusion is the dominant physical phenomenon in the mixing process of materials with different fluid properties, such as a gaseous fuel and air. The process of diffusion can also be divided into two main categories: molecular diffusion, which causes material transportation by molecular motion, and turbulent diffusion, which causes material transportation by turbulent eddy motion. Research has been carried out into the use of turbulent diffusion in engines to improve mixing and enhance combustion.<sup>(9)</sup> At the same time, since hydrogen has an extremely high molecular diffusion coefficient, it may be possible to realize a good mixture without relying on turbulent diffusion. Therefore, the molecular diffusion coefficient of hydrogen was compared quantitatively with the in-cylinder turbulent diffusion coefficient obtained by engine calculations.

The molecular diffusion coefficient was calculated using Equation (1), which is the formula for obtaining the Chapman-Enskog intermolecular diffusion coefficient.<sup>(10)</sup> In this equation,  $M_{im}$  is the molecular weight,  $\sigma_{im}$  is the collision diameter, and  $\Omega^{(1,1)*}$  is the diffusion collision integral. Since the molecular diffusion coefficient correlates with temperature and pressure, and changes over time in accordance with the temperature and pressure inside the cylinder, the time history of the molecular diffusion coefficient was calculated using temperature and pressure values obtained in engine

calculations. As well as hydrogen, this research also examined the effects with isooctane to compare the differences due to chemical species.

In contrast, the turbulent diffusion coefficient was calculated using Equation (2). In this equation, the turbulent kinetic viscosity coefficient  $\nu_t$  was set to the average value inside the cylinder and the turbulent Schmidt number was set to 0.5.

**Fig. 11** compares the molecular diffusion coefficient and turbulent diffusion coefficient calculated as described above. The molecular diffusion coefficient of hydrogen is approximately ten times higher than that of isooctane, with an order of magnitude difference between the values. However, the in-cylinder turbulent diffusion coefficient is seventy times higher than the hydrogen molecular diffusion even at an engine speed of 1,000 rpm, a difference that amounts to two orders of magnitude. This difference only expands as the engine speed increases further.

Therefore, when a gaseous fuel mixes with air in an engine cylinder, turbulent diffusion retains a dominant effect even with hydrogen, which has a high molecular diffusion coefficient. Consequently, it is important to maximize the effects of turbulent diffusion.

$$D_{im} = \frac{2.66 \times 10^{-7} T^{3/2}}{p M_{im}^{1/2} \sigma_{im}^2 \Omega^{(1,1)*}} \dots \dots \dots (1)$$

$$D_t = \frac{\nu_t}{Sc} \dots \dots \dots (2)$$

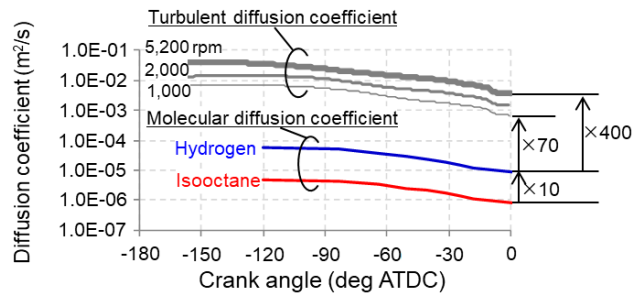


**Fig. 11 Comparison of Molecular Diffusion Coefficient and Turbulent Diffusion Coefficient**

**3.3 Guidelines for Achieving Homogeneous Mixture Formation**

As described in the previous section, maximizing the effects of turbulent diffusion is important for achieving a good mixture in a hydrogen DI engine. To intensify turbulent flow in this type of engine, it should be possible to utilize the properties of tumble or swirl flow. Tumble is widely used to realize high-speed combustion in gasoline engines and swirl is widely adopted to enhance mixing in diesel DI engines. Since hydrogen is being considered for both heavy-duty commercial diesel and compact passenger gasoline engines, this research

analyzed and made comparisons with both types of engines from the perspective of gaseous fuel mixture formation.

This study adopted the following operating conditions using the engine described in **Table 2**: engine speed = 2,800 rpm, BMEP = 0.95 MPa,  $\lambda = 2.0$ . The calculation start timing was set to 140 deg BTDC after intake valve closure (IVC). Tumble and swirl flows with a predetermined intensity were applied as initial conditions. As shown in **Fig. 12**, the hydrogen gas injector was mounted below the intake ports and the gas was injected at a downward angle of approximately 30 degrees from the horizontal plane toward the center of the bore. Unlike swirl, which is not intensified by the fuel jet since the fuel is injected toward the center of the eddy, the fuel jet does have a potential intensification effect on tumble flow.

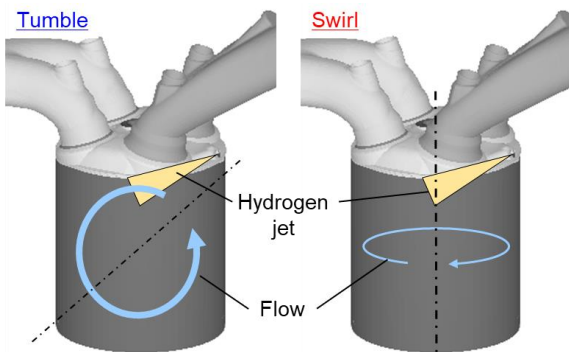


**Fig. 12** Layout of Flows and Hydrogen Jet Direction

**Fig. 13** shows the correlation of the mixture NO<sub>x</sub> index with the tumble and swirl ratios. It demonstrates that the NO<sub>x</sub> index might fall as the tumble ratio intensifies. In contrast, no decrease in the NO<sub>x</sub> index is suggested as the swirl ratio intensifies. This is because, although mixing is promoted as the swirl flow becomes stronger, mixture dilution is not sufficiently promoted until an equivalence ratio with a low amount of NO generation is reached.

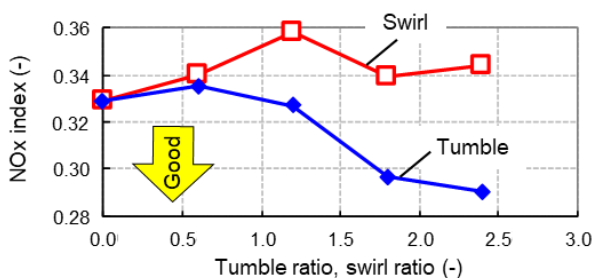


**Fig. 13** Effects of Tumble and Swirl on Hydrogen Mixture Formation

**Fig. 14** shows the time history of physical quantities inside the cylinder at tumble and swirl ratios of 1.8. The NO<sub>x</sub> index decreases more rapidly with tumble flow than with swirl flow. The bottom left graph in **Fig. 14** shows the average in-cylinder turbulent diffusion coefficient. During the injection period, the turbulent diffusion coefficient increases rapidly with both tumble and swirl flows. Subsequently, with swirl flow, the turbulent diffusion coefficient rapidly attenuates. Although tumble flow also attenuates immediately after injection, it remains virtually steady between 90 deg BTDC and TDC. The top right graph in **Fig. 14** shows the rotational kinetic energy around the center of gravity inside the cylinder, and the bottom right graph shows the in-cylinder turbulent energy. These figures may be explained as follows. With tumble flow, the fuel jet intensifies the rotational kinetic energy. In addition, a large longitudinal eddy almost the same scale as the bore diameter decays due to compression by the piston and transforms into smaller scale eddies (i.e., turbulent energy). As a result, the effects of turbulent diffusion are maintained until close to TDC.

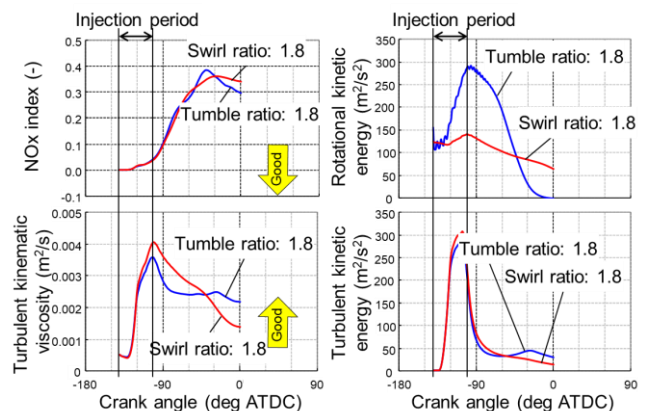


**Fig. 14** Time History of In-Cylinder Physical Quantities

With the LPDI concept, it is important to maximize the effects of turbulent diffusion to achieve a good mixture. A favorable way of realizing this objective involves using the intense turbulence generated when the piston compresses and causes the decay of tumble flow that has been strengthened by the fuel jet.

### 3.4 Study of mixing process due to in-cylinder flows

The previous section described that tumble is more suitable than swirl for the LPDI concept. In contrast, it has been reported that a combination of swirl and multi-hole nozzles are an effective approach for the HPDI concept.<sup>(8)(11)</sup> This section examines what flows and injection systems would be more suitable depending on the concept. As described above, diffusion is the dominant physical phenomenon in the mixing process of

materials with different fluid properties. In addition, turbulent diffusion is predominant in engine cylinders compared to molecular diffusion.

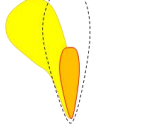
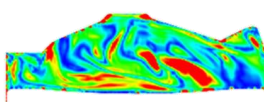
Equation (3) shows Fick's law, which defines material diffusion.

$$J = -D \frac{dc}{dx} \dots\dots\dots(3)$$

where,

- J: diffusion flux
- D: diffusion coefficient
- Fraction: concentration gradient

Two methods are available for increasing the diffusion flux: (1) increase the diffusion coefficient and (2) increase the concentration gradient. This research examined the mixture promotion effect of flows from these perspectives. In a mixing process involving the injection of gaseous fuel into air, flows can promote mixing through the utilization of two effects: advection and turbulence. **Fig. 15** presents an outline of these two effects.

|        | Effects of advection  | Effects of turbulence   |
|--------|---|---|
|        |  <ul style="list-style-type: none"> <li>- A subsequent hydrogen jet enters the fresh mixture that propelled the previous hydrogen jet.</li> <li>- Particularly effective for improving mixtures created by a multi-hole injector.</li> </ul> |  <ul style="list-style-type: none"> <li>- Momentum created by small eddies due to tumble decay and shear flow, and material transportation.</li> </ul> |
| Swirl  | Good  | Poor  |
| Tumble | Good  | Excellent   |
| Squish | Good  | Excellent   |

**Fig. 15 Effects of Flows on Mixing Process**

First, the effects of advection are discussed below. When fuel is injected into a static field in a series of jets, subsequent hydrogen jets penetrate the high-concentration mixture created by previous hydrogen jets, adversely affecting the concentration gradient. In contrast, in a field that contains a lateral flow with respect to the injection axis, the mixture created by the previous hydrogen jets is pushed away by that flow. As a result, the subsequent hydrogen jets penetrate low-concentration mixture. In other words, a high concentration gradient can be created, and mixing is promoted by increasing the diffusion flux as described above. Although this effect can be obtained by either swirl or tumble, it is thought that swirl is particularly

effective when combined with multi-hole nozzles as is the case in a diesel engine.

In addition to advection, turbulence has the effect of promoting turbulent diffusion. This results in material transportation due to eddy motion. This transportation is most active at locations where tumble decays and shear flow occurs. As described in the previous section, tumble has a greater effect than swirl inside an engine cylinder.

Next, this research analyzed the applicability of in-cylinder tumble and swirl flows to the concepts from the perspective of identifying which effects are generated at which timings. **Fig. 16** shows an outline of this analysis.

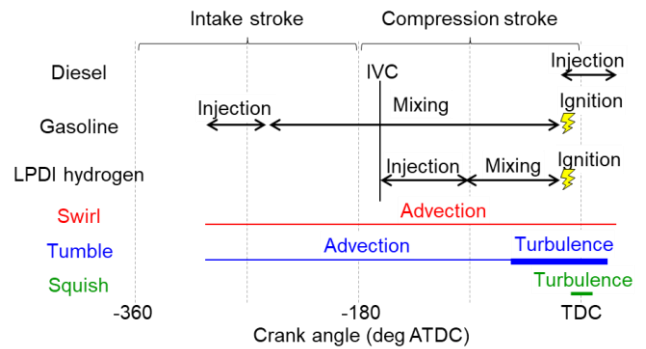


**Fig. 16 Time Chart of Effects of In-Cylinder Flows on Mixing Process**

Swirl realizes the advection effect over a long period of time from the compression stroke to the expansion stroke. In contrast, tumble realizes the advection effect up to the first half of the compression stroke and then realizes the turbulent effect in the second half of the compression stroke. Squish only realizes the turbulent effect close to the TDC of the compression stroke.

A diesel engine must complete the injection and mixing processes in an extremely short period close to the TDC of the compression stroke. For this reason, high-pressure injection using multi-hole nozzles, swirl, and squish are generally utilized in these engines. Tests have confirmed that this same approach (multi-hole nozzles, swirl, and squish) is also effective in a hydrogen engine that adopts the HPDI concept and carries out injection close to TDC.<sup>(8)(11)</sup>

Gasoline engines are not affected by issues such as a drop in volumetric efficiency and abnormal combustion caused by fuel injection. Therefore, fuel can be injected at an early timing in the intake stroke and mixing promoted over the available time until the TDC of the compression stroke. In addition, gasoline engines generally use tumble flow from the perspective of utilizing turbulence to realize high-speed combustion. In a hydrogen engine adopting the LPDI concept, since injection after IVC is usually selected mainly from the perspective of ensuring volumetric efficiency, the mixing period before the TDC of the compression stroke is shorter than in a gasoline engine. A favorable way of

achieving a good mixture in this limited time involves using the intense turbulence generated when the piston compresses and causes the decay of tumble flow that has been strengthened by the fuel jet.

#### 4. Conclusions

This research studied an MBD technique for simulating a gas jet and used it to examine guidelines for achieving homogeneous mixture formation. The following knowledge was obtained.

- (1) A gas jet was visualized in a static field and quantitative data for the penetration and jet angle were measured. A gas jet MBD technique was then constructed to simulate this measured data. This technique was applied to engine calculations. A NO<sub>x</sub> index based on the extent of mixture inhomogeneity was confirmed to correlate closely to the NO<sub>x</sub> emissions of an actual engine.
- (2) To realize both high efficiency and low NO<sub>x</sub>, the SOI timing needs to be retarded to maximize the pressure recovery effect. At the same time, the mixing process must be promoted within a limited time window to reduce the occurrence of a locally rich mixture.
- (3) Although the molecular diffusion coefficient of hydrogen is approximately ten times higher than that of isooctane, the in-cylinder turbulent diffusion coefficient is seventy times higher than the hydrogen molecular diffusion even at an engine speed of 1,000 rpm, a difference that amounts to two orders of magnitude. Turbulent diffusion has a dominant effect in an engine cylinder even with hydrogen. Consequently, it is important to maximize the effects of turbulent diffusion.
- (4) Tumble is more suitable than swirl for the LPDI concept. Tumble flow, which is intensified by the injection process, decays due to piston compression, and is suitable for creating turbulence that maximizes turbulent diffusion. In contrast, for the HPDI concept, the use of multi-hole nozzles, swirl, and squish is an effective approach when injection occurs close to TDC.

#### References

- (1) L. Walter et al. "The H<sub>2</sub> Combustion Engine - The Forerunner of a Zero Emissions Future." *42nd International Vienna Motor Symposium* (2021).
- (2) R. Dreisbach et al. "The Heavy-Duty Hydrogen Engine and its Realization until 2025." *42nd International Vienna Motor Symposium* (2021).
- (3) P. Kapus et al. *43rd International Vienna Motor Symposium* (2022).
- (4) R. Scarcelli et al. "Mixture Formation in Direct Injection Hydrogen Engines: CFD and Optica Analysis of Single- and Multi-Hole Nozzles." *SAE Paper No. 2011-24-0096* (2011).
- (5) N. Matsubara et al. "A Study of Abnormal Ignition in Hydrogen Combustion Engine." *Proceedings of the JSAE Annual Congress (Autumn)* (2022).
- (6) H. Murozumi et al. "Measurement of Atmospheric Induction of Liquid Sprays and High-Pressure Jets Using Time-Series PIV" (in Japanese). *Proceedings of the Symposium on Atomization Vol. 27* (2018).
- (7) S. Tanno et al. "Investigation of a Novel Leaner Fuel Spray Formation for Reducing Soot in Diffusive Diesel Combustion." *SAE Paper No. 2019-01-2273* (2019).
- (8) S. Tanno et al. "High-Efficiency and Low-NO<sub>x</sub> Hydrogen Combustion by High Pressure Direct Injection." *SAE Paper No. 2010-01-2173* (2010).
- (9) H. Sakai et al. "Model-Based Development for Super Lean Burn Gasoline Engine Using Kolmogorov Microscales." *SAE Paper No. 2023-01-0201* (2023).
- (10) R.C. Reid et al. *The Properties of Gases and Liquids*. 4th ed. McGraw-Hill, Inc., New York (1987).
- (11) T. Kato et al. "A Study of Rising Thermal Efficiency Using an Argon Circulated Hydrogen Engine (Third Report)." *Proceedings of the JSAE Annual Congress (Autumn)* (2013).

**Authors**



J. Miyagawa



Y. Miyamoto



S. Tanno



Y. Tsukamoto



T. Omura



D. Takahashi



K. Nakata

# The WAVEBASE Cloud-Based Material Data Analysis Service

Masao Yano<sup>\*1\*2</sup>Takeo Yamaguchi<sup>\*1</sup>Ryo Aoki<sup>\*1\*2</sup>Kazuto Ide<sup>\*1\*2</sup>Hanae Ikeda<sup>\*1\*2</sup>Yasuhiro Toyama<sup>\*2</sup>Yusuke Murai<sup>\*2</sup>Kanta Ono<sup>\*3\*1</sup>Tetsuya Shoji<sup>\*1\*2</sup>

## Abstract

This article describes the WAVEBASE cloud-based material data analysis service, including the background behind its technical and system development, use cases, efforts to commercialize the service and make it available around the world, and its future prospects.

**Keywords:** *material research and development, DX, materials informatics (MI), dimensionality reduction, machine learning, latent space*

## 1. Introduction

More than five years have passed since it was announced that the automotive industry was standing on the verge of a once-in-a-century transformation. In response to this situation, Toyota has initiated various activities to sow the seeds of new businesses for the future with the idea of making use of dormant assets within the company while its core business remains profitable. The project described in this article is part of this approach. Focusing on fundamental technologies developed by the material engineering divisions to understand various materials, this project was started up to see whether it might be possible to monetize these fundamental technologies in some way. Although a wide range of fundamental material analysis technologies have been examined in the past, most of these were put aside after being used once to explain a particular phenomenon and now exist simply as a report in storage. To escape this wasteful cycle and help strengthen the competitiveness of the materials industry in Japan by making the technologies and know-how accumulated in this way more widely available to the industry as a whole, Professor Kanta Ono of Osaka University started working on a concept called Characterization as a Service (CaaS) in 2019. At this point in time, the adoption of technologies based on artificial intelligence (AI) (i.e., the utilization of materials informatics (MI))

had started to become a rising global trend in material research and development. From the outset of this trend, the utility of AI technologies was studied from the perspective of applying robotic process automation (RPA: the use of algorithms to automate work normally carried out by people) to analyze data obtained from materials analysis and measurement systems. However, as free-of-charge proof-of-concepts (PoCs: tests and experiments designed to verify a hypothesis by a process that confirms whether a service has value) accumulated, discussions between people in various industries suggested a need to rethink this hypothesis: Was there really a future need for this approach? Wouldn't it be more important to provide methods to help develop a deeper understanding of the data? Should efforts be directed into creating even larger scale services that incorporate digital transformation (DX) technologies? Consequently, a number of studies were carried out from the perspective of somehow extracting information contained within images and spectra. The focus then shifted to the ideas of latent variables and latent space in terms of AI technologies. Initially, various algorithms were tried out. Techniques such as t-distributed Stochastic Neighbor Embedding (t-SNE)<sup>(1)</sup> and Uniform Manifold Approximation and Projection (UMAP)<sup>(2)</sup> were applied to perform dimensionality reduction and project structural information into a latent space. However, in general terms, although latent variables in machine learning are able to extract certain information, the difficulty of interpretation encountered when analyzing this information remained an issue. Therefore, technological development adopted the concept of highly interpretable AI technology, and the objective of development shifted to the implementation of cloud-

<sup>\*1</sup> Advanced Data Science Management Div., Advanced R&D and Engineering Company

<sup>\*2</sup> Advanced Material Engineering Div., Advanced R&D and Engineering Company

<sup>\*3</sup> Graduate School of Engineering, Osaka University

based systems that would allow anyone to easily use developed analytical techniques. In addition to the interpretability of analysis results obtained by developed technologies, the initiative described in this article focused on designing a screen navigation process and user interface (UI) that would be intuitive and as easy-to-understand as possible. The aim was to avoid the sort of UI that can only be understood by experts, something commonly found in engineering-related business-to-business (B-to-B) software. Despite the objective of producing interpretable analysis results, since the project was developing a specialist analytical tool, it was realized that the results might still be impossible to understand without further intervention. Therefore, the development of the algorithms and UI proceeded from the standpoint of aiding interpretation of the results. Another focus of the development was the incorporation of DX technologies. Utilizing the advantages of a web-based cloud system, secure workspaces were prepared for each customer. In addition to the embedding of data, the intent was to enable the accumulation and analysis of data, which can then be shared throughout an organization via a URL.

This project named WAVEBASE, a portmanteau of the English words “wave,” which refers to both the properties of the light waves used in materials measurement and the wave behavior that acts as the foundation of this analytical technique, and “base,” which is taken from the word database and the concept of fundamental (base) technologies. The project was conducted with the idea of making a wide contribution to industry as a whole by providing the type of service that only a company like Toyota, whose business is not focused on materials per se or measurement instrumentation, is capable.

The following section describes the approach behind this project based on the issues that needed to be addressed. This is followed by an explanation of the developed technologies, an outline of the system, case studies of analysis conducted using WAVEBASE, an outline of the services provided by the project, and an overview of the activities carried out to commercialize these services. Finally, this article concludes with a discussion of the application of DX to research and development, and the prospects for the future.

## 2. Development of Technologies for WAVEBASE

Conventionally, people working in the material development field have obtained data by structural and component analysis using microscopes and X-rays, but have mainly developed materials based on intuition, learned techniques, and experience using only a part of the information contained in that data. Critically speaking, cases have occurred in the past in which the

level of experiments was insufficient, making it impossible to assess the validity of development targets or the validity of the definition of the experimental space under development. Therefore, to escape this situation, it was decided to develop technology focusing on appropriately defining the data space and making effective use of the available data. The value to be delivered by this project was proposed as follows: Might it be possible to research and develop materials more efficiently even with limited resources by providing an environment that allows anyone to easily use MI (**Fig. 1**)? This project analyzed the situation surrounding the development process and found that, although experiments were being carried out to fabricate and measure material samples and to obtain data about the material in question, the amount of time required for data analysis meant that thorough analysis was not being carried out, and that the obtained data was only being examined on a qualitative basis. Consequently, it was hypothesized that the obtained data might not be in a usable state. This led to the hypothesis that the data was not being analyzed by machine learning or other techniques, thereby obscuring the advantages of MI or data utilization (**Fig. 2**). Through interviews with several tens of companies, several reasons for this lack of MI-usable data were identified as follows. First, there is a lack of set data analysis techniques and analysis is too time consuming. Second, data and analysis results are scattered throughout companies and cannot be used even when the desire to use it is present. Third, there is insufficient know-how about efficient material development using statistical processing (**Fig. 3**). In response, it was proposed that a system capable of automatic analysis of material analytics data, functioning as a centralized database of scattered data, and able to perform data analysis might be an effective way of addressing the issues expressed by these reasons. It was decided to develop a system with these functions and implement it on the cloud. However, since the use of MI and the analysis of the subsequent results requires a certain level of technical skills and acclimatization, it was decided to propose a solution that would also include support for the analysis process (**Fig. 4**). This section describes the development and concept of the system designed to embody these technologies, focusing on an explanation of the technical aspects of extracting information embedded within data and the technological development carried out for analysis.

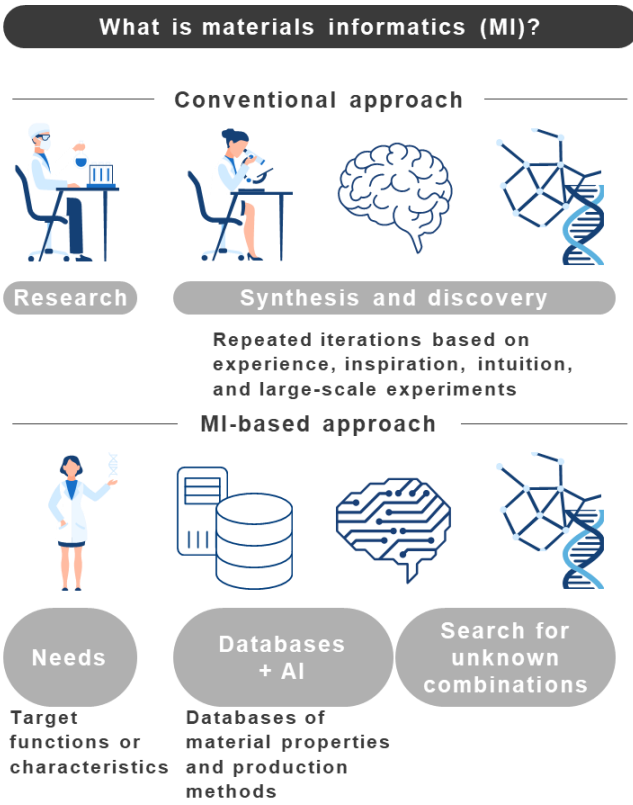


**Fig. 1 Comparison of Conventional Approach to Material Development and Approach Using MI**

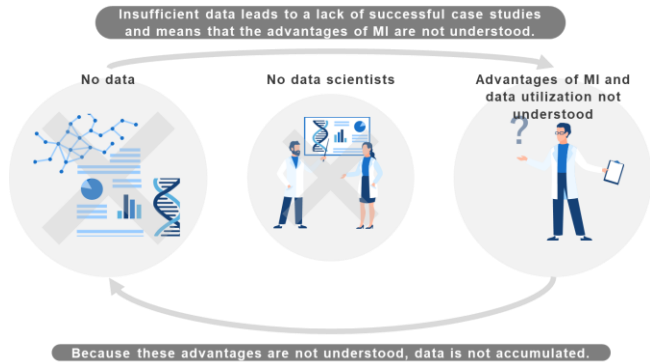


**Fig. 2 Reasons for Lack of Penetration of MI in Materials Industry**

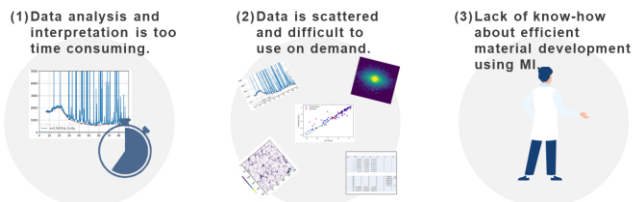


**Fig. 3 Issues Preventing Utilization of Analysis Data with Materials**

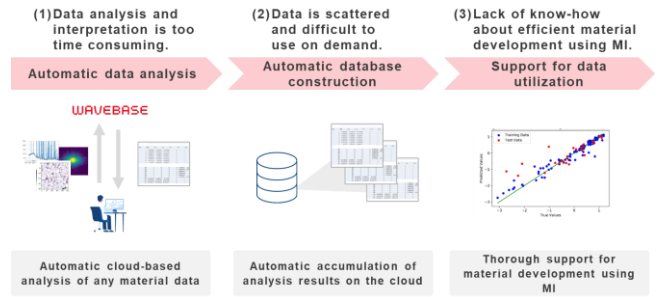


**Fig. 4 Three Solutions Provided by WAVEBASE**

**2.1 Issues to be addressed**

Generally speaking, the objective of material research and development is to identify process conditions and internal material structures capable of satisfying material performance requirements. Alternatively, the objective is to identify process conditions and internal material structures that cause normal or abnormal results in quality control (Fig. 5(a)). To achieve these objectives using machine learning, data related to compounding and processes, data related to the internal material structures (i.e., microscope images or spectra), and data related to material performance must be collected (Fig. 5(b)). Of this data, data related to internal material structures includes data that is expensive to obtain and data that can be obtained at low cost. The selection of this data is an extremely important factor in considering the efficiency of the development. Typical examples of high-cost measurement techniques include transmission electron microscopy (TEM), which is capable of observing structures to an extremely microscopic level. In addition, the technique selected for analyzing the obtained data, and for analyzing the subsequent results is dependent on individual skills, which is one reason why this data cannot be used to its full extent, and is another issue that needed to be addressed.

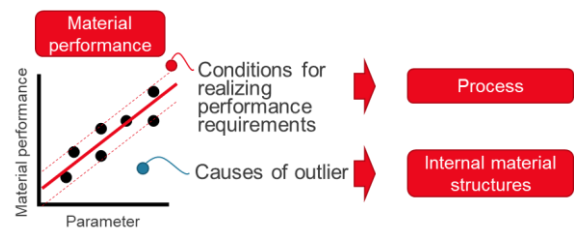


**Fig. 5(a) Target Scenarios for MI**

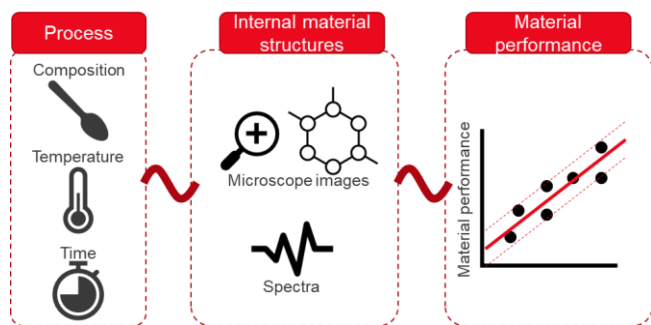


Fig. 5(b) Required Data Sets for Utilizing MI

Several examples of the state of measured material data utilization are introduced below. For example, X-ray diffraction (XRD) is a measurement technique for obtaining information about structural alignments on an atomic level. XRD uses a principle in which a material is exposed to X-rays and information about the atomic alignment of the materials is converted from the X-rays into a characteristic waveform. Conventionally, as shown in **Fig. 6**, the peak positions of XRD data are converted into interatomic distances within the crystal structure, and atomic alignment information is cross-matched with a database and used to identify the structure type. In addition, microscope images can be used to observe the microstructure of the material. This data can be used, for example, to derive the characteristic size of the microstructure and its distribution. These forms of data analysis can be recognized manually and selectable quantities can be obtained. However, characteristics outside the original assumptions and information that is not recognizable manually may be missed. Therefore, this project aimed to develop a method of extracting information from data that eliminates human bias. As an example, the project focused on feature extraction using unsupervised learning. The utilization of machine learning-based feature quantity extraction methods allows a single waveform to be plotted in a latent space as a single point, thereby enabling the overall visualization of changes or correlations between data. For example, coloring the target performance values or the like in the resulting graph enables intuitive understanding of the relationship between waveform characteristics and performance. However, realizing that a simple visualization technique would not be sufficient, the project began examining the extent of characteristics that need to be extracted to enable target performance evaluations.

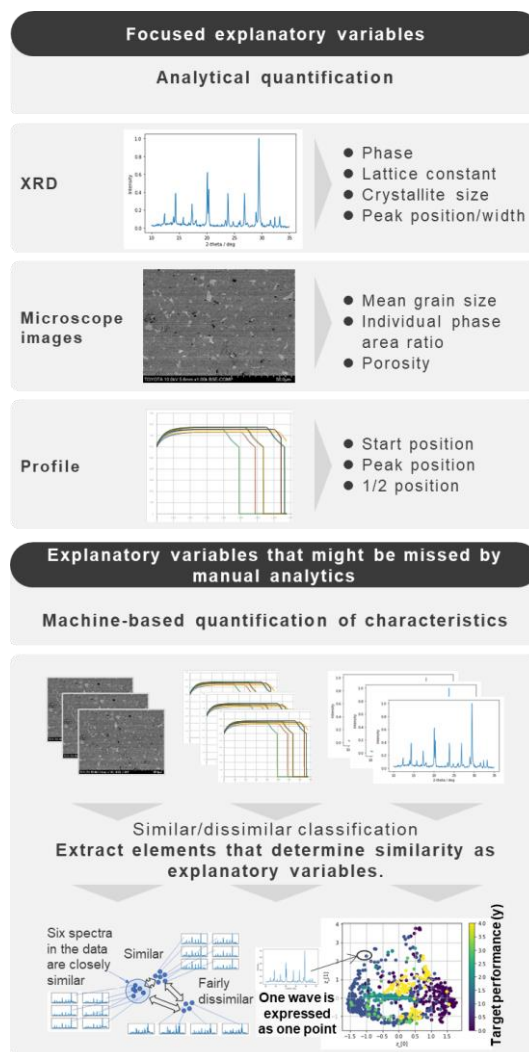
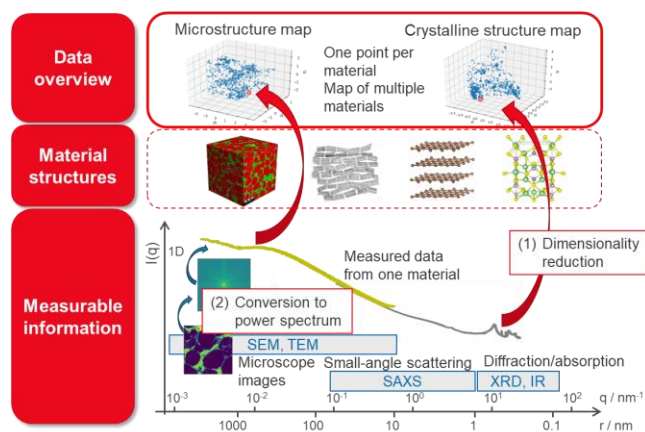


Fig. 6 Comparison of Techniques for Quantifying Characteristics from Material Analytics Data

## 2.2 Diversity and information contained within material analysis data

In the same way that the method of cooking will affect the taste and texture of food even if the same ingredients are used, the materials (steel, plastics, or the like) used in an industrial product will result in different performance depending on the way that the materials are compounded and the manufacturing processes adopted. As an example, if the deliciousness of a bowl of rice depends on the softness and internal components of each grain, the performance of a material will also depend on the alignment and composition of the microstructure. To identify information about the internal nature of a material, such as structural alignments and compositions that affect material performance, it is necessary to select the appropriate analysis technique that matches the size and form of the required internal information, and then to obtain that data. For example, XRD using short-wavelength X-rays can be applied to measure interatomic distances, which is one item of information about the regular alignment of atoms in metallic

crystalline structures (Fig. 7). In addition, scanning electron microscopy (SEM) can be used to observe the state of grains 1,000 times larger than XRD (these grains are still only one-tenth the size of a human hair). It is possible to examine the effects on material performance by expressing the characteristic quantities obtained using XRD and SEM data as numerical values. Material analytics does not only involve techniques for observing structures on multiple scales, such as XRD and SEM. A myriad of other techniques are also available, including techniques capable of observing the compound status of elements contained in the material, as well as internal magnetic and electrical states. A key technology for enabling this analysis data to be utilized by MI is called dimensionality reduction. This technology converts the material analysis data obtained by each of these techniques into data that can be continuously interpreted based on an approach firmly rooted in physical phenomena, and extracts features within a range that can be interpreted manually, while maintaining the data in a machine-readable state.



**Fig. 7 Illustration of Scale Covered by Material Analytics and Utilization of Measured Data**

### 2.3 Development of dimensionality reduction technique for waveforms

The waveform data handled in material analysis is numerical information consisting of between several hundred and several thousand points. Since the values for each measurement point are regarded as variables, waveform data has a high degree of dimensionality, featuring between several hundred and several thousand dimensions. Dimensionality reduction converts this into low-dimensional data while minimizing the loss of information. High-dimensional data is complicated to handle and difficult to interpret. In addition, rather than the number of dimensions, machine learning requires sufficiently large sample sizes. In other words, with small sample sizes, it is necessary to reduce the dimensions of variable data. For this purpose, dimensionality reduction must be used to express data in

fewer dimensions. In addition, dimensionality reduction can also be used to visualize the relationship between each sample by embedding high-dimensional data in a low-dimensional space. This enables analysis that focuses on the cohesion between samples, such as clustering or classification.

Known dimensionality reduction techniques include t-SNE<sup>(1)</sup> and UMAP.<sup>(2)</sup> Either of these techniques is capable of visualization while maintaining non-linear data structures. With high-dimensional data, non-linear structures often appear that cannot be expressed as simple straight lines or planes. Therefore, these techniques, which are capable of embedding non-linear structures in a low-dimensional space while maintaining non-linearity are capable of identifying data characteristics more accurately. However, since it is difficult to understand the axes of data embedded in low-dimensional spaces, the results of data visualization must be interpreted, meaning that a follow-up process is required. Consequently, these techniques are difficult to use for this reason.

In contrast, principal component analysis (PCA) is a long-standing technique that enables the simple interpretation of axes after dimensionality reduction. With PCA, dimensionality reduction is carried out by dividing and organizing each item of data into principal component vectors and principal component scores. When PCA is applied to a data set consisting of multiple items of waveform data, the obtained principal component vectors represent common data waveforms. That is, it is a technique capable of accurately expressing differences between data. In addition, the principal component score can be regarded as expressing the contribution of each principal component to the original waveform data. In Fig. 8, PCA has been applied to a data set consisting of 48 waveforms and two principal component vectors have been extracted. Since each item of waveform data can be expressed by linear coupling between the principal component vectors and principal component scores, a single item of waveform data can be expressed as a single point in latent space by organizing the data based on the principal component scores as shown on the right of Fig. 8. When PCA is used to perform dimensionality reduction, the similarity of data can be read based on the position of the data in the latent space. In addition, since the size of the principal component scores between the data items has a linear relationship, these principal component scores can be used as explanatory variables in machine learning. This technique is not just limited to material analysis data and can also be applied to various types of waveform data.

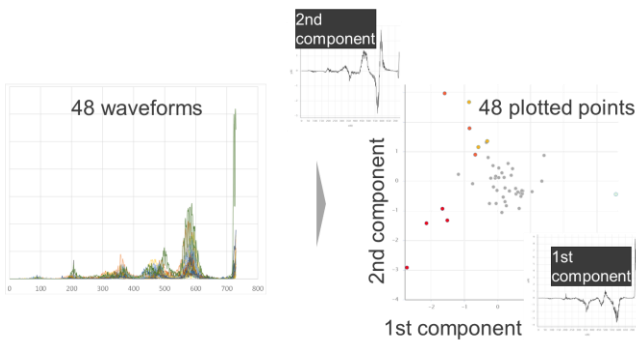


**Fig. 8 Illustration of Dimensionality Reduction by Applying PCA to Waveforms**

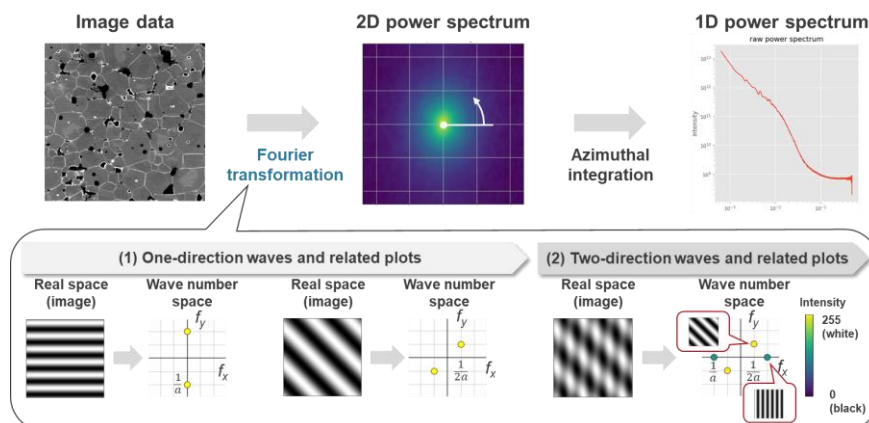
## 2.4 Development of technique to convert image data to waveform data

Image data consists of approximately 1,000 values lined up in the vertical and horizontal directions. In the same way as waveform data, image data is another typical type of high-dimensional data. In material development, the characteristics of samples are frequently identified using images, such as those obtained using a microscope. One point of concern in this process is that data obtained from observation using a microscope only amounts to local information relevant to a portion of the sample. For example, if a material with a size of  $1 \text{ cm}^3$  is assumed to consist of grains with a size of  $1 \mu\text{m}$ , the material will include roughly one trillion such grains. Microscope images frequently depict a visual field containing, at most, around 100 grains and can only show a tiny fraction of the total 1 trillion grains. Therefore, a method capable of quantitatively assessing the periodic nature of grains in an image is regarded as a way of obtaining information that is as significant as possible from observed images.<sup>(3)</sup>

If certain rows can be obtained from image data, these rows can be regarded as waveform data pertaining to brightness information. The same can be said of the row

direction. In other words, image data can be treated as two-dimensional waveform data. Based on its utilization in sound frequency analysis, Fourier transformation is known as method of parsing waveform data into frequency components. Two-dimensional (2D) Fourier transformation that expands the method into two dimensions can be used to extract frequency information pertaining to the size and distance between grains in an image. Values obtained by squaring the amplitude of each frequency component extracted using Fourier transformation are referred to as a power spectrum. Since a power spectrum expresses the intensity of each frequency component, it can also be used to identify the characteristics of image data.

**Fig. 9** shows an example of Fourier transformation applied to image data. If the image data contains black and white stripes at a certain cycle, the power spectrum will show an image of the intensity at each position of the stripe cycle along the stripe cycle direction. Similarly, if the image data contains multiple cycles, points will be plotted at positions corresponding to the respective cycle directions and cycles. The intensity of the plotted points reflects the intensity of the frequency components. In this way, statistical information of any kind of periodic structure in an image can be expressed as a form inside a power spectrum. Accordingly, the Fourier transformed 2D power spectrum for the center part of the microscope image on the left side of **Fig. 9** contains all the periodic information of the original microscope image. When this 2D power spectrum is integrated in the circumferential direction, the result is the one-dimensional (1D) power spectrum shown on the right of **Fig. 9** (a logarithmic expression of the vertical and horizontal axes). As described above, dimensionality reduction was carried out by converting images into power spectra and treating the images as waveform data, enabling the differences between the statistical information for the structures in the images to be visualized in a latent space.



**Fig. 9 Technique for Converting 2D Image Data to 1D Waveforms by Fourier Transformation and Circumferential Integration**

## 2.5 System development

With the aim of propagating the technologies described above into a material analytics and data analysis system, a cloud-based web application that can be used easily by anyone without requiring any coding was developed. The system concept was as follows. It must enable the simple analysis of data by non data scientists, provide an overview of the characteristics of data inputted into the system in any format, include a data analytics function that shapes data into a format compatible with feature quantity-based machine learning, enable the sharing of data inside and outside an organization as required, and be equipped with DX-related functions that enable the utilization and sharing of data states and results whenever necessary. A system was developed to realize this concept. The objectives of implementing a system with these functions were to enable users to perform each stage of the process from data acquisition to analysis, utilization, and accumulation without outside assistance, and to promote the accumulation of data as an organization. This section describes an outline of the developed system.

### 2.5.1 Coding-free system

This system is constructed as a cloud-based web application. Data is logged into the system by dragging and dropping measured data using a browser window. The logged data is automatically analyzed, and the feature quantities extracted from the data are also accumulated as measured data and data sets (**Fig. 10**). Analysis results can be viewed on the web or downloaded as numerical or graph data. In addition, by specifying an arbitrary value as an objective variable, the system can propose and analyze the next experimental level using regression analysis or Bayesian optimization. If, for example, the obtained results indicate that principal components extracted from the spectra will have an impact on material performance, the system incorporates tools for interpreting the results that can demonstrate the meaning of the applicable principal components to the user.

To encourage users with little aptitude for data analysis to utilize these functions, the screens and screen navigation have been designed to be non-confusing and enable most analysis to be performed by mouse operations alone. The objective is to use simple screens to facilitate ongoing use of the system by a wide variety of users.

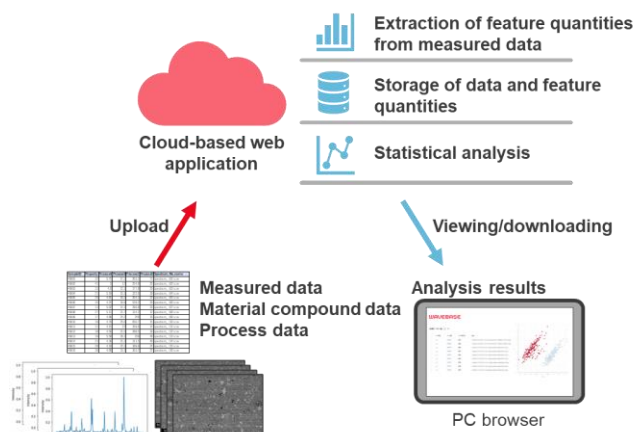


**Fig. 10 Overview of WAVEBASE System**

### 2.5.2 Conversion of data into usable formats for machine learning

This system carries out analytical feature quantity extraction and machine-based automatic extraction of feature quantities using material analysis data logged into the system (**Fig. 6**). In the case of XRD, analytical feature extraction refers to the identification of phases in the material and the calculation of crystallite sizes. In the case of microscope images, it refers to the extraction of the size and number of grains in the image as quantitative values. In contrast, machine-based feature extraction uses a dimensionality reduction technique that focuses on the similarity between data.

As described in Section 2, there are various types of material analysis data, including electron microscope images, X-ray diffraction patterns, infrared (IR) spectra, and so on. Generally speaking, even when the same analytical technique is used, different device manufacturers tend to adopt different data output formats. For these types of data, the system incorporates an algorithm that automatically determines and extracts supplemental information (such as measurement conditions, specifications, and the like) and measured data. The user can then handle the data without concern for the device or file format. Consequently, if the data read by the system is, for example, waveform data consisting of x (horizontal) and y (vertical) axes as shown in **Fig. 11(a)**, the scope of x and the interval between measurement points is often likely to differ between measured data items. Therefore, the system performs automatic pre-processing to make the scope of x and the interval between points uniform (**Fig. 11(b)**). This conversion process creates data in which the scope of x and the number of measurement points are aligned, enabling the dimensionality reduction described in the previous section. The developed system calculates a uniform upper-level principal component score for a wide range of material analysis data such as waveforms from XRD and IR, as well as images from electron microscopy and the like. As a result, in the same way as

process settings that originally consisted of numerical values or performance data and the like that can be obtained as numerical values, this system enables the application of values processed from images and waveform data in machine learning (Fig. 12).

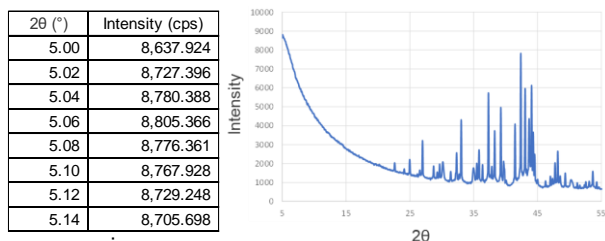


Fig. 11(a) Example of Measured Waveform Data

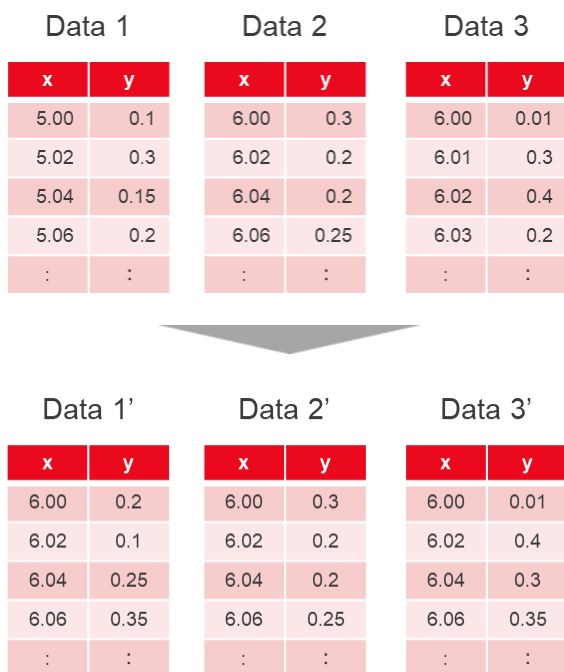


Fig. 11(b) Comparison of Multiple Measured Data Items Before and After Processing

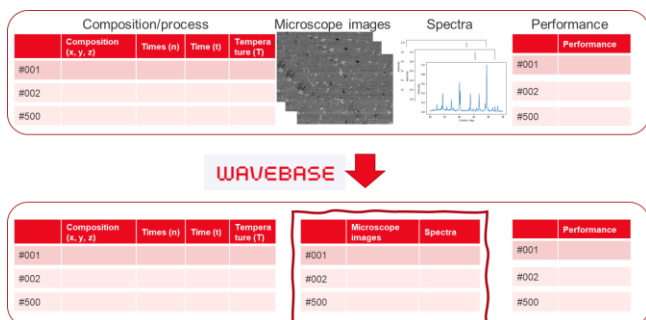


Fig. 12 Illustration of Data Tables Compatible with Machine Learning Obtained by Using WAVEBASE

### 2.5.3 Sharing of data and analysis results

Data is stored in securely compartmentalized regions in workspaces created for each company or organization to which the users belong. As a result, data cannot be viewed or obtained by different companies or organizations. Within that company or organization, the analysis results can be shared via a browser URL, providing immediate access to the same data for people registered in the system.

At the same time, it is likely that some development projects will be carried out while sharing data between different companies. The system allows the assignment of access rights to individual users in other organizations limited to specific data only. This enables data and analysis results to be shared flexibly in project or work units across different companies or academic institutions. Since this function can be used to share, for example, data and analysis results between companies engaged in joint material research in real-time, the system eliminates the effort required to save data or send data by email, helping to create an environment that facilitates research projects.

## 3. Case Studies of Analysis Using WAVEBASE

### 3.1 Development of rare-earth magnet materials

Background and objectives:

In a material development project, it is necessary to determine the development policy based on only a small number of data points. In addition, since information about the material structure at varying degrees of scale, from nanometer-order crystalline structures to micrometer- and millimeter-order structures will affect the target performance, it is extremely important to understand which factors will determine the performance of the material. This section introduces a case study involving the analysis of magnet materials, which was carried out following the themes of small data analysis, multi-modal analysis, and model analysis. Feature quantities were extracted from XRD spectra, which allow the analysis of nanometer-order or smaller magnet crystalline structures, and SEM images, which allow observation of micrometer-order structures. The factors affecting magnet performance were then analyzed based on an extremely small number of data points from twelve samples.

Extraction of feature quantities from spectra and images:

XRD is a measurement technique capable of identifying the average data of an extremely large number of grains with a low degree of variation between measurements. Therefore, it is sufficient to acquire data from one spectrum per sample.

Feature quantity extraction by XRD is carried out as

described in the previous section. Here, the principal components XRD\_PC1 to XRD\_PC10 were obtained. In contrast, SEM images may, by chance, include grains that have suffered abnormal growth or foreign objects. This creates the issue of large potential variation in each visual field depending on the magnification. Therefore, it was decided to obtain images from ten visual fields per sample for this analysis and calculate the average power spectra. Principal components SEM\_PC1 to SEM\_PC10 were extracted from the images by applying PCA to these average spectra.

Performance estimation model and its interpretation:

**Fig. 13** shows the regression results for correlation with magnet performance using the extracted feature quantities. Although this is just a simple linear model (lasso), it can be used to explain magnet performance. As shown in **Fig. 14**, by simulating XRD spectra for directions that result in improved performance (i.e., by increasing XRD\_PC1 and reducing XRD\_PC3), specific crystal plane orientations strengths can be confirmed as falling (red arrows in **Fig. 14**). This indicates that crystal orientation affects magnet performance. The analysis also found that that, in addition to XRD feature quantities, SEM\_PC2 also makes a contribution to magnet performance. **Fig. 15** shows images restored using phase information. The images emphasize grain interfaces and indicate that performance improves as the number of white precipitate grain boundaries increases. The key point of this case study is that the principal components that affect performance can be identified even without input from a magnet expert. This should help to increase development efficiency since the experts only need to select the expressions used in the final interpretation.

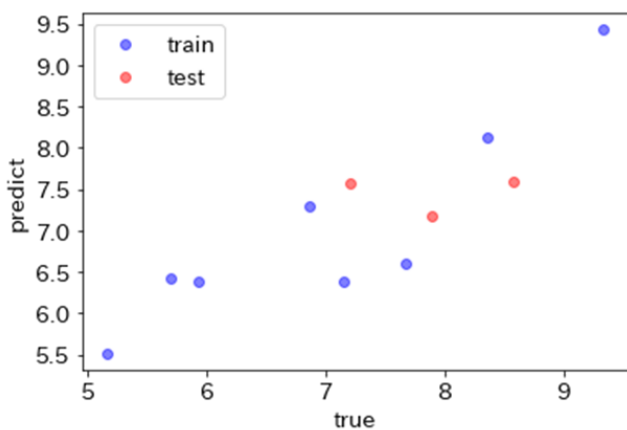


**Fig. 13(a) Accuracy of Performance Estimation Model**

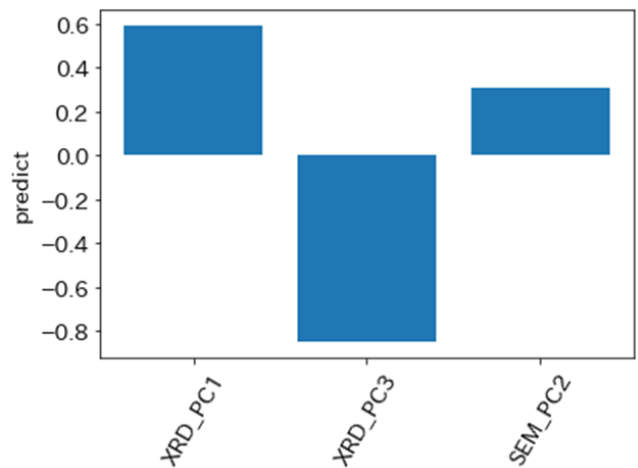


**Fig. 13(b) Contribution Ratio of Explanatory Variables**

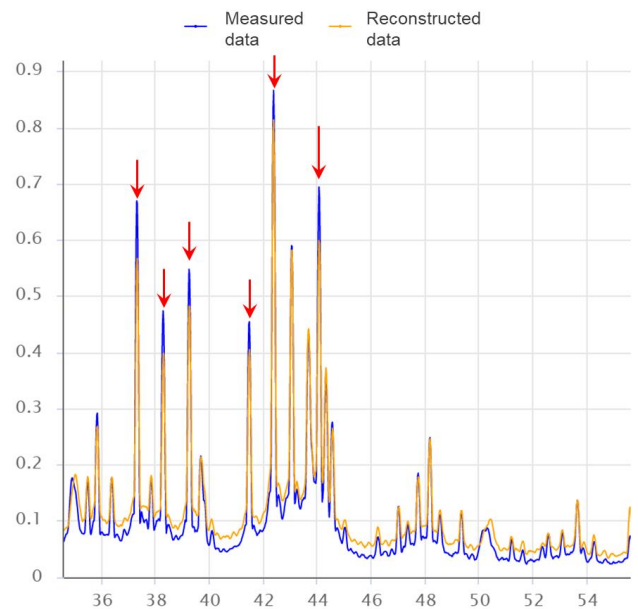


**Fig. 14 Original XRD Patterns (Blue) and Restored Patterns (Orange)**

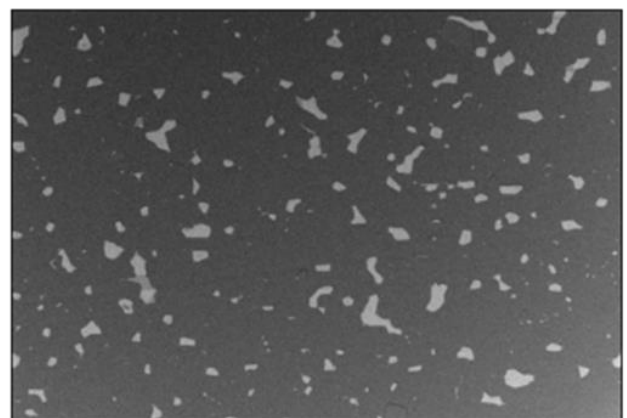


**Fig. 15(a) Magnet SEM Image**

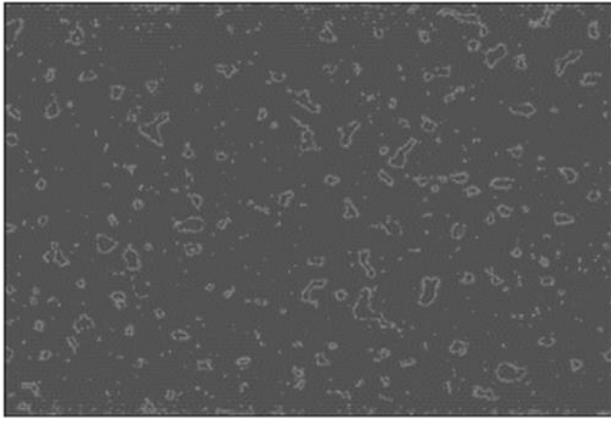


**Fig. 15(b) Restored Phase Image of PC2**

#### Conclusions:

As described above, the factors that increase or reduce magnet performance could be estimated even with experimental data from only twelve samples. The acquisition of data with less variation, multi-modal analysis that combines different types of scale information, and the identification of interpretable performance estimation models are extremely important for analyzing small data.

### 3.2 Rubber material development for tires

#### Background and objectives:

Requirements for tire rubber material development include identifying the relationship between the internal structure of the material and performance, and the mechanism by which that performance is realized. Therefore, it is necessary to quantify the internal structure of the material, which varies depending on the type of material used and a wide range of environmental factors.

#### Issues:

To identify the mechanism by which the performance of tire rubber is realized, the development project used data obtained by the large synchrotron radiation facility SPring-8. This data was regarded as being potentially useful for analyzing structural changes in the material as the rubber deforms. Since this analysis technique is capable measuring large volumes of data in a short period of time, it has the merit of obtaining large quantities of dynamic structural information. In contrast, due to the massive number of obtained data points, the duration of data analysis is a bottleneck in the process for identifying the mechanism and performing material development (**Fig. 16**).

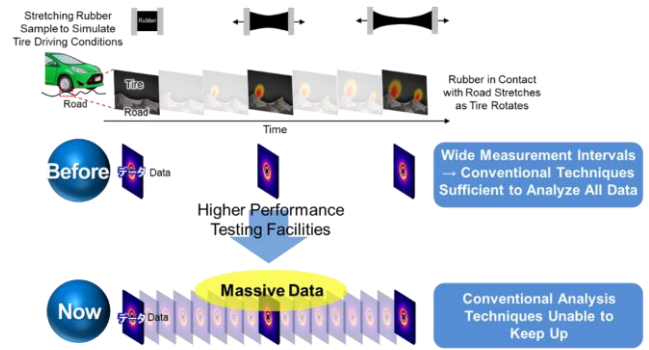


**Fig. 16 Issues of Using Big Data**

Source: [https://www.srigroup.co.jp/english/newsrelease/2022/sri/2022\\_032.html](https://www.srigroup.co.jp/english/newsrelease/2022/sri/2022_032.html)

#### Experiment:

Rubber material test pieces were fabricated and stretched. Mechanical properties (stress-strain curves) and small-angle X-ray scattering (SAXS) patterns were then obtained in this state. SAXS is a non-destructive analytical technique used to investigate the microstructure of materials. Samples are exposed to X-rays and the angular distribution of the scattered X-rays is measured. This enables analysis of factors such as the internal microstructure and forms of the sample, the molecular weight, distance between molecules, and so on. Approximately 2,000 data points (approximately 50 material types  $\times$  degrees of stretching) were obtained (**Fig. 17**).

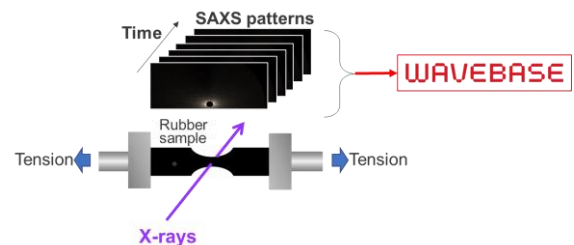


**Fig. 17 Illustration of SAXS Measurement Tests Using Stretched Rubber**

#### Results:

The WAVEBASE system was used to plot the feature quantities extracted from every SAXS pattern onto a single map. This created an easily interpretable overview of structural changes during the stretching process consisting of around 2,000 data points. The system visualized changes over time in accordance with changes in these trends. Differences in these trends could then be traced by comparing materials with different mechanical properties (**Fig. 18**). As a result, the mechanical properties of the material could be described using feature quantities extracted from SAXS, including internal material structural information.

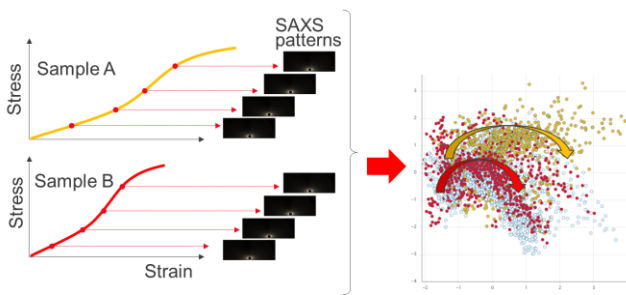


**Fig. 18 Mechanical Properties (Stress-Strain Curves) and Feature Quantity Map of SAXS Patterns**

In the future, it may be possible to identify material development policies based on the mechanisms causing changes in rubber structures that affect performance by interpreting the principal components with a major impact on the material properties and investigating the correlation between material production conditions and SAXS feature quantities.

### 3.3 Development of carbon-neutral fuels

Background and objectives:

Carbon-neutral fuels such as bioethanol are being increasingly regarded as a potential way of reducing or even eliminating CO<sub>2</sub> emissions. However, since these fuels have different physical properties to gasoline, which has a long history of use in vehicle engines, new research must be carried out to examine the effects of factors such as fuel injection, mixing, ignition, and combustion. This case study analyzed high-speed camera video data of the injection states of various fuels used in vehicle engines, and identified the differences in injection shapes due to the composition of the fuel, and the relationship with combustion states.

Experiment:

High-speed cameras were used to video the appearance of fuel injected under various pressures. Continuously changing images were then extracted from these videos and analyzed using the WAVEBASE system.

Results:

The obtained video data was pre-processed to split into image files of one frame each (Fig. 19). The image data was converted by the system into power spectra and plotted onto a latent space by PCA. As shown in Fig. 20(a), applying different colors to the plotted points for each injection pressure creates a uniform color appearance for each pressure. This indicates that, although the characteristics of the images appear to be similar under the same injection pressures, the characteristics actually change at different pressures. As shown in Fig. 20(b), when two types of fuel are compared, separate plots are displayed for each fuel. Fig. 20(c) compares images at each plotted point. From these

results, even differences between the images that are difficult to spot manually can be automatically extracted and quantified as coordinates in a latent space.

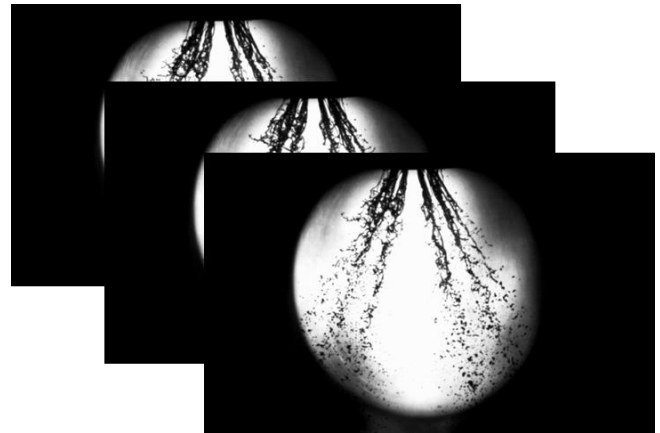


**Fig. 19(a) Videos Obtained in Tests**

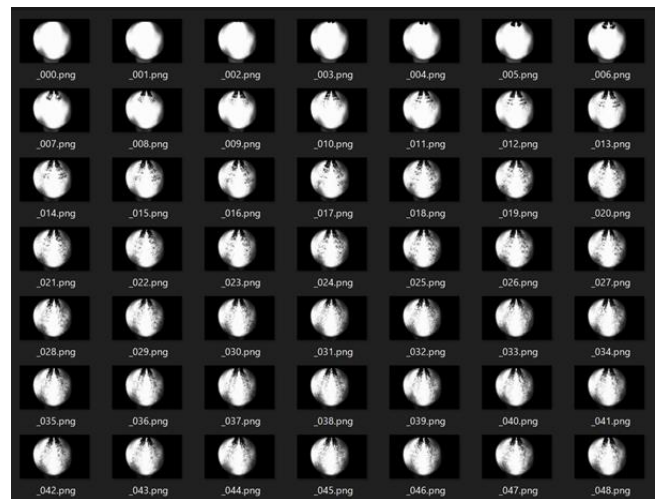


**Fig. 19(b) Resulting Single Frame Images Obtained from Videos**

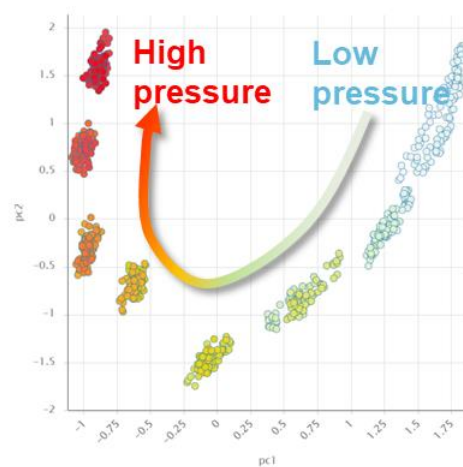


**Fig. 20(a) Principal Component Scores of Images at Nine Injection Pressure Levels**

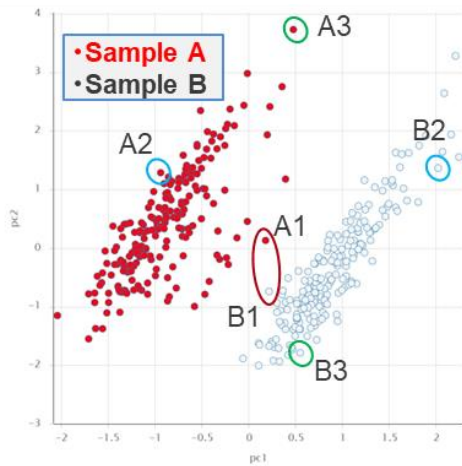


**Fig. 20(b) Principal Component Score Plots of Images at Same Injection Pressure for Two Fuel Types**

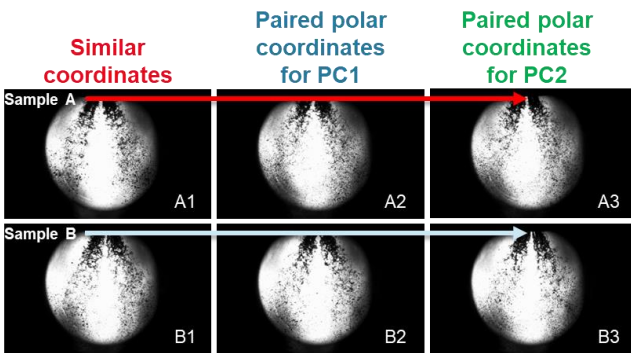


**Fig. 20(c) Image-Based Comparison of Two Points in Fig. 20(b)**

Next, the meaning of these coordinates must be interpreted. As shown in Fig. 21, a feature quantity interpreting tool capable of reproducing power spectra at arbitrary points in the latent space was used to find that the high-frequency components in the power spectra drop conspicuously from right to left on the PC1 axis. Since the high-frequency components of the power spectra correspond to relatively smaller pieces of information in the image, these results can be interpreted as meaning that the number of smaller elements in the fuel states in the images is decreasing.

As described above, this system can be used to quantify the states of injected fuel, which change depending on the injection conditions and type of fuel, into an interpretable form. Linking these results with performance data enables fuel injection conditions that optimize performance to be determined by data analysis. Therefore, by using this technique, it should be possible to accumulate and utilize data that quantifies various fuel states to help accelerate the development of carbon-neutral fuels.

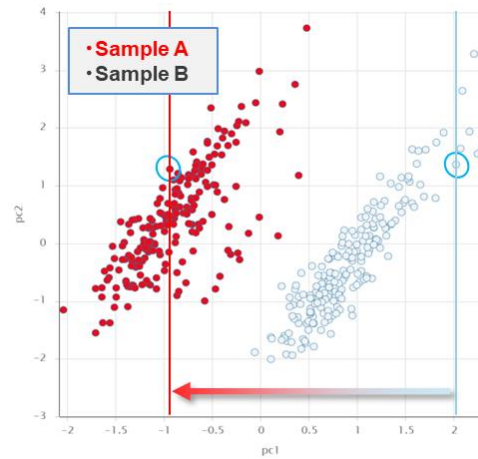


**Fig. 21(a) PC1 and PC2 Space Plots for Two Samples**

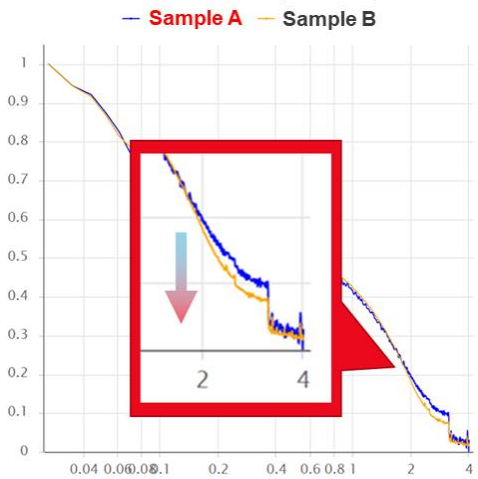


**Fig. 21(b) Comparison of Power Spectra at Two Points**

#### 4. Initiatives for Commercialization

The concept of a business originating from in-house technological development might appear to conform to the idea of product-out business development. However, the project to commercialize the WAVEBASE service was actually focused on creating a customer-centric product. This section describes how this service was started up using this approach.

In 2019, as part of Toyota’s efforts to respond flexibly to changes in the times and continue providing value for customers, it was decided to set up a business creation platform called “Be-Creation” as a support framework for starting new businesses using the company’s own assets. This new initiative provided the motivation to simultaneously start studying the commercialization of the WAVEBASE service. The processes that led to the current activities are described in the previous sections. The business development support offered by Be-Creation essentially follows the lean start-up concept.

Lean start-up is a management method that aims to realize true customer requirements via repeated rapid cycles of prototype creation incorporating the minimum necessary levels of products, services, and functions over a short period of time, and the validation of hypothetical customer needs. Since the project to commercialize the WAVEBASE service adopted this approach, it began by confirming the requirements of customers without massive investment in product development at an early phase, even though WAVEBASE is a technology-based product. More specifically, the project repeatedly validated hypotheses by providing the service in a manually accessible form without using funds to conduct interviews or construct systems. Through this process, the project was able to proceed from an initial hypothesis (that the processing of large volumes of data such as XRD or SEM images is probably too time-consuming for customers) to the determination of an eventual definite requirement to be satisfied by the service (customers want to effectively utilize low volumes of data).

In general terms, once an existing business attains a certain scale, the promotion of new businesses based on an organization that has been optimized for that existing business is often regarded as difficult. In the rapidly changing environment of recent years, this can affect the survival of the business at an existential level. The mission of Be-Creation is to nurture people in the art of creating new businesses, revolutionize workplace cultures, and bring the existing business up to date. The WAVEBASE service is an emblematic case study for this mission. The WAVEBASE business was established based on material development technologies nurtured for the vehicle business. As an analytical technique refined by addressing issues faced by the customer, it has the potential to revolutionize working practices in Toyota's main business.

## 5. Conclusion

Using MI techniques that emphasize interpretability, WAVEBASE is capable of extracting feature quantities by the application of dimensionality reduction and visualizing the latent spaces of those quantities as low-dimensional spaces. Through this process, it can extract knowledge indispensable to the research and development of materials from analytical and measurement data accumulated within a company or organization. In addition to greatly improving the efficiency of the material research and development process, this can create substantial value from data left idle because the potential uses, analytical techniques, or methods of interpretation are difficult to understand by ordinary people.

Currently, feature quantities specific to individual materials are being extracted and latent spaces constructed. One major step for the future is likely to

involve identifying optimum feature quantities for a wider range of material groups such as battery and magnetic materials, and using the resulting latent spaces. These latent spaces visualize factors such as the similarities between materials, structures, and functional correlations in low-dimensional spaces while maintaining interpretability. These can be truly referred to as material maps. The WAVEBASE service differs from the conventional method of using MI technology, namely, to simply obtain massive data sets and use existing MI techniques with the aim of discovering new materials. This is a new cross-organizational human-centric research and development process that uses material maps to facilitate moments of inspiration in engineers and researchers, ultimately leading to the discovery of new materials that conventional approaches would not have achieved. The creation of highly versatile material maps that are easy to use by engineers and researchers involved in manufacturing is regarded as an important accomplishment. In addition to improving the research and development capabilities of an individual organization, it should also raise national industrial competitiveness, and help to address social issues from a global perspective as expressed by the Sustainable Development Goals (SDGs). In the creation and use of these material maps, methodologies to improve the performance of the maps by all users of WAVEBASE while protecting the confidential information of individual organizations will also be important.

The goal of material development is not to generate multiple virtual candidate materials inside a computer, but to identify useful real-world materials based on various restrictions, such as raw material and manufacturing costs, processes, and environmental impacts. Material development technologies capable of bringing candidate materials created on a computer screen to life in the real world via MI or other AI techniques or material maps will also be necessary. The use of cutting-edge robot technologies and AI techniques to automate material development in the real world and feedback measured data from the created materials for the purpose of discovering new materials, as well as for identifying and optimizing the mechanisms that define material functions or manufacturing processes, is becoming a trend in Europe and the U.S. The next step for WAVEBASE, which aims to generate value by extracting knowledge from material data, is to create even greater value and enable technological development that contributes to society. This can be accomplished by creating material maps as compilations of extracted knowledge and actually giving birth to new materials through the formation of synergy between people and material maps and the enabling of autonomous research and development into materials using AI and robots.

The development of AI technology as typified by Chat GPT is having an increasingly disruptive impact. The

appropriate use of AI technology and access to information that people would find difficult to identify will undoubtedly play an indispensable role in future technological development projects. In contrast, some parts of development will depend on the five senses of human perception and the so-called sixth sense of intuition and learned techniques. Many unproductive aspects of research and development remain. By addressing these aspects, it may be possible to devote more time to understanding and interpreting research cycles, as well as to the creative process of ideation for the next development cycle. For this purpose, it will be important to create an environment that enables basic functions such as accumulating data that is easily accessible by as many engineers and researchers as possible, extracting information from that data, and interpreting the correlations between the data. These basic functions will include, for example, visualizing the differences between basic and advanced analysis to assess the validity of the analytical techniques being used. To realize that, it will probably be necessary to realize a world-view focused on the more creative utilization of human intuition and ideas.

## Acknowledgments

The initiatives described in this article are the result of the invaluable support received from many people inside and outside Toyota in algorithm and system development, as well as for commercialization of the service. Field testing of the WAVEBASE service relied on data and support provided by Sumitomo Rubber Industries, Ltd. Data for the development of rare-earth magnet materials was obtained and provided by the Advanced Material Engineering Division and data for the development of carbon-neutral fuels was obtained and provided by the Carbon Neutral Development Division. The authors would like to take this opportunity to express their sincere gratitude to everyone involved.

## References

- (1) L. Maaten, Hinton. "Visualizing Data Using t-SNE." *Journal of Machine Learning Research* Vol. 9 (2008) p. 2579.
- (2) L. McInnes et al. "UMAP: Uniform Manifold Approximation and Projection for Dimension Reduction." *arXiv* No. 1802.03426 (2018).
- (3) S. Koizumi et al. "New Attempt to Combine Scanning Electron Microscopy and Small-Angle Scattering in Reciprocal Space." *Journal of Applied Crystallography* Vol. 52 (2019) pp. 783-790.

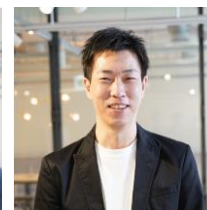
## Authors



M. Yano



T. Yamaguchi



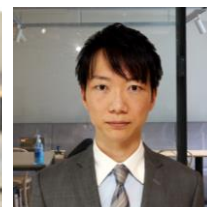
R. Aoki



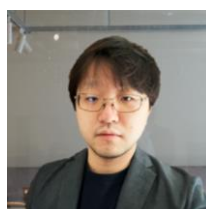
K. Ide



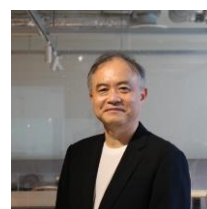
H. Ikeda



Y. Toyama



Y. Murai



K. Ono



T. Shoji

Chairman's Award of the 2022 JSPMI Prizes  
2022 JSME Medal for New Technology

The JSAE Technological Development Award (73rd JSAE Awards)

# Development of Remote Control Autonomous Driving System

Takuro Sawano\*<sup>1</sup>

Takeshi Kanou\*<sup>2</sup>

Shogo Yasuyama\*<sup>1</sup>

Kento Iwahori\*<sup>1</sup>

Keigo Ikeda\*<sup>3</sup>

## 1. Background

As innovation continues to advance in the new fields of connected, autonomous (or automated), shared, and electric (CASE) technologies, the fundamental concept of what a vehicle can be is beginning to undergo major changes. At the same time, companies in Japan are experiencing increasingly severe labor shortages as the working population shrinks in size. With this background, it is becoming necessary to identify new forms of vehicle manufacturing capable of realizing dramatic improvements in productivity.

This article describes the automation of vehicle transportation in assembly plants, which has been a major issue in efforts to raise productivity. This initiative made maximum use of CASE technologies to develop a remote control autonomous driving system (RCD) as an unmanned system for transporting mass-production vehicles. This is the first such system in the world to be adopted on mass-production lines, and it has had a substantial labor-saving effect (Fig. 1).



Fig. 1 Images of Unmanned Vehicle Transportation by RCD

## 2. System Outline

RCD performs the cognition, decision making, and operation processes of driving using a control system located outside the vehicle and performs autonomous transportation by wireless communication with the vehicle (Fig. 2). The control flow is as follows. (1) Vehicle position estimation is carried out by sensing via infrastructure cameras and image processing in real-

time. (2) The control system calculates the vehicle motion control command values based on comprehensive inputs such as position information, the target path, vehicle state, and so on. (3) Wireless communication is used to transmit the motion control command values to the vehicle. (4) The vehicle is driven autonomously in accordance with the received motion control command values by the actuators in the powertrain, steering, brakes, and the like. Remote autonomous vehicle motion control is then realized by repeating these controls in a low-delay/high-speed cycle.

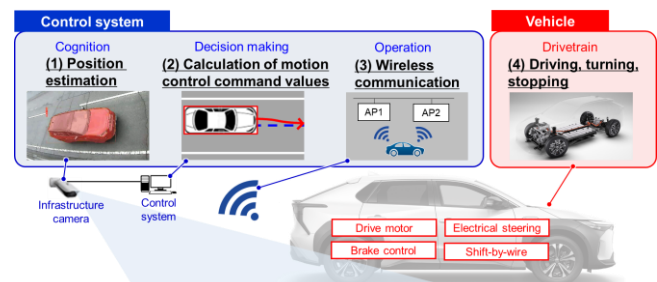


Fig. 2 Outline of RCD Controls

## 3. Main Technologies

### 3.1 High-accuracy vehicle position estimation by infrastructure cameras

The vehicle coordinates and orientation angle calculated in the positioning process form the basis for computing the motion control command values, and therefore must be extremely accurate. Current technologies used for this purpose include onboard sensors that detect the situation outside the vehicle, as well as light detection and ranging (LiDAR). However, these technologies are difficult to adopt widely for cost reasons.

Therefore, RCD uses infrastructure cameras and incorporates an image processing model capable of simultaneous high-speed object detection and segmentation. This approach enables rapid and accurate estimation of the external shape of the vehicle and allows highly precise calculation of the vehicle coordinates and orientation angle.

\*<sup>1</sup> Motomachi Plant Vehicle Quality Div., Production Group

\*<sup>2</sup> Chassis Development Div. No. 2, Vehicle Development Center

\*<sup>3</sup> Automated Driving & Advanced Safety System Planning Div., Vehicle Development Center

### 3.2 Motion control value calculation method for target path following

The purpose of motion control is to enable the vehicle to follow a target path. Issues in the development of this control included communication, creating a calculation formula that factors in the dead time caused by computation delay, and overcoming the effects of deterioration in the orientation angle signal-noise (S-N) ratio on image processing, which cannot be completely avoided.

The following two measures were adopted to counter these issues. First, a two degrees of freedom control structure was adopted consisting of feed forward (FF) control that determines the steering angle from the curvature of the target path and feedback (FB) control that derives the actual steering angle from the lateral deviation between the vehicle position and the target path. Then, to ensure stability and reduce dependence on the FB control, the FF control is used for the path-following function (Fig. 3).

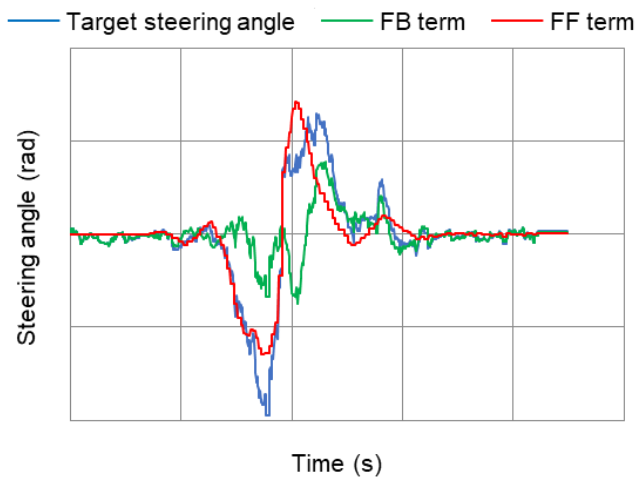


Fig. 3 Calculation of Target Steering Angle

Second, estimation of the orientation angle does not depend on image processing alone. Accuracy was improved by also incorporating information from onboard sensors. Although image processing is capable of obtaining absolute values, this merit is offset by a deterioration in the S-N ratio. In contrast, onboard sensors have a good S-N ratio, but are affected by the accumulation of integration errors. Consequently, the accuracy of orientation angle estimation was enhanced by taking advantage of the merits of both image processing and onboard sensor integration (Fig. 4). By adopting these measures, it was possible to realize the target control accuracy.

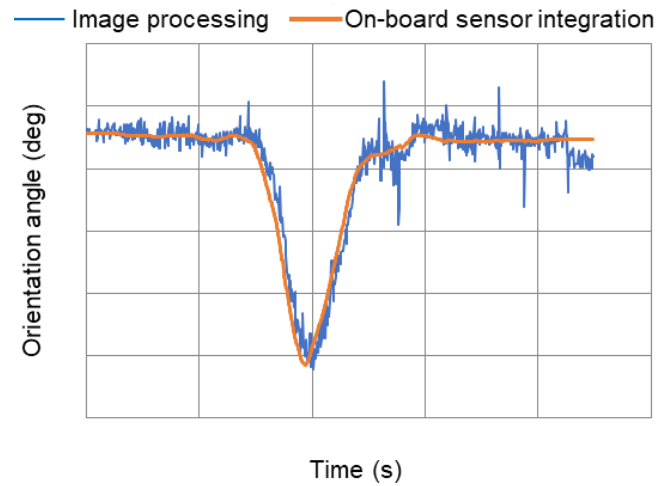


Fig. 4 Orientation Angle Estimation

### 3.3 Stabilization technology for wireless communication

Remote vehicle control requires the transmission and reception of control values over a high-speed cycle by wireless communication. An important aspect of this is stabilizing communication quality. However, the quality of wireless communication is affected by deterioration risks due to radio wave interference, noise, and phasing. Therefore, redundancy was incorporated into the RCD wireless communication system, and logic was adopted that constantly evaluates indicators related to communication quality (such as the strength of radio waves and the like) and selects the higher quality communication path based on a comprehensive judgment process (Fig. 5). This approach greatly reduces the probability that communication will be delayed or disrupted. In addition, if disruption does occur, the vehicle detects the disruption and brakes automatically to a stop, thereby deactivating the autonomous driving control and ensuring safety.

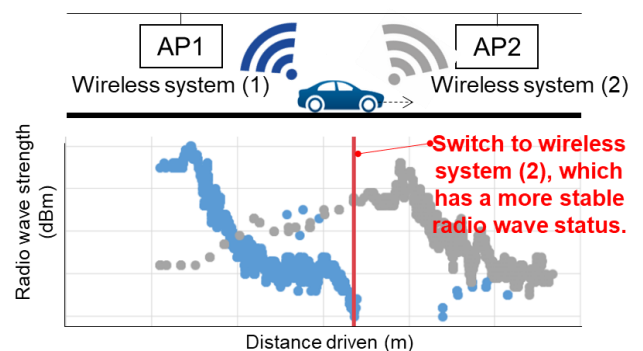


Fig. 5 Redundancy in Wireless Communication

## 4. System Reliability

Since RCD is equivalent to a level 4 system under the Society of Automotive Engineers' (SAE) definitions of autonomous driving systems, the safety of the entire system must be ensured. To realize this, a basic approach of mitigating the potential damage of a single malfunction was adopted. Because RCD applies to mass-production models with different specifications, it is difficult to adopt satisfactory failsafe functions on an individual vehicle level. Therefore, a system was constructed to mutually supplement the functions of both RCD and the vehicle. For example, if an error occurs in a vehicle, this would be detected by RCD, which would then apply the brakes and bring the vehicle to a complete stop. If communication between RCD and the vehicle is interrupted for a predetermined time, the vehicle would identify that situation and automatically stop itself.

Additionally, evaluations for introducing RCD to actual manufacturing sites can only be conducted on non-operational days, making it difficult to secure adequate development time. Therefore, the vehicle motion was modeled and a simulation environment created that couples the plant environment with the control system (Fig. 6). The standard deviation and dead time of the positioning coordinates were incorporated into the model and iterations of development were carried out by defining specifications and calibrating constants theoretically. This helped to shorten the development period and improve reliability.

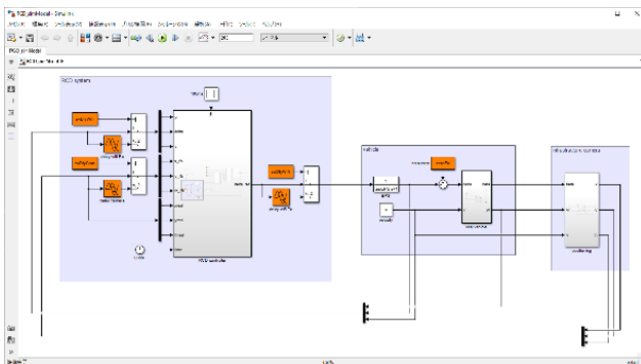


Fig. 6 Simulation Environment

In addition, actual vehicle verification environments were set up both indoors and outdoors to enable repeated evaluations and improvements under different preconditions over a three-year period (Fig. 7). Outdoor evaluations were carried out under a range of uncontrollable factors, including the weather conditions, time, and the like, to strengthen the AI model and logic. Indoors, a low ceiling of approximately 2.5 meters was assumed to evaluate different conditions such as camera height and the like. As a result, since the adoption of RCD in the Motomachi Plant, it has realized safe and

highly efficient unmanned transportation of more than 50,000 vehicles. Toyota continues to enhance the system under real-world mass-production environments with the aim of delivering even greater value.



Fig. 7 Outdoor and Indoor Evaluation Environments

## 5. Conclusion

RCD is a versatile technology that uses an external system to control vehicle motion. Since it has minimal requirements for vehicle equipment and functions, it should be relatively simple to adopt in other situations. The Toyota Technical Workshop held in June 2023 included an announcement about a self-propelled production line using RCD (Fig. 8). This has the potential to reduce the investment required to transport vehicles on a production line by several billion yen. The resulting flexible line layout should also dramatically reduce the lead-time for new model changeovers. Furthermore, in addition to raising plant productivity, RCD also has the potential to enhance the safety, peace of mind, and convenience of a wide range of other services.

However, since RCD combines various CASE-related technologies, a continuous series of advances will be required before it is ready for adoption in a wider range of use cases. Toyota intends to continue building up its real-world manufacturing technologies and exploring the potential of mobility.

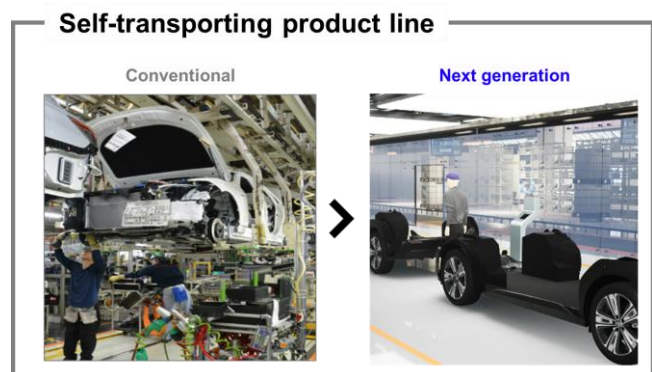


Fig. 8 Self-Propelled Production Line

2022 Energy Conservation Grand Prize (ECCJ Chairman's Award) of the Energy Conservation Center, Japan

# Initiatives to Reduce Power Demand through Peak Shifting and Demand-Response

Yoshitaka Ohtake\*<sup>1</sup>Iwao Akaida\*<sup>1</sup>Nobutake Suzuki\*<sup>1</sup>

## 1. Background

As Japan promotes the introduction of solar power generation and other forms of renewable energy, it has become increasingly important to expand the adoption of new supply and demand adjustment functions to help resolve the following issues: (1) fluctuations in the amount of solar power generation depending on the weather and the time of day or night and (2) the deactivation and decommissioning of fossil fuel power generation facilities due to aging equipment (**Fig. 1**). Consequently, Toyota launched initiatives in 2019 to stabilize its power supply and demand by reducing the amount of power required by production processes at peak times and utilizing in-house generation systems.

## 2. Initiative Details

### 2.1 Reduction in power required by production processes at peak times (peak shifting)

This section describes Toyota's initiative to shift its peak power demand. This initiative complements the company's ongoing efforts to reduce its total energy consumption (**Fig. 2**). In promoting this initiative, Toyota adopted the innovative approach of encouraging the involvement of every team member at its plants in helping to shift its peak power demand. By doing so, Toyota aimed to nurture awareness in its employees and firmly establish this initiative throughout the company (**Fig. 3**).

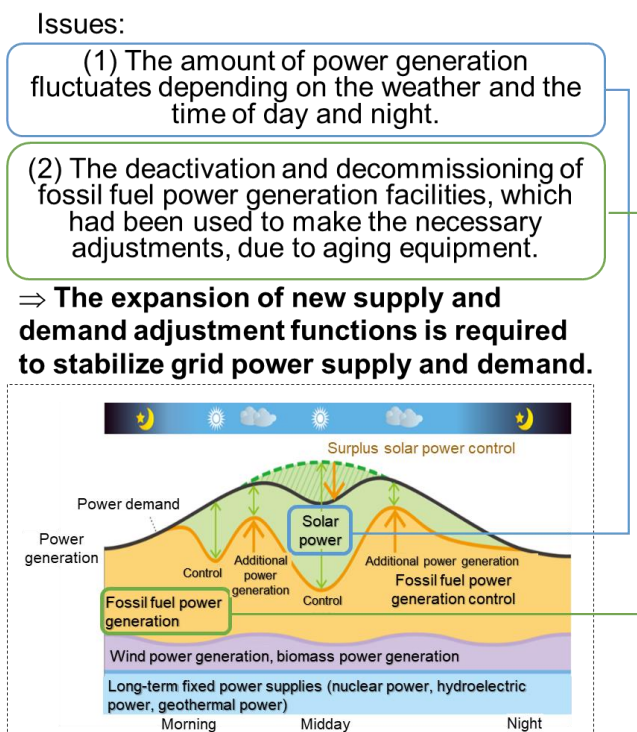
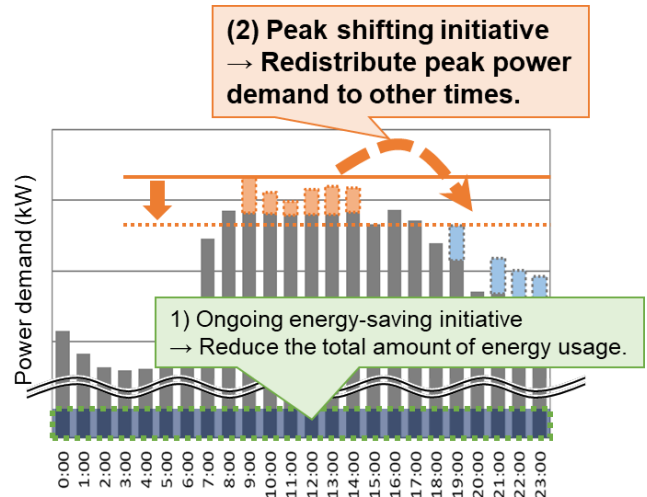


**Fig. 1 Outline of Power Supply<sup>(1)</sup>**



Methods of reducing peak power demand:

- 1) Energy-saving: continue ongoing initiative
- 2) Peak shifting: start new initiative

**Fig. 2 Hourly Plant Power Demand**

\*<sup>1</sup> Plant & Environmental Engineering Div., Production Group

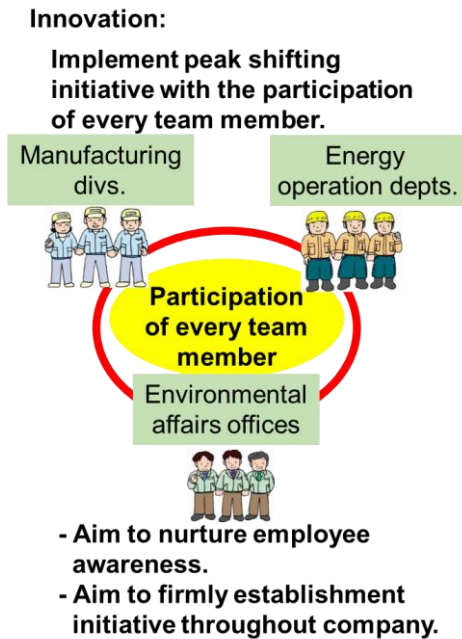


**Fig. 3 Innovative Approach to Peak Shifting**

More specifically, the peak shifting initiative involved collaborating with people with expert knowledge about equipment capable of shifting the timing of power loads in production processes, identifying feasible cases, and studying how to implement the shifts in power demand.

The following describes two examples of peak shifting that were adopted.

Example 1: Shifting the battery charging times of internal logistics vehicles

Battery-powered forklifts and compact electric tow tractors called Tugnovas (Fig. 4-1) are used for internal logistics. Before the start of this initiative, these vehicles were charged unsystematically whenever a low battery level was reached (Fig. 4-2). The method of operation was studied with the involvement of the manufacturing divisions, which verified that plant operations and production would not be affected by shifting charging outside the period of peak power demand. Adopting this approach in actual operations helped to lower peak power consumption (Fig. 5).



**Fig. 4-1 Forklift and Tugnovas**



**Fig. 4-2 Battery Charging Station**

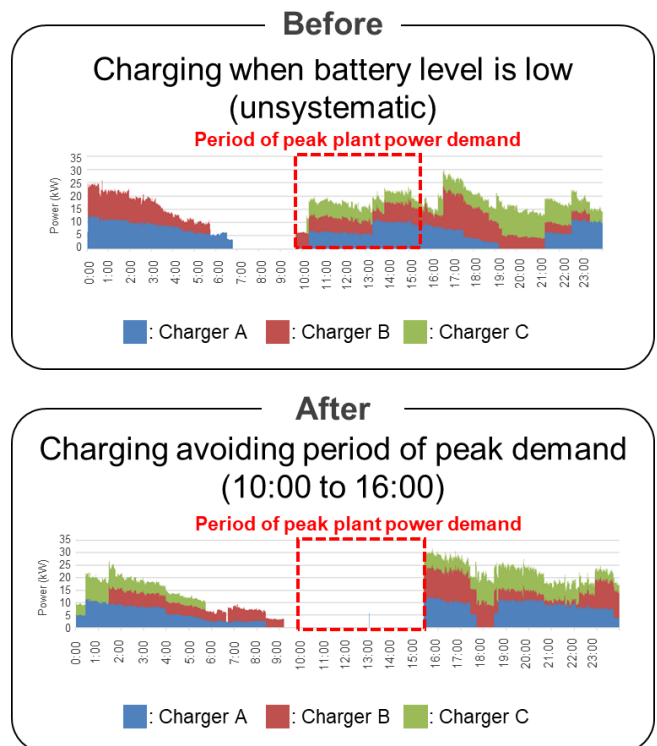


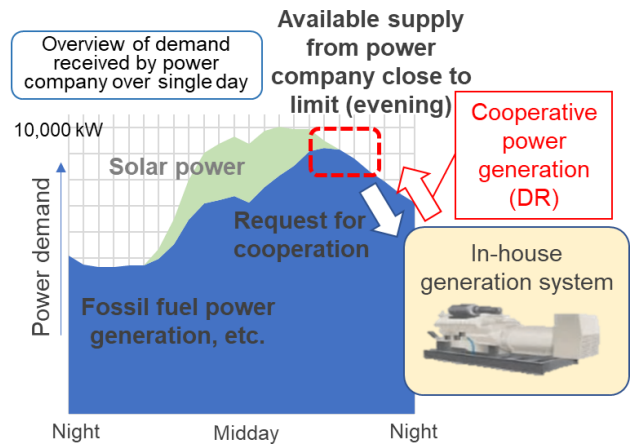
**Fig. 5 Operation before and after Initiative**

Example 2: Shifting power demand by changing operating pattern of cast iron smelting furnaces

This initiative also addressed the cast iron smelting furnaces (Fig. 6) used in the casting process for making engine parts and other components. The casting process involves the heating and forming of metal materials. The process studied in this initiative uses two smelting furnaces. Before the initiative was started, both smelting furnaces were started up at the same time. However, during the collaboration with the manufacturing divisions about the operation method, it was verified that production was possible even if the start-up time of one furnace was shifted to a different time, thereby reducing peak power consumption (Fig. 7).



**Fig. 6 Image of Smelting Furnace**



Adjust the amount of demand by activating/deactivating in-house generation systems in response to power company requests.

**Fig. 8 Illustration of Overall Demand Received by Power Company**

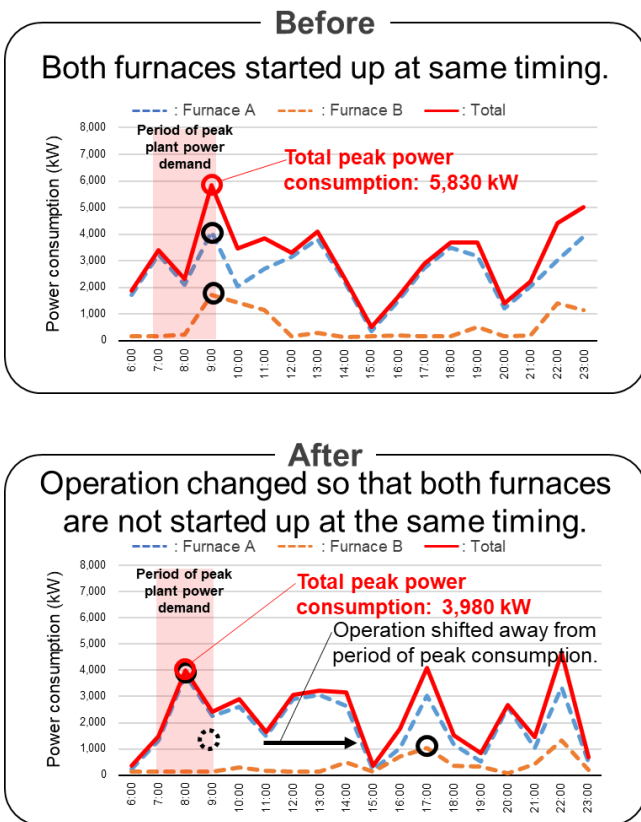


**Fig. 7 Operation before and after Initiative**

**2.2 Utilization of in-house generation systems (demand-response)**

Demand-response (DR) is a method that helps to adjust grid power demand by accepting requests from power companies to activate in-house generation systems when the available grid power supply is close to its limits (Fig. 8). This initiative adopted an innovative approach to implementing DR by working as a team with the energy operation departments to effectively utilize the time in which in-house generation systems are normally on standby (Fig. 9).

**Innovation:**

| Plant       | Generators              | Generators usually in operation | Generators normally on standby |
|-------------|-------------------------|---------------------------------|--------------------------------|
| Head Office | Diesel generator        |                                 | ○                              |
|             | Diesel generator        |                                 | ○                              |
|             | Gas engine generator    | ○                               |                                |
| Motomachi   | Diesel generator        |                                 | ○                              |
|             | Gas engine generator    | ○                               |                                |
|             | Gas engine generator    | ○                               |                                |
| Kamigo      | Diesel generator        |                                 | ○                              |
|             | Diesel generator        |                                 | ○                              |
|             | Diesel generator        |                                 | ○                              |
| Takaoka     | Diesel engine generator |                                 | ○                              |
|             | Gas engine generator    | ○                               |                                |

Effectively utilize the time in which in-house generation systems are normally on standby.

**Fig. 9 Operation before and after Initiative**

A specific example involving DR is described below  
Example: DR

There are two types of DR, depending on the request from the power company: response to lower demand on the grid by activating in-house generation systems, and response to raise demand from the grid by deactivating in-house generation systems (Fig. 10). Based on the operational status of the generators, response to lower demand on the grid is mainly carried out by the twenty-two diesel generators that

are normally on standby, and response to raise demand from the grid is mainly carried out by the five gas engine generators that are usually in operation. As a result, this approach helps to adjust grid power demand by responding to requests from power companies to activate in-house generation systems (Fig. 11). In addition, a notification system was set up with the involvement of the energy operation departments so that the in-house generation systems can be activated or deactivated accurately and promptly in response to a power company request issued three hours in advance of the required DR period (Fig. 12).

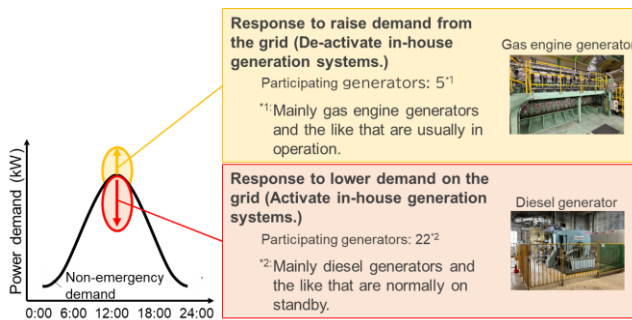


Fig. 10 In-House Generation Systems Participating in DR

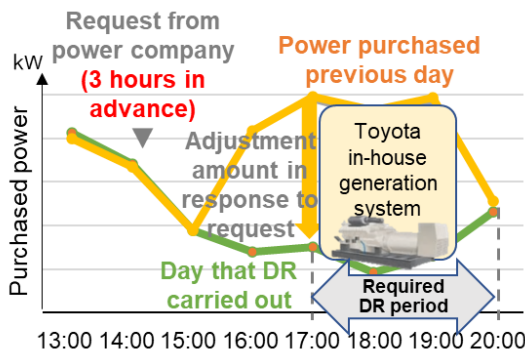


Fig. 11 Effects of Response to Lower Demand on Grid

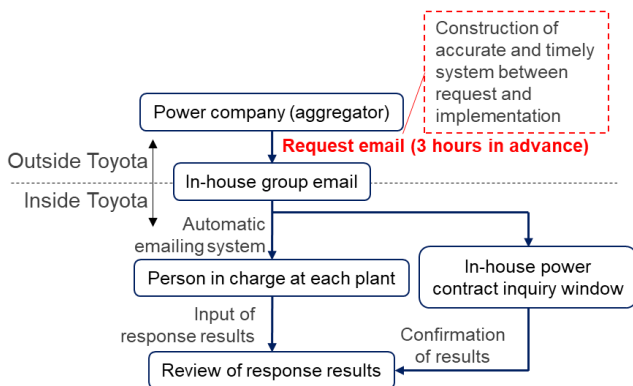


Fig. 12 DR Notification System

### 3. Initiative Effects

The effects of the peak shifting initiative were as follows. Peak power demand was reduced by 4,191 kW, an energy saving effect of 3,064 MWh (Table 1). In addition, Table 2 shows the effect of power generation allocation through DR adjustments. Power adjustments equivalent to approximately 10% of the peak power consumption of Toyota’s eleven domestic plants were achieved, particularly due to the effects of lowering demand on the grid.

Table 1 Effects of Peak Shifting

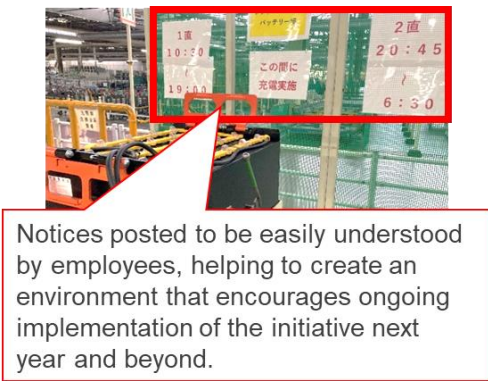
| Theme   | Reduction in peak power demand (kW) | Energy saving (MWh) |
|---|-------------------------------------|---------------------|
| Shifting battery charging times of logistics vehicles   | 174                                 |                     |
| Shifting sand filter backwash times at wastewater treatment sites                                   | 21                                  |                     |
| Changes to operating format of cast iron smelting furnaces  | 1,850                               |                     |
| Changes to casting work-in-progress   | 700                                 |                     |
| Reduction in air conditioning load by scattering water on external air conditioner compressor units | 480                                 | 542                 |
| Integration and consolidation of deodorization equipment  | 47                                  | 180                 |
| Other examples (14)   | 919                                 | 2,342               |
| Total   | 4,191                               | 3,064               |

Table 2 Effects of DR

|                | Lowering of demand on grid (kW) | Raising demand from grid (kW) |
|----------------|---------------------------------|-------------------------------|
| Adjusted power | 38,550                          | 14,800                        |

### 4. Initiative Continuity

The main target of the peak shifting initiative was the summer months (between July and September) when the power demand of plants increases. Various system- and people-centric measures were carried out to remind team members of the initiative, such as posting notices on target peak shifting equipment (Fig. 13) and sending regular notifications to every manufacturing division (Fig. 14). As part of the DR initiative, a system was created to enable ongoing participation through annual consultation with the operation and maintenance departments to formulate maintenance plans that ensure that the required DR periods do not overlap with maintenance times.



Notices posted to be easily understood by employees, helping to create an environment that encourages ongoing implementation of the initiative next year and beyond.

**Fig. 13 Notices Posted on Target Peak Shifting Equipment**

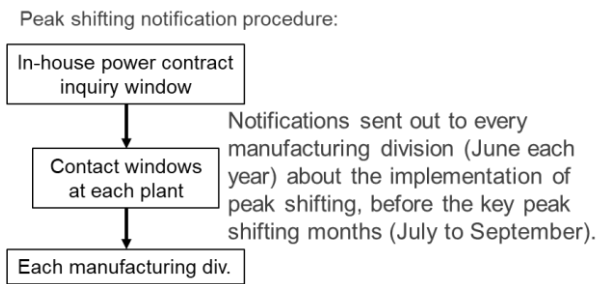


**Fig. 14 Notifications to Manufacturing Divisions**

## 5. Future Issues and Initiative Plans

As part of the peak power demand reduction initiative, a system is being considered that will allow the demand reduction effect to be reported as a result in the existing Energy Saving Proposal form (Fig. 15) used internally by Toyota. Another suggestion under consideration is to adopt an internal award system for the best examples to nurture even greater employee awareness of peak shifting and to encourage people to continue coming up with new ideas. At the same time, the DR initiative is considering an activity to raise the reliability of aging equipment by reducing failures and so on, as well as expanding opportunities to apply DR through automatic controls or the like.

**Fig. 15 Illustration of Energy Saving Proposal Form**

As highlighted in this article, Toyota intends to continue promoting energy management initiatives to help improve the balance between supply and demand when the public energy grid is close to its limits.

## Reference

- (1) *Energy in Japan 2021*. Agency for Natural Resources and Energy. <https://www.enecho.meti.go.jp/about/pamphlet/energy2021/007/#section1> (accessed May 30, 2022).

## List of Externally Published Papers of FY2022

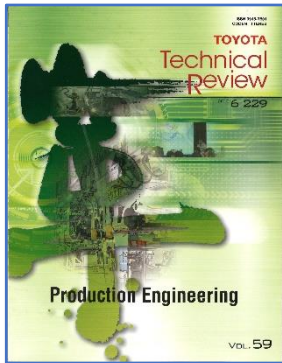
| Publication Name   | Title   | Presenter   | Affiliation  |
|--|---|---|--|
| Transactions of the Society of Automotive Engineers of Japan, Inc. | A Study of Object Detection Methodologies Applicable to Walking Assistant Devices to Identify Crosswalks and Signals      | Hiroaki Kawamura<br>Kohei Shintani<br>Hiroki Mima<br>Mashio Taniguchi   | Toyota Motor Corporation<br>(same as above)<br>(same as above)<br>(same as above)  |
|  | Powertrain On Board Diagnosis Development by Model Application - Efficient Development Process -                          | Kazuki Tsurumi<br>Shinji Satoh<br>Masaya Sunago<br>Takuya Matsumoto<br>Tomoyuki Tsuji<br>Takuya Atsumi  | Toyota Motor Corporation<br>(same as above)<br>(same as above)<br>(same as above)<br>(same as above)<br>(same as above)  |
|  | Application of CAE/ML Technique for Multifunctional Trade-Off Study between Mass and Performances                         | Yoshio Fujita<br>Shigeki Kojima<br>Kosho Kawahara   | Toyota Motor Corporation<br>(same as above)<br>(same as above)   |
|  | Extracting of High Contributing Body Vibration Mode to Road Noise using Operational Data Measured Separately              | Yuri Arai<br>Miho Nakatsuka<br>Masashi Komada<br>Junji Yoshida  | Toyota Motor Corporation<br>(same as above)<br>(same as above)<br>Osaka Institute of Technology  |
|  | Integrated Vehicle Dynamics Control Ordered by Six-Component Force at Center of Gravity with Brakes Mounted on Each Wheel | Sota Ukai<br>Manabu Nagasaka<br>Etsuo Katsuyama   | Toyota Motor Corporation<br>ADVICS CO., LTD.<br>Toyota Motor Corporation   |
|  | Impacts of Transboundary Air Pollution from East Asia on Air Quality in Japan in 2050                                     | Yoshiaki Yamadaya<br>Kentarou Hayashi<br>Tazuko Morikawa<br>Hiroyuki Yamada<br>Kotaro Tanaka<br>Shinichiro Okayama<br>Yoshiaki Shibata<br><br>Hiroe Watanabe<br>Toru Kidokoro | Ibraki University<br>Tokyo Denki University<br>Japan Automobile Research institute<br>Tokyo Denki University<br>Ibraki University<br>Nissan Motor co., Ltd.<br>Institute of Integrated Atmospheric Environment<br>Nissan Motor co., Ltd.<br>Toyota Motor Corporation |
|  | Effects of Fuel Components on Lean and EGR Diluted Combustion in Gasoline Engine  | Kazuki Kaneko<br>Naoyoshi Matsubara<br>Nozomi Yokoo<br>Koichi Nakata<br>Taketora Naiki<br>Ken Obata<br>Manabu Watanabe  | Toyota Motor Corporation<br>(same as above)<br>(same as above)<br>(same as above)<br>ENEOS Corporation<br>(same as above)<br>(same as above)   |
|  | Road-Embedding and Evaluation of Dynamic Power Transfer System for Outdoor Use Auto Guided Vehicle                        | Osamu Shimizu<br>Kazuyoshi Hanabusa<br>Kota Arasaki<br>Daisuke Gunji<br>Yuto Sakai<br>Hiromori Ikeda<br>Fuminori Matuoka  | The University of Tokyo<br>TDK Corporation<br>TDK-Lambda Corporation<br>NSK Ltd.<br>SHINMEI INDUSTRY CO., Ltd<br>TOYOTA T&S CONSTRUCTION CO.,LTD.<br>Toyota Motor Corporation  |
|  | Proposal of Data-Based Preview Controller for Active Vehicle Suspension   | Hiroki Furuta<br>Jin Hozumi<br>Shuta Yokota<br>Toru Takashima   | Toyota Motor Corporation<br>(same as above)<br>(same as above)<br>(same as above)  |
|  | Analysis of Unsprung Mass Vibration of Rigid Suspension during Vehicle Starting   | Shingo Koumura<br>Shumei Matsuda  | Toyota Motor Corporation<br>(same as above)  |
|  | Reduction of Longitudinal Vibration by Side-View Arrangement of Suspension  | Kazuaki Sugiyama<br>Shingo Koumura<br>Hiroki Kanbe<br>Tsuyoshi Yoshimi  | Toyota Motor Corporation<br>(same as above)<br>(same as above)<br>(same as above)  |
|  | Driving Dialogue Dataset Collection and Analysis for a Transformer-Based Conversational System that Talks About Scenery   | Ko Koga<br>Toshifumi Nishijima<br>Hiroaki Sugiyama  | Toyota Motor Corporation<br>(same as above)<br>NTT Communication Science Laboratories  |
|  | Reduction Technologies of Rear Differential Gear Whine Noise by Controlling Vibration Characteristics of Leaf Suspension  | Jun Kokaji<br>Masashi Komada<br>Hideo Satoh<br>Junzo Tamari<br>Koji Suzuki<br>Taira Sugiyama  | Toyota Motor Corporation<br>(same as above)<br>(same as above)<br>ESTECH Corporation<br>(same as above)<br>(same as above)   |

| Publication Name   | Title  | Presenter   | Affiliation   |   |
|--|--|---|---|---|
| Transactions of the Society of Automotive Engineers of Japan, Inc. | A Study of the Mechanism of Abnormal Ignition in H2 Engine   | Naoyoshi Matsubara<br>Yoshinori Miyamoto<br>Shiro Tanno<br>Jun Miyagawa<br>Yuya Abe<br>Nozomi Yokoo<br>Kazuki Kaneko<br>Daishi Takahashi<br>Koichi Nakata | Toyota Motor Corporation<br>(same as above)<br>(same as above)<br>(same as above)<br>DENSO Corporation<br>Toyota Motor Corporation<br>(same as above)<br>(same as above)<br>(same as above) |   |
|  | Prediction Methodology for xEV Motor Durability against Random Vibration   | Yoshifumi Nasuno<br>Tomotaka Nishimura<br>Kazuya Arakawa  | Toyota Motor Corporation<br>(same as above)<br>(same as above)  |   |
|  | Evaluation of Receiving Power Control for Dynamic Wireless Power Transfer Using Pulse Density Modulation   | Sakahisa Nagai<br>Toshiyuki Fujita<br>Hiroshi Fujimoto<br>Ryosuke Ikemura<br>Shogo Tsuge<br>Toshiya Hashimoto   | The University of Tokyo<br>(same as above)<br>(same as above)<br>Toyota Motor Corporation<br>(same as above)<br>(same as above)   |   |
|  | Power Control in Dynamic Wireless Power Transfer - Low-Speed Vehicle Testing with Active Rectification -   | Ryosuke Ikemura<br>Shogo Tsuge<br>Toshiya Hashimoto<br>Sakahisa Nagai<br>Toshiyuki Fujita<br>Hiroshi Fujimoto   | Toyota Motor Corporation<br>(same as above)<br>(same as above)<br>The University of Tokyo<br>(same as above)<br>(same as above)   |   |
|  | Research of the Correlation Between the Number of Training Data and Machine Learning Prediction Accuracy in Vehicle Crash Analysis   | Shota Hashimoto<br>Shigeki Kojima<br>Kosho Kawahara   | Toyota Motor Corporation<br>(same as above)<br>(same as above)  |   |
|  | A Feasibility Study for Quantum Computing Methodologies in Automotive Advanced Material Investigation - Application to Molecular Dynamics (MD) Study of Hydrogen Systems - | Yoshinori Suga<br>Sho Koh<br>Toru Shibamiya<br>Tennin Yan   | Toyota Motor Corporation<br>QunaSys Inc.<br>(same as above)<br>(same as above)  |   |
|  | Construction of a Predicting Method for Radiated Noise from Motor System Bench Below 30 MHz  | Ayumi Yamashita<br>Soichiro Ota<br>Hirotoshi Izawa<br>Daisuke Funahashi   | Toyota Motor Corporation<br>(same as above)<br>(same as above)<br>(same as above)   |   |
|  | Set-Based Design Method for Rigid Axle Suspension using Bayesian Active Learning   | Hideki Shiraiishi<br>Kohei Shintani<br>Motofumi Iwata<br>Yasuaki Takada   | Toyota Motor Corporation<br>(same as above)<br>(same as above)<br>(same as above)   |   |
|  | Accident Reduction Effect Analysis of Driving Load Reduction System Based on Market Data   | Masaru Otsuki<br>Tsuyoshi Shimizu<br>Yuji Ikedo   | Toyota Motor Corporation<br>(same as above)<br>(same as above)  |   |
|  | Shape Optimization of Dynamic Structural Member in Isogeometric Analysis   | Hozumi Oshika<br>Shin-ichi Arimoto<br>Kosho Kawahara<br>Ki-ichi Furuhashi<br>Yuta Yokoyama<br>Hirofumi Sugiyama<br>Shigenobu Okazawa                      | University of Yamanashi<br>Toyota Motor Corporation<br>(same as above)<br>University of Yamanashi<br>(same as above)<br>(same as above)<br>(same as above)                                  |   |
|  | A Study on Selection Method of Survey Cooperators Considering Psychological Distance Scale in Concept Test   | Masaya Ando<br>Akira Saito<br>Motoki Maekawa<br>Hideki Kobayashi  | Chiba Institute of technology<br>Toyota Motor Corporation<br>(same as above)<br>(same as above)   |   |
|  | International Journal of Automotive Engineering (IAE)  | Proposal of Risk Estimation Index from Driver Behaviour for Approaching and Overtaking Vulnerable Road User   | Manh-Dung Vu<br>Sueharu Nagiri<br><br>Hirofumi Aoki<br>Tatsuya Suzuki<br>Quy Hung Nguyen Van<br>Shouji Itou<br>Akira Hattori  | Nagoya University<br>Nagoya University,<br>Institute of Innovation for Future Society<br>(same as above)<br>Nagoya University<br>Toyota Motor Corporation<br>(same as above)<br>(same as above) |
|  |  | The Study of Connected System Specification for Traffic Flow Control with Effective Lane Utilization  | Yoshiaki Irie<br>Daisuke Akasaka  | Toyota Motor Corporation<br>MathWorks Japan   |
| SAE Technical Paper  | Deployment of OTA-Upgradable Teammate Advanced Drive   | Tomoya Kawasaki<br>Kaiji Itabashi<br>Derek Caveney<br>Masaki Kitago<br>Yuichiro Nara<br>Takashi Oda   | Toyota Motor Corporation<br>Woven Core, Inc.<br>Toyota Motor North America, Inc.<br>Woven Core, Inc.<br>(same as above)<br>Toyota Motor Corporation   |   |

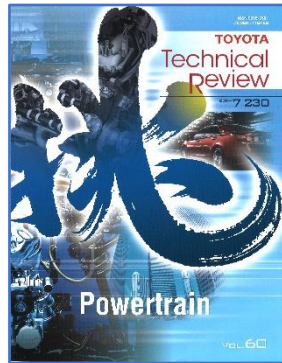
| Publication Name    | Title   | Presenter  | Affiliation   |
|---------------------|---|--|---|
| SAE Technical Paper | Development of Automatic Door Lock System to Help Prevent Collisions between Opened Doors and Approaching Vehicles When Exiting Vehicle                           | Koji Takeuchi<br>Masaho Ishida   | Toyota Motor Corporation<br>(same as above)   |
|                     | Road Crossing Assistance Method Using Object Detection Based on Deep Learning   | Hiroaki Kawamura<br>Kohei Shintani<br>Hiroki Mima<br>Mashio Taniguchi  | Toyota Motor Corporation<br>(same as above)<br>(same as above)<br>(same as above)   |
|                     | Cabin Comfort Improvement and Heating Energy Reduction under Cold-Condition by Using Radiative Heater   | Hiroataka Sasaki<br>Daisuke Sakamoto   | Toyota Motor Corporation<br>(same as above)   |
|                     | Effect of Aero Covers on Underfloor Wind Noise; Conclusions from a Wind Tunnel Validated Aero-Vibro-Acoustic Model  | Susumu Terakado<br>Paul Bremner  | Toyota Motor Corporation<br>AeroHydroPLUS   |
|                     | Variable Axial Composite Lightweight Automotive Parts Using Anisotropic Topology Optimization and Tailored Fiber Placement  | Tsuyoshi Nomura<br>Yoshihiro Iwano<br>Atsushi Kawamoto<br>Katsuharu Yoshikawa<br>Axel Spickenheuer   | Toyota Central R&D Labs., Inc.<br>Toyota Motor Corporation<br>Toyota Central R&D Labs., Inc.<br>Tokai Industrial Sewing Machines Co., Ltd.<br>Leibniz Institute of<br>Polymer Research Dresden e.V.                                       |
|                     | Development of In Mold Coating Clear Coat Paint for Carbon Fiber Sheet Molding Compound Roof  | Katsunori Ito<br>Keiji Ambo  | Toyota Motor Corporation<br>(same as above)   |
|                     | Research on Ultra-High Viscosity Index Engine Oil: Part 1 - "Flat Viscosity" Concept and Contribution to Carbon Neutrality  | Kazuo Yamamori<br>Yuta Uematsu<br>Satoshi Hirano<br>Noriya Ishizaki<br>Shunsuke Mori<br>Takashi Koyama<br>Takashi Suzuki<br>Kotaro Wada  | Toyota Motor Corporation<br>(same as above)<br>(same as above)<br>(same as above)<br>(same as above)<br>(same as above)<br>(same as above)<br>(same as above)<br>ENEOS Corporation  |
|                     | Research on Ultra-High Viscosity Index Engine Oil: Part 2 - Influence of Engine Oil Evaporation Characteristics on Oil Consumption of Internal Combustion Engines | Takashi Koyama<br>Takashi Suzuki<br>Kazuo Yamamori<br>Yuta Uematsu<br>Satoshi Hirano<br>Noriya Ishizaki<br>Kotaro Wada   | Toyota Motor Corporation<br>(same as above)<br>(same as above)<br>(same as above)<br>(same as above)<br>(same as above)<br>(same as above)<br>ENEOS Corporation   |
|                     | Development of a Ceramic EHC  | Takahiro Sadamitsu<br>Toshinori Oki<br>Shingo Korenaga<br>Shigemasa Hirooka<br>Shingo Iwasaki<br>Tatsuo Iida   | Toyota Motor Corporation<br>(same as above)<br>(same as above)<br>(same as above)<br>(same as above)<br>NGK Insulators Ltd.<br>Toyota Motor Corporation   |
|                     | Vehicle Surge Reduction Technology during Towing in Parallel HEV Pickup Truck   | Shingo Okaya<br>Jun Kokaji<br>Luis Quinteros<br>Yoshio Hasegawa<br>Seiji Masunaga  | Toyota Motor Corporation<br>(same as above)<br>Toyota Motor North America, Inc.<br>Toyota Motor Corporation<br>(same as above)  |
|                     | Toyota's New Hybrid Unit "L4A0"   | Guodong Tan<br>Masashi Ikemura<br>Yoshio Hasegawa<br>Takao Ohki<br>Masayuki Baba<br>Atsuro Nakamura<br>Craig Herring<br>Atsushi Niinomi<br>Makoto Hamano<br>Yasuhiro Mizoguchi | Toyota Motor Corporation<br>(same as above)<br>(same as above)<br>(same as above)<br>(same as above)<br>(same as above)<br>(same as above)<br>Toyota Motor North America, Inc.<br>AISIN Corporation<br>(same as above)<br>(same as above) |
|                     | Development of Safety Performance for FC Stack in the New Toyota FCEV   | Kei Enomoto<br>Atsushi Ida<br>Takashi Harada<br>Hiroaki Takeuchi   | Toyota Motor Corporation<br>(same as above)<br>(same as above)<br>(same as above)   |
|                     | Data-Driven Set Based Concurrent Engineering Method for Multidisciplinary Design Optimization   | Kohei Shintani<br>Atsuji Abe<br>Minoru Tsuchiyama  | Toyota Motor Corporation<br>(same as above)<br>(same as above)  |
|                     | Development of Steering Control Method for Steer-by-Wire System Requiring No Changes in Steering Wheel Hand Position  | Toru Takashima<br>Yoshio Kudo<br>Kenji Shibata<br>Takashi Koderu<br>Isao Namikawa  | Toyota Motor Corporation<br>(same as above)<br>(same as above)<br>JTEKT Corporation<br>(same as above)  |

| Publication Name  | Title  | Presenter  | Affiliation   |
|---|--|--|---|
| Transactions of the JSME<br>(in Japanese)                               | A method of calculating the reflection and transmission coefficients required for controlling the nodal positions of a mode shape as desired in a three-dimensional beam structure | Yuichi Matsumura<br>Haruto Katsuno<br>Tomo Yamada<br>Masashi Komada<br>Hidenori Morita   | Gifu University<br>Graduate School of Gifu University<br>(same as above)<br>Toyota Motor Corporation<br>Toyota Motor Kyushu, Inc.   |
|   | Approximate estimation of stresses and displacements of a thin-walled square cross-section beam after torsional buckling   | Katsuya Furusu<br>Tatsuyuki Amago<br>Toshiaki Nakagawa<br>Tsutomu Hamabe<br>Norihisa Aoki  | Toyota Central R&D Labs., Inc.<br>(same as above)<br>(same as above)<br>Toyota Motor Corporation<br>(same as above)   |
|   | An automation system for vehicle driveability evaluation using machine learning  | Hisashi Tajima<br>Kohei Shintani<br>Azuki Ogoshi<br>Shota Kitano<br>Motofumi Iwata   | Toyota Motor Corporation<br>(same as above)<br>(same as above)<br>(same as above)<br>(same as above)  |
|   | Research on compliance steers of strut type front suspension subject to lateral force and self aligning torque during cornering  | Tetsuaki Kawata<br>Tadashi Kouno<br>Hitoshi Sakuma   | Daihatsu Motor Co., Ltd<br>(Incumbent Aichi institute of Technology)<br>Toyota Motor Corporation<br>(same as above)   |
|   | Study on kingpin axis behavior of front suspension under the turning lateral force.  | Tetsuaki Kawata<br>Tadashi Kouno<br>Hitoshi Sakuma   | Daihatsu Motor Co., Ltd<br>(Incumbent Aichi institute of Technology)<br>Toyota Motor Corporation<br>(same as above)   |
| Journal of Advanced<br>Mechanical Design, Systems,<br>and Manufacturing | Non-destructive depth analysis of acidic phosphate ester boundary layers by hard X-ray photoelectron spectroscopy  | Naoko Takechi-Takahashi<br>Kensuke Matsushima<br>Noritake Isomura<br>Satoru Kosaka<br>Mamoru Tohyama<br>Hiroshi Moritani<br>Takayuki Aoyama<br>Toshinari Sano<br>Satoru Maegawa<br>Fumihito Itoigawa | Toyota Central R&D Labs., Inc<br>Nagoya Institute of Technology<br>Toyota Central R&D Labs., Inc<br>(same as above)<br>(same as above)<br>(same as above)<br>(same as above)<br>Toyota Motor Corporation<br>Nagoya Institute of Technology<br>(same as above) |
|   | A set-based approach to dynamic system design using physics informed neural network  | Kohei Shintani<br>Eiji Nakatsugawa<br>Minoru Tsuchiyama  | Toyota Motor Corporation<br>(same as above)<br>(same as above)  |

# Back Number Index



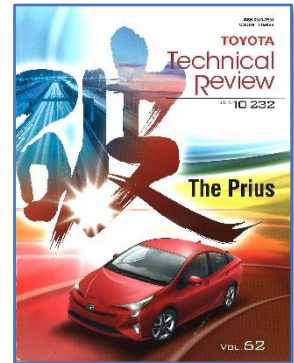
**Vol.59(2013/6)**  
Special Feature:  
Production Engineering



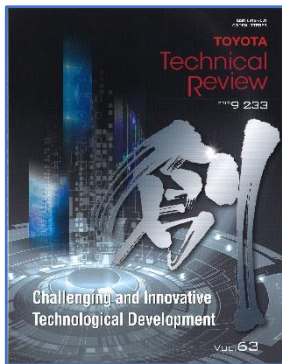
**Vol.60(2014/7)**  
Special Feature:  
Powertrain



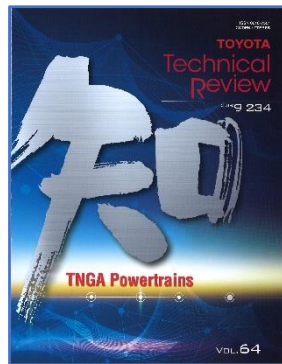
**Vol.61(2015/6)**  
Special Feature1:  
The Mirai FCV  
Special Feature2:  
Advanced Driving  
Support Systems



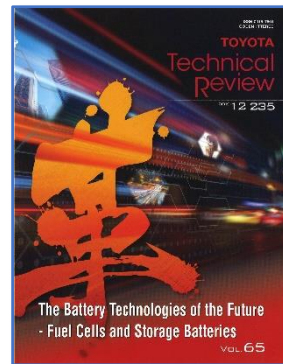
**Vol.62(2016/10)**  
Special Feature:  
The Prius



**Vol.63(2017/9)**  
Challenging and  
Innovative Technological  
Development



**Vol.64(2018/9)**  
Special Feature:  
TNGA Powertrains



**Vol.65(2019/12)**  
Special Feature:  
The Battery Technologies  
of the Future – Fuel Cells  
and Storage Batteries



**Vol.66(2021/3)**  
Special Feature:  
Contrasts in Value and  
Manufacturing – The  
Second-Generation Mirai  
and New GR Yaris –



**Vol.67(2022/3)**  
Special Feature:  
Toyota's initiatives for  
building a society  
through sports in which  
everyone can participate  
in peace and equality, and  
for realizing a sustainable  
society through mobility



**Vol.68(2023/4)**  
Special Feature:  
Toyota's Full Lineup  
Strategy for Carbon  
Neutrality

## **TOYOTA Technical Review Vol.69 No.1**

© 2023 TOYOTA MOTOR CORPORATION

( All rights reserved )

Publisher's Office

R&D and Engineering management Div.

TOYOTA MOTOR CORPORATION

1 Toyota-cho, Toyota, Aichi, 471-8572 Japan

81-565-28-2121 (Operator)

Publisher

Tetsuya Kohigashi

Planning

Midori Mori , Chieko Hirahara , Mayuka Kubo

Editor

Shingo Kato

(Publishing Office)

Administration Support Dept.

Toyota Office

TOYOTA ENTERPRISE INC.

Published

December 20, 2023